1998

Uncertainty and Variability Analysis in the Estimation of Human Exposure to Mercury from Seafood Consumption Using Two-Dimensional Monte Carlo Simulations

J. Keith Bangerter
Medical University of South Carolina

Uncertainty and Variability Analysis in the Estimation of Human Exposure to Mercury from Seafood Consumption Using Two–Dimensional Monte Carlo Simulations

by

J. Keith Bangerter

A dissertation submitted to the faculty of the Medical University of South Carolina in partial fulfillment of the requirements for the degree of Doctor of Philosophy in the College of Graduate Studies

Department of Biometry and Epidemiology

1998

Approved by:

Eberhard O. Voit, Ph.D., Professor
Chairman, Advisory Committee
Department of Biometry and Epidemiology

Karen G. Burnett, Ph.D., Associate Professor
Department of Microbiology and Immunology

Rebecca G. Knapp, Ph.D., Professor
Department of Biometry and Epidemiology

G. Malcolm Meaburn, Ph.D.
National Ocean Service

Philip F. Rust, Ph.D., Associate Professor
Department of Biometry and Epidemiology

Acknowledgments

I do not boast in my own strength, nor in my own wisdom ... Yea, I know that I am nothing; as to my own strength I am weak; therefore I will not boast of myself, but I will boast of my God, for in His strength I can do all things.

The Book of Mormon, Alma 26:11–12

First and foremost, I want to thank a loving Heavenly Father and His son Jesus Christ for the beautiful gospel that they have provided. It is this gospel that inspires me strive for self–improvement in all facets of life: mental, physical, emotional, and spiritual. At this time, I also want to express my gratitude for the desire to learn and a mind capable of learning.

This would not have been possible without my wonderful wife, Deitra, who has encouraged me all along the way. I want to thank her for the time that she spent without me while pursuing this degree, and for the remarkable way that she is raising our beautiful daughter, Mallory. Now I hope that these two women will get more of the husband and father that they deserve.

I have had the good fortune of an outstanding advisory committee to help me write this dissertation. Dr. Eberhard Voit, my mentor and committee chair, has continuously provided consultation, comments, and guidance to keep me on the correct path. He has pushed me to complete a dissertation that I am proud of authoring. I would like to thank Dr. Malcolm Meaburn for his patience in teaching me about seafood safety issues, for the opportunity to work with him at the National Ocean Service, and for the funding he has obtained to support my work. Dr. Rebecca Knapp has not only provided assistance with my dissertation, but she has helped to prepare me for the professional job market throughout my stay at MUSC. I would like to thank Dr. Phil Rust for his thoughtful questions, which inspired me to do more than I thought was possible. Finally, I want to thank Dr. Karen Burnett for her support. I know she has a busy schedule, yet she always managed to find time for me.

I would like to thank Lori Schwacke for the Mathcad programs and approximation equations that she provided. She is a truly gifted programmer. In addition, thanks are in order for Al Fortner from the National Ocean Service who used his GIS skills and software to provide the lobster sampling sites map. Finally, I want to thank Reneé Hebert for everything from statistical opinions to a listening ear. She has been my best friend and most trusted confidante at MUSC.

Table of Contents

List of Figures

List of Tables

Acronyms and Abbreviations

ADI	Acceptable Daily Intake
ATSDR	Agency for Toxic Substances and Disease Registry
CDF	Cumulative distribution function
cm	Centimeter
CNS	Central nervous system
DDST	Denver Developmental Screen Test
EPA	Environmental Protection Agency
FDA	Food and Drug Administration
g	Gram
GI	Gastrointestinal
IAEA	International Atomic Energy Agency
kg	Kilogram
LOAEL	Lowest–Observed–Adverse–Effect Level
mg	Milligram
mm	Millimeter
MRL	Minimal Risk Level
NCHS	National Center for Health Statistics
NHANES	National Health and Nutrition Examination Survey
NMFS	National Marine Fisheries Service
NOS	National Ocean Service
NPD	National Purchase Diary
PDF	Probability density function
oz	Ounce
ppm	Parts per million
r	Sample correlation coefficient
RfD	Reference Dose
RNA	Ribonucleic acid
SRI	Stanford Research Institute
WHO	World Health Organization
WHO/IPCS	World Health Organization's International Programme for Chemical Safety
μg	Microgram
μ	Mean
σ	Standard Deviation

Abstract

Fish and shellfish are a beneficial food source due to their high protein content, low saturated fat content, and low cholesterol content; they possess beneficial omega–3 fatty acids and antioxidants such as vitamin E and selenium. Recent studies identified a decreased risk of sudden cardiac death in seafood consumers.

Per capita seafood consumption increased 27% from 1975 to 1990, with nearly 95% of the U.S. population consuming some kind of fish or shellfish product each year. But seafood consumption may pose health risks which need to be weighed against benefits. One of potential risks is the toxicity of methylmercury. Mercury accumulates dramatically in the aquatic food web, where nearly all is converted into methylmercury. Almost all fish and shellfish contain at least trace amounts of methylmercury, and seafood consumption is the source of nearly all human methylmercury exposure. Major methylmercury poisonings provide evidence that the health effect of greatest concern from methylmercury exposure is neurotoxicity in the fetus and infant.

Exposure assessments are the crucial step in identifying populations at risk of deleterious effects. Although several methods are currently available to project exposure, additional techniques may be necessary to accurately characterize exposure. One major complication in assessing exposure is the fact that all contributing factors are subject to variability, uncertainty, or to both. *Variability* describes heterogeneity in a well–characterized population, while *uncertainty* accounts for partial ignorance about a characteristic.

Unfortunately, current exposure estimation techniques fail to simultaneously represent the full range and probability of exposures, account for dependencies among variables, and partition effects of variability from uncertainty. Thus, an innovative statistical methodology is developed here to overcome these deficiencies. Statistical techniques are also utilized to determine those input variables that are most critical to exposure.

The different methods discussed and developed here may be used to estimate contaminant exposure from seafood consumption. Among other contaminants and marine species, methylmercury exposure from the consumption of Northern lobster, *Homarus americanus*, is currently of interest. Lobster is one of the more commonly consumed marine species, and it has the potential to bioaccumulate high methylmercury levels.

Chapter 1

INTRODUCTION

Issue

Seafood consumption is associated with documented health benefits, yet high levels of methylmercury exposure from seafood consumption present potential health risks. In order to weigh seafood consumption benefits properly against possible risks, it is necessary to evaluate exposure using modern mathematical means.

Rationale

Fish and shellfish are a beneficial food source due to their high protein content, low saturated fat content, and low cholesterol content; they possess substantial amounts of beneficial omega–3 fatty acids and antioxidants such as vitamin E and selenium (Egeland and Middaugh, 1997). Two recent studies both concluded that men who consume at least eight ounces (one serving) of fish or shellfish per week decrease the risk of sudden cardiac death by 50–60% compared with those who consumed less fish and shellfish (Daviglus *et al.*, 1997; Albert *et al.*, 1998).

Consumption of fish and shellfish has risen over the last 25 years. In fact, per capita seafood consumption increased 27% from 1975 to 1990 as Americans

became more and more health conscious (Ruffle *et al.*, 1994; EPA, 1997c; Johnson and Doré, 1993). Nearly 95% of the U.S. population consume some kind of fish product each year (Rupp *et al.*, 1980; Lipfert *et al.*, 1996).

But seafood consumption may pose health risks which need to be weighed against the benefits. One of these potential risks is the toxicity of methylmercury. Mercury accumulates most efficiently in the aquatic food web, where almost all is converted into the organic form of methylmercury. Almost all fish contain at least trace amounts of methylmercury, and fish consumption is the source of nearly all human methylmercury exposure (ATSDR, 1993; Marsh *et al.*, 1995; Lipfert *et al.*, 1996).

The first major methylmercury poisoning as a result of seafood consumption occurred in Minamata, Japan. In 1953 human health effects, including developmental effects, were recorded (ATSDR, 1993; EPA, 1997b). The toxic effects included high rates of developmental abnormalities in newborns and young children, the hospitalization of hundreds of poisoning victims, and even death (Eisler, 1987).

In 1971–1972 Iraq experienced a large poisoning event (Lee, 1972; Rom, 1992; EPA, 1997b). The U.S. sent to Iraq grain treated with organo–mercurial fungicide. The U.S. intended the grain to be used as seed; the hungry citizens of Iraq made bread with the grain, not realizing it was toxic. The poisoning produced adverse effects, including developmental outcomes, similar to those observed in Minamata (Lee, 1972; ATSDR, 1993; Waldron and Scott, 1994; EPA, 1997b).

Both the Minamata and Iraqi poisonings provide evidence that the health effect of greatest concern from methylmercury exposure is neurotoxicity in the fetus and infant. Methylmercury is a potent neurotoxicant for young children, especially the fetus, since the central nervous system is rapidly developing during this stage of life (ATSDR, 1993; EPA, 1994, 1997b). Methylmercury easily crosses both the placental barrier and the blood–brain barrier (ATSDR, 1993; EPA, 1994).

Two major long–term epidemiological studies in the Seychelles Islands and the Faroe Islands evaluated the relationship between fetal methylmercury exposure from high fish consuming populations and neurotoxic effects in childhood development (Davidson *et al.*, 1995, 1998; Myers *et al.*, 1995; Grandjean *et al.*, 1997). Neither study identified significant developmental abnormalities in children from mothers consuming vast amounts of seafood.

The Environmental Protection Agency (EPA) is extremely concerned about risks from mercury exposure. In fact, EPA recently published the *Mercury Study Report to Congress* (1997b) consisting of eight volumes with over 1,800 pages which stirred enormous discussion among federal and state agencies. It is estimated that natural and anthropogenic sources contribute approximately equal amounts of mercury to the environment. The Mercury Study Report provides an assessment of anthropogenic mercury emissions and the health and environmental implications from those emissions. This includes the potential hazard of methylmercury exposure to humans and wildlife from the consumption of contaminated seafood. Combustion point sources such as coal–fired utility

boilers, waste incinerators, and commercial/industrial boilers account for over 85% of the U.S. anthropogenic mercury emission. EPA notes the link between anthropogenic releases of mercury and methylmercury levels in fish.

Exposure assessments are the crucial step in identifying populations at risk of deleterious effects, and several methods are currently available to project exposure. Traditionally exposure was determined using point estimates, but more recently Monte Carlo simulation techniques have been used to characterize exposure. One major complication in assessing exposure is the fact that all contributing factors are subject to variability and uncertainty. *Variability*, or true biologic variability, describes heterogeneity or diversity in a well–characterized population, while *uncertainty* accounts for partial ignorance or lack of total knowledge about a characteristic. It is useful to distinguish between variability and uncertainty because uncertainty may be reduced through additional measurement or study, while true biologic variability is irreducible.

Unfortunately, current exposure estimation techniques fail to represent the full range and probability of exposures, fail to account for dependencies among the variables used to predict exposure, and do not separate the effects of variability from uncertainty. Point estimates do not render information as to where the estimates lie on the distribution of exposures, and no current simulation technique simultaneously accounts for dependencies among input variables while distinguishing between variability and uncertainty. Thus, an innovative statistical methodology is developed here to overcome these deficiencies.

Several methods have been used to predict the degree of methylmercury exposure from the consumption of variuos seafood species; for example, EPA (1997c) used point estimates, Lipfert *et al.* (1996) traditional Monte Carlo simulations, Balthis *et al.* (1996) hierarchical Monte Carlo simulations, and MacIntosh *et al.* (1994) and Carrington *et al.* (1997) used two-dimensional Monte Carlo simulations. This effort is intended to identify the circumstances that are most appropriate for each of several exposure estimation techniques. Risk assessors may use this information to select the most appropriate exposure estimation techniques for a given problem. All of the methods mentioned above along with the new methodology developed here are compared using identical data sets to predict methylmercury exposure from the consumption of Northern lobster, *Homarus americanus*. Lobster is the most desired seafood, and it is also one of the more commonly consumed marine species (NOAA, 1991). Northern lobster take approximately five to seven years to attain the minimum legal harvest weight of one pound; consequently, they have the potential to bioaccumulate high methylmercury levels.

Objectives

The primary goal of this research is to estimate methylmercury exposure from seafood consumption while considering the uncertainty and variability for each input variable and dependencies among input variables. To accomplish this the following tasks were performed:

1. **Develop a simulation technique to account simultaneously for both variability and uncertainty within individual input variables and dependencies among input variables.**

One major complication in assessing exposure is the fact that all contributing factors are subject to variability, uncertainty, or to both. Throughout this report the term variability is used to represent true biological variability. *Variability* describes heterogeneity or diversity in a well–characterized population. *Uncertainty* accounts for partial ignorance or lack of a complete knowledge about a characteristic. Parameter uncertainty quantifies the uncertainty resulting from the estimation of input parameters. This uncertainty may result from small sample sizes, sampling error (both random and systematic), or measurement error (IAEA, 1989; Morgan and Henrion, 1990).

Some investigators refer to variability as *Type A Uncertainty* and uncertainty as *Type B Uncertainty* (IAEA, 1989; Hoffman and Hammonds, 1994). It is useful to distinguish between variability and uncertainty because uncertainty may be reduced through additional measurement or study, while true biologic variability is irreducible.

In addition to variability and uncertainty, it is necessary to account for dependencies among input variables. Dependencies among input variables occur when two or more variables are correlated. For example, a relationship exists between body weight and food consumption.

In the past, NOS has relied on methods of exposure estimation that account for dependencies, yet fail to differentiate between variability and

uncertainty. Additional exposure estimation techniques distinguish between variability and uncertainty without considering dependencies. But under certain circumstances, it may be beneficial to simultaneously account for dependencies while distinguishing between variability and uncertainty. Thus, an innovative exposure estimation technique was developed.

2. **Perform an uncertainty analysis to rank contributions to the overall uncertainty from uncertainties in individual input variables. Include a sensitivity analysis to determine how changes in individual input variables influence the outcome.**

It is useful to determine those input variables that are most critical to a model's output. Uncertainty analysis techniques quantify the potential reduction in uncertainty from the acquisition of additional data for each input variable. Sensitivity analysis ranks the influence of fluctuations in the individual input values on the outcome. The most sensitive variables should be characterized by reliable data. The results obtained from the uncertainty and sensitivity analyses provide direction for future research efforts, such that maximum benefit may be obtained. Results from the uncertainty analysis may be used to direct the collection of additional data in order to reduce the greatest amount of uncertainty, while results from the sensitivity analyses may be used to identify variables that require an accurate characterization because they exert the most influence on the outcome.

3. Perform a detailed analysis of methylmercury exposure from the consumption of Northern lobster, *Homarus americanus*.

The techniques presented in tasks 1 and 2 above were used to predict methylmercury exposure from the consumption of Northern lobster. One of the missions of the National Ocean Service in Charleston is to conduct multi–disciplinary research activities related to environmental contaminants and their impact on public health and risk assessment; the exposure analyses proposed here assist in this charge.

4. Fit mercury concentration distributions for some of the most frequently consumed marine species. Perform simulations with these distributions to characterize methylmercury exposure from the consumption of multiple species.

Fish consumption advisories offer consumption guidelines that protect individuals from adverse toxic effects. Unfortunately, fish consumption advisories are often calculated under the assumption that individuals consume only a single species. Ignoring exposure to methylmercury from multiple species will cause the total risk to be underestimated, and this may lead to the overestimation of safe consumption quantities. It could cause individuals who consume multiple seafood species to be under–protected. To help remedy this problem, distributions of methylmercury concentrations were fitted for multiple species. As an example of potential benefits from these distributions, a

simulation was performed to characterize methylmercury exposure from the consumption of these most frequently consumed species.

Chapter 2

REVIEW OF THE LITERATURE

History

Mercury has been known to be toxic for a long time. The Chinese have known of the hazardous effects of mercury since 3000 B.C., and during the 18th and 19th centuries the deleterious effects of mercury were commonly observed in syphilis patients treated with mercurial ointments, mirror makers who used an amalgam of mercury and tine to silver mirrors, and hat makers who treated felt with mercuric nitrate (Rom, 1992; Waldron and Scott, 1994).

The first major mercury poisoning as a result of seafood consumption occurred in Minamata, Japan. Initially, many animals, e.g., cats, dogs, crows, waterfowl, and pigs, from the area were noted to have irregular behavior followed by death; an unusual number of dead fish were floating in the bay (Eisler, 1987). In 1953 human health effects such as paresthesia (tingling sensation in extremities), loss of hearing and vision, slurred speech, muscle weakness, personality changes (irritability and depression), memory loss, and sleeping difficulties were recorded (Officer and Ryther, 1981; ATSDR, 1993; EPA, 1997b). The most alarming effect was that some infants from mothers who consumed mercury contaminated seafood during pregnancy experienced varying degrees

of neuronal damage. For example, approximately 6% of the babies born in the Minamata region at this time had cerebral palsy, compared to 0.5% elsewhere (Eisler, 1987). The consequences also included 111 documented mercury poisonings by 1960, 41 deaths by 1965, and over 1,800 verified human mercury poisoning victims by 1982 from a regional population of 200,000 (Eisler, 1987). The total number of victims is difficult to establish and thus remains unconfirmed.

Not until 1968 did the Japanese government officially announce that mercury from industrial waste was the cause of the "Minamata Disease" (Officer and Ryther, 1981). Between 260 and 600 tons of mercury were discharged into Minamata Bay from 1932 to 1968 by an acetaldehyde plant, which used inorganic mercury (Eisler, 1987). The plant discontinued discharging mercury after 1971.

The second major mercury poisoning event occurred in Iraq from 1971–1972 (Lee, 1972; Rom, 1992; EPA, 1997b). A large quantity of grain was treated with an organo–mercurial fungicide to prevent fungal disease prior to germination. Although the grain was intended to be used as seed; hungry Iraqi citizens made bread with the toxic grain. Adverse consequences, particularly the developmental abnormalities, paralleled those observed in Minamata (ATSDR, 1993; EPA, 1997b). The poisoning eventually resulted in over 6,500 persons being hospitalized and more than 500 deaths primarily from central nervous system failure (Lee, 1972; ATSDR, 1993; Waldron and Scott, 1994; EPA, 1997b).

The Japanese and Iraqi poisonings spurred awareness of the toxic effects from mercury. In 1967 the Swedish Medical Board banned the sales of fish from approximately 40 rivers and lakes because of high mercury concentrations in fish (Lee, 1972). In 1969 the United States and Canada were informed of potentially dangerous mercury concentrations in fish when a zoology student at the University of Western Ontario notified authorities in Canada about mercury levels above 7 parts per million (ppm) in fish from Lake St. Clair and the St. Clair River, which connect Lake Huron and Lake Erie. By April 2, 1970 the United States Food and Drug Administration (FDA) set the mercury guideline for commercial seafood at 0.5 ppm.

Within six months of FDA's new guideline announcement, 33 states had reported mercury hazards and 16 states had some type of ban. A temporary ban followed in the tuna industry. Canned tuna, from supermarket shelves, was found to contain levels of mercury above the 0.5 ppm guideline, and once the Food and Drug Administration confirmed these findings, 12.5 million cans of tuna were removed from supermarket shelves (Jukes, 1975).

Early in 1971 FDA discovered that approximately 90% of the swordfish tested for mercury contained levels which exceeded 0.5 ppm, with most swordfish in the range 0.75–0.99 ppm (Officer and Ryther, 1981). This was one of the most destructive mercury contamination findings to the fish industry. From 1970 to 1971 U.S. swordfish landings toppled from 1.6 million pounds to just 23,000 pounds (Lipton, 1986).

Eight years later, in 1978, the U.S. Courts changed FDA's guideline from 0.5 ppm to 1 ppm after considering the evidence that the 1 ppm guideline would not result in a significant increase in adverse effects. The U.S. Courts also considered the fact that a large portion of the mercury in seafood comes from natural sources.

Characteristics of Mercury

Mercury is found in the environment primarily in three forms. Pure mercury is called *metallic* or *elemental mercury*. *Inorganic mercury* is mercury that has combined with elements such as chlorine or sulfur to form mercuric chloride or mercuric sulfide (cinnabar), respectively. Mercury also combines with carbon to form *organic mercury* compounds such as methylmercury. Mercury is naturally transformed from one form to another.

Mercury enters the environment in approximately equal amounts from both natural and anthropogenic sources (ATSDR, 1993). Natural sources of mercury include both terrestrial and oceanic volcanic activity, natural weathering of the earth's crust, and hot springs which commonly release cinnabar (Eisler, 1987; ATSDR, 1993). Anthropogenic sources of mercury have caused a significant change in the environmental distribution of mercury. The principal anthropogenic source of mercury is the emission from the combustion of coal or garbage (ATSDR, 1993; EPA, 1997b). Mercury is mined and used in industry to manufacture chlorine gas, sodium hydroxide, thermometers, barometers, batteries, and electrical switches (Lee, 1972; ATSDR, 1993; EPA, 1993, 1997b).

It is often used to control slime in the pulp and paper mill industry and to extract gold (Lee, 1972; ATSDR, 1993; EPA, 1993, 1997b). In the dental industry, mercury currently makes up about 50% of dental amalgams (ATSDR, 1993; Richardson and Allan, 1996). Agricultural uses were first introduced in the United States in the 1920s (Lee, 1972). In agriculture, numerous pesticides contain organic and inorganic mercury, while mercury containing fungicides prevent fungal diseases in plants, fruits, vegetables, and seeds prior to germination (Lee, 1972; ATSDR, 1993; EPA, 1997d). The use of mercury in fungicides has been banned since the 1970s (ATSDR, 1993).

Mercury research in the aquatic environment was very limited before 1970. Consequently by 1970, when rigorous research started, it was not possible to find the "natural" background level of mercury in water because agriculture and industry had been using mercury for approximately 20 years (Lee, 1972). Eisler (1987) proposes that concentration changes in oceanic waters have been insignificant.

Most of the mercury released into the hydrosphere is in the form of the inorganic salt or metallic mercury (Lee, 1972). Microorganisms in the hydrosphere convert inorganic and elemental mercury to methylmercury, and methylmercury is readily absorbed by aquatic organisms. Persistent chemicals, such as methylmercury, have a high potential for bioaccumulation. Older fish typically have higher levels because they have had more time to accumulate the chemicals. Methylmercury is bioaccumulated near the bottom of the aquatic food webs as small creatures eat plants and microorganisms that contain

methylmercury, and it is biomagnified up to 100,000 times the concentration in the water as trophic levels increase to the top predators in aquatic food webs (ATSDR, 1993). Thus, top predators usually have contaminant concentrations which exceed concentrations in other fish because predators store most of the methylmercury from the fish they consume.

Pharmacokinetics

Most lipophilic toxins accumulate in the fatty tissues of fish; in addition, methylmercury binds to protein, and thus it also accumulates in the edible portions of fish (Lee, 1972; EPA, 1994; Marsh *et al.*, 1995). This means that methylmercury, unlike other contaminants, cannot be removed simply by trimming off the fatty parts of fish (EPA, 1994).

Approximately 95% of methylmercury ingested from fish consumption is absorbed, although methylmercury has no known physiologic function in humans (Lee, 1972; WHO, 1990; ATSDR, 1993; EPA, 1996). After ingestion, methylmercury is absorbed through the gastrointestinal (GI) tract into the blood, and from the blood, it can affect all parts of the body. Methylmercury easily passes through the phospholipid bilayer because it is lipophilic. Due to the ability to penetrate all membranes and to bind to protein, methylmercury is essentially found in all human body tissues; however, the human body concentrates methylmercury in the brain, liver, and kidneys, with the highest concentration in the kidneys (Lee, 1972; ATSDR, 1993; EPA, 1994, 1996). Thus, methylmercury is the most toxic form of mercury to humans because it accumulates in the most

sensitive tissues (ATSDR, 1993). The distribution process takes between four to six days to complete in humans (EPA, 1996).

Once inside, most human tissues slowly transform organic mercury compounds, such as methylmercury, into inorganic mercury via the oxidation reduction cycle (ATSDR, 1993; EPA, 1994). The inorganic mercury can either be stored in the tissue or excreted in the urine or feces (ATSDR, 1993).

Methylmercury crosses the placental barrier with fetal organs often exhibiting higher concentrations than the corresponding maternal organs (ATSDR, 1993; EPA, 1994). In addition, methylmercury has been found in breast milk with a concentration of about five percent of that found in the mother's blood (McKinney, 1981; ATSDR, 1993; EPA, 1994).

Methylmercury has a half–life between 70–79 days in humans and between 500 and 1,000 days in many marine species, which contributes to the bioaccumulation problem in marine species (Lee, 1972; ATSDR, 1993; EPA, 1996). Inorganic mercury has a half life between 42–60 days in humans (ATSDR, 1993).

Ingested methylmercury is primarily eliminated in the feces (bile), although some is discharged during lactation (ATSDR, 1993; EPA, 1994, 1996). Essentially all mercury excreted in the feces is in the form of inorganic mercury, as methylmercury and elemental mercury are reabsorbed prior to excretion (ATSDR, 1993; EPA, 1996).

Acute Toxicity

Acute exposures to methylmercury are a concern because of the ability of fish to bioaccumulate methylmercury and the large sizes of some seafood meals (EPA, 1994). An acute exposure may be particularly harmful to susceptible populations like the developing fetus or infants (EPA, 1994). Clarkson (1997), a leading authority on methylmercury toxicity, reported that peak exposure, rather than chronic exposure, was the best determinant of deleterious effects. Acute high level exposures to methylmercury may result in detrimental effects such as renal damage or failure, gastrointestinal damage, cardiovascular collapse, shock, and death (EPA, 1994). The Agency for Toxic Substances and Disease Registry (ATSDR) reported 10 to 60 mg of methylmercury per kilogram of body weight as the acute lethal dose for individuals of all ages (ATSDR, 1993).

Chronic Toxicity

Studies of the Japanese and Iraqi poisonings have revealed that one of the most sensitive organs for methylmercury toxicity is the central nervous system (CNS). The human brain retains mercury longer than most other organs and can accumulate a mercury level four to five times higher than that found in the blood (McKinney, 1981). Common neuronal adverse effects include decreased performance on behavioral tests (e.g., the Denver Developmental Screen Test), personality changes (irritability, shyness, and nervousness), memory loss, insomnia, paresthesia, weakness, ataxia (loss of coordinated muscle movement), slurred speech, loss of speech, loss of vision, loss of

hearing, neuronal degeneration, tremors, paralysis, coma, and death (Lee, 1972; Eisler, 1987; Rom, 1992; ATSDR, 1993).

Another sensitive organ for methylmercury toxicity is the kidney, although the CNS is usually more sensitive than the kidney (ATSDR, 1993; EPA, 1994). Common adverse effects include renal damage and failure.

Developmental Toxicity

The Environmental Protection Agency (EPA) defines developmental toxicity as "adverse effects on the developing organism that may result from exposure prior to conception (either parent), during prenatal development, or postnatally to the time of sexual maturation" (1994, p. 5–12).

Methylmercury is a potent neurotoxicant for young children, especially the fetus, since the central nervous system is rapidly developing during this stage of life (ATSDR, 1993; EPA, 1994, 1997b). Some plausible reasons for the increased sensitivity of the CNS in the neonate are that methylmercury destroys microtubules, disturbs sulfhydryl enzyme systems, and reduces RNA in nerve cells of the dorsal root ganglia and cerebellum (McKinney, 1981; Marsh *et al.*, 1987; ATSDR, 1993; EPA, 1994). Cell division and migration are obstructed without microtubules; consequently, the development of the nervous system may results in abnormalities. This hypothesis is supported by autopsy data from Japanese and Iraqi children who were prenatally exposed to methylmercury. The children's autopsies revealed significant central nervous system abnormalities without regional specificity; adults exposed to methylmercury

poisonings exhibited a high degree of regional specificity in CNS abnormalities (EPA, 1994). Methylmercury particularly seems to disrupt microtubules in the developing cerebellum; consequently, the increased sensitivity of neonates compared to adults may be explained because mitosis and migration of granule cells in the cerebellum typically end shortly after birth (ATSDR, 1993).

Additional factors contribute to the increased sensitivity of neonates. Children seem to exhibit an increased absorption and longer retention of mercury (ATSDR, 1993). This phenomenon may be explained in the fetus because both the blood–brain barrier and the transport system within the blood–brain barrier are not fully mature (ATSDR, 1993). Additionally, enzyme detoxification systems are not entirely mature until two to three months after birth (ATSDR, 1990). The Environmental Protection Agency also advises that children may have an enhanced susceptibility because the human immune system is immature up to 12 years of age (ATSDR, 1990). Additionally, animal studies have shown that females and infants excrete mercury slower than males and adults, respectively (ATSDR, 1993; EPA, 1994). Although children typically consume less than adults, they often consume more per kilogram body weight than adults (EPA, 1994, 1997c). ATSDR (1993) indicates that children may be more sensitive to neurotoxic effects because a higher percentage of methylmercury is stored in the brains of young children than adults.

Typical neurologic signs from neonatal and childhood exposure to methylmercury include paresthesia, neuromuscular weakness, incoordination, inability to move, blindness, inability to speak, seizures, irritability, mental

retardation, delayed development, cerebral palsy, congenital malformation of the cerebellum, congenital malformation of the visual cortex, and death (Lee, 1972; Rom, 1992; ATSDR, 1993; EPA, 1994). ATSDR (1993) remarks that the prevailing central nervous system pathological feature from methylmercury poisoning is degeneration of the cerebellum. While some of the adult effects of methylmercury toxicity are reversible, most of the developmental effects are permanent structural changes in the brain (EPA, 1994).

Animals prenatally and lactationally exposed develop immunotoxicity, liver toxicity, kidney damage, and CNS effects similar to those detected in human infants (ATSDR, 1993).

Mutagenicity

ATSDR (1993) reports that methylmercury may have some mutagenic potential. Study results have been mixed, but methylmercury concentrations have been shown to be correlated with chromosome aberrations (ATSDR, 1993).

Carcinogenicity

EPA (1996) has classified methylmercury as a Class C carcinogen, indicating possible human carcinogenicity. This assignment is, however, based on insufficient data in humans and limited evidence in animals (EPA, 1996).

Special Susceptibilities

As described under the heading *Developmental Toxicity*, the fetus and infant have an increased risk of adverse neurological effects from methylmercury exposure (ATSDR, 1993).

It has also been suggested that the elderly, ill, malnourished (particularly those with insufficient levels of zinc, glutathione, antioxidants, or selenium), and individuals with impaired kidney, CNS, or liver function also have an elevated susceptibility to methylmercury toxicity (ATSDR, 1993).

Sport and subsistence fishers are at an increased risk, but not an increased susceptibility, due to unusually high consumption rates.

Interactive Effects

Selenium, which bioaccumulates in an atomic ratio of approximately one-to-one with methylmercury in seafood, may reduce the toxicity of methylmercury (Calabrese, 1981; McKinney, 1981; ATSDR, 1993; EPA, 1996). Selenium treatment was sometimes able to decrease common renal, neurologic, and fetal effects (Calabrese, 1981).

Epidemiological Studies

Marsh *et al.* (1987) provided the research that most influenced the current reference dose (RfD). The authors studied neurologic effects of the Iraqi poisoning on 81 mother–child pairs. Methylmercury exposure was estimated from maternal hair samples. The neurologic effects that were considered included delayed onset of walking (after 18 months), delayed onset of talking

(after 24 months), mental symptoms, seizures, cranial nerve signs, involuntary movement, as well as impairment in limb tone strength, deep tendon reflexes, plantar responses, coordination, dexterity, primitive reflexes, sensation, and posture. Delayed walking, delayed talking, cerebral palsy, altered muscle tone, and altered deep tendon reflexes were detected in children exposed *in utero*. The neurologic signs detected in the mothers included paresthesia, ataxia, reduced visual fields, and hearing impairments. The significant problem with using this study to justify the RfD is that extremely high levels of methylmercury were consumed in a relatively short period of time, and fish consumers typically have long–term rather than short–term exposure. In addition, these women were exposed to methylmercury from grain consumption, not fish consumption.

Lipfert *et al.* (1996) investigated the probability of neurological effects from consuming fish with high methylmercury levels. The two neurological effects they studied were adult paresthesia and congenital neurological effects. The study assumed a daily consumption rate of 24.7 g/day, which consisted of 4.5 g/day canned tuna, 10.3 g/day freshwater finfish, and 9.9 g/day other marine seafood. A Monte Carlo simulation was performed to estimate exposure levels. The results showed that adults were more than ten times below the level of exposure that caused adult paresthesia in the Iraqi poisoning. However, the results for congenital neurological effects were just under the levels which caused similar effects in Iraq, consequently the authors advised that pregnant women should avoid frequent consumption of predatory freshwater sportfish.

Cree Indian infants from northern Quebec were studied by McKeown–Eyssen *et al.* (1983) because Cree Indians typically consume large amounts of seafood. The authors studied 247 children for abnormalities that would be consistent with methylmercury exposure. The most common abnormalities were altered deep tendon reflexes and altered muscle tone. It was noted that each additional 10 μg of fetal methylmercury exposure per gram of fetal weight resulted in a sevenfold increase in the prevalence of muscle tone or reflex abnormalities. The principal weakness of this study was the failure to account for the confounding factors of maternal smoking and alcoholism.

Studies of fetal exposure to methylmercury also were performed in New Zealand in the late 1980s by Kjellstrom, Kennedy, Wallis, and Mantell (EPA, 1996, 1997d). Approximately 11,000 mothers were surveyed to find consumption patterns and demographic data. The survey produced 31 high seafood consuming mothers that were matched with low seafood consuming mothers by ethnic group, maternal age, child's birthplace, and child's birth date. Exposure was then estimated using maternal hair samples. Children were studied at age four using the Denver Developmental Screen Test (DDST), which identifies abnormalities in gross motor skills, fine motor skills, language skills, and personal–social skills. Each area was scored as normal, questionable, or abnormal. The high exposure group resulted in 2 abnormal and 14 questionable scores, while the low exposure group had 1 abnormal and 4 questionable scores. The fine motor and language skills were the most common developmental delays. Standard vision and sensory tests revealed delayed

development in 52% of the children from the high consumption group and only 17% from the control group. It is interesting to note that children from the high consumption mothers were more likely to be born prematurely (before 37 weeks) and to have low birth weights (< 2,500 g). The results of this study were limited due to the presence of confounding variables and a low participation rate of 44%.

The New Zealand study was followed up two years later when the children were age six (EPA, 1996, 1997d). Sixty–one children from high consumption mothers were compared to three control groups. Mothers from each control group had both fish consumption rates and mercury hair levels less than mothers from the study group. Confounding was controlled by using linear multiple regression and by matching children from high consumption mothers to three controls by maternal age, smoking status, ethnic group, place of residence, and the child's gender. The children were tested using various academic, psychological, and behavioral tests. Average maternal mercury hair levels of 13–15 mg/kg during gestation were associated with decreased test scores, but the small sample size limited the power to identify differences among the lower exposure groups. EPA (1996) feels that this study did not use the most appropriate tests for detecting methylmercury effects.

Recently a study was carried out in the Republic of the Seychelles (Davidson *et al.*, 1995, 1998; Marsh *et al.*, 1995; Myers *et al.*, 1995; Shamlaye *et al.*, 1995). This particular population was selected because a diet with a median of 12 fish meals per week during pregnancy results in high exposure levels. In

addition, potential confounding factors such as extreme alcohol consumption, high infant mortality rates, and small population sizes are not a problem with the Seychellois. Methylmercury exposure during gestation was estimated using maternal hair samples for 740 mother–infant pairs. Children were examined periodically from 6 ½ months through 66 months using a neurologic examination, a revised DDST, the Fagan test of visual recognition memory, and the Bayley Scales of Infant Development for both mental and psychomotor development. No association between fetal methylmercury exposure and neurodevelopment through 66 months of age was identified.

In the Faroe Islands, Grandjean *et al.* (1992, 1995, 1997) examined the potential effects of fetal and infant methylmercury exposure. The confounding effect from alcohol consumption was not a problem as Faroese women typically do not consume alcohol during pregnancy. The primary source of methylmercury exposure for the Faroese is from eating pilot whale meat. Fetal methylmercury exposure was estimated using maternal hair samples and cord blood samples taken at birth, while infant methylmercury exposure was estimated using hair samples from the child taken at both twelve months and seven years of age. Over 900 infants born between 1986 and 1987 were examined at age seven using a battery of physical exams, neurophysiological tests, and neuropsychological tests. Grandjean *et al.* found some association between increased mercury exposure and a decreased performance in language skills, even at levels of exposure currently considered safe. It was reported that doubling mercury exposure could potentially cause a two month delay in several

developmental areas. This study had some likely sources of bias: the exposure was primarily from the consumption of pilot whale meat which has high levels of other contaminants such as PCBs that produce effects similar to mercury; the reported associations were weak and possibly statistically significant only because of the large sample size; and the authors made no multiple comparison correction to account for the numerous test that were performed.

Summary of Risk Values

Table 2–1 presents different risk values. Risk assessors and risk managers may use any of these risk values in risk assessments and the decision making process, albeit in the U.S. the Environmental Protection Agency's reference dose (RfD) is typically selected among these values.

EPA's Reference Dose (RfD)	0.1 µg/kg/day for populations including women of childbearing potential and young children
FDA's Acceptable Daily Intake (ADI)	0.47 µg/kg/day for the average adult
ATSDR's Minimal Risk Level (MRL)	0.5 µg/kg/day for populations including women of childbearing potential and young children
WHO/IPCS's Value	0.47 µg/kg/day for adults

Table 2–1. Summary of Risk Values

The reference dose estimates the daily exposure that protects even the most sensitive subgroup from harmful effects over a lifetime. EPA recommends an oral RfD of 0.1 µg of methylmercury per kilogram of body weight per day for the ingestion of methylmercury (EPA, 1996). The RfD for methylmercury is

based on developmental neurologic abnormalities primarily from the Iraqi poisoning (EPA, 1994; EPA, 1996; EPA, 1997b). Neurologic abnormalities in adults were also considered, but developmental endpoints were more sensitive (EPA, 1996). This finding is verified by epidemiological data from the Minamata poisoning showing healthy females who gave birth to brain damaged children (ATSDR, 1993; Lee, 1972). An uncertainty factor of ten was applied to the RfD for the use of a lowest–observable–adverse–effect level (LOAEL). This uncertainty factor is more conservative that the uncertainty factor used just a few years ago, and the use of this more conservative uncertainty factor resulted in the reduction of the RfD from 0.3 to 0.1 μg/kg/d.

It is interesting that EPA's Reference Dose is approximately five times more conservative than the other daily intake recommendations in Table 2–1, since some of the other risk values are also intended to protect the most sensitive subgroups of the population.

The Food and Drug Administration has offered an Acceptable Daily Intake (ADI) of 0.47 μg of methylmercury per kilogram of body weight per day. The ADI is approximately five times greater than the RfD in part because the ADI is only designed to protect the average adult (excluding the fetus and infants), while the reference dose is designed to protect even the most sensitive subgroups (including the fetus). Studies suggest that the fetus is up to five times more sensitive than adults to methylmercury toxicity (Marsh *et al.*, 1987; EPA, 1994).

ATSDR's Minimal Risk Level (MRL) estimates the daily exposure that is likely to be without an appreciable risk of deleterious noncancerous effects for a chronic duration of exposure, one year or longer. ATSDR (1998) recommends an MRL of 0.5 μg of methylmercury per kilogram of body weight per day for chronic oral exposures to methylmercury. The MRL for methylmercury is based on developmental delays observed in Seychellois children (Davidson *et al.*, 1995; Marsh *et al.*, 1995; Myers *et al.*, 1995; Shamlaye *et al.*, 1995). Even though ATSDR did not characterize any of the reported decreases in children's activity levels at 29 months of age as adverse, the midpoint of all hair levels, rather than the maximum level, was used for the no–observable–adverse–effect level (NOAEL) because activity levels appeared to decrease with increasing mercury hair concentrations in boys above the overall median value (ATSDR, 1998). No uncertainty factor was applied to the MRL.

The MRL is approximately equal to the ADI, despite the fact that the two values are designed for different populations. The MRL is intended to protect sensitive subgroups such as the fetus, while the ADI is calculated to protect the average adult.

WHO/IPCS calculated a daily methylmercury intake of 0.47 μg of methylmercury per kilogram of body weight per day (EPA, 1997b). WHO/IPCS's recommendation is almost identical to FDA's Acceptable Daily Intake, as both are designed to protect adults from adverse effects.

Chapter 3

METHODS

Exposure Equations

Using risk assessment and risk management to set fish consumption advisories is a very difficult process due to all of the factors which must be considered. It should be noted that throughout this section the term fish is used to denote both fish and shellfish. Fish consumption may pose health risks which need to be weighed properly against the benefits; economic and social impacts also weigh heavily on the decision making process (EPA, 1994). Different state governments and federal agencies use numerous methods to calculate the risk to human health from seafood consumption (EPA, 1994).

EPA (1994) estimates the exposure to a contaminant from seafood consumption using the following equation:

$$E_m = \frac{C_m \cdot CR}{BW} \qquad (3.1)$$

where:

E_m = Exposure to contaminant m from fish consumption (μg/kg/day),

C_m = Concentration of contaminant m in a given species of fish (μg/g),

CR = Consumer consumption rate of a given species of fish (g/day), and,

BW = Consumer body weight (kg).

Equation (3.1) is useful for calculations involving a single species, yet the equation needs to be modified as follows to account for multiple species:

$$E_m = \frac{\left(\frac{\sum_{j=1}^{n} (C_{mj} \cdot CR_j)}{\sum_{j=1}^{n} CR_j} \right) \left(\sum_{j=1}^{n} CR_j \right)}{BW} = \frac{\sum_{j=1}^{n} (C_{mj} \cdot CR_j)}{BW} \qquad \textbf{(3.2)}$$

where:

E_m = Exposure to contaminant m from fish consumption (μg/kg/day),

C_{mj} = Concentration of contaminant m in species j (μg/g),

CR_j = Consumer consumption rate of species j (g/day), and,

BW = Consumer body weight (kg).

Uncertainty Analysis

An evaluation of uncertainty is necessary, yet frequently ignored (Morgan and Henrion, 1990; EPA, 1992, 1994; Hoffman and Hammonds, 1994; Carrington and Bolger, 1998). An uncertainty analysis ranks the contributions to overall uncertainty from uncertainties in the input variables. It is especially important to consider uncertainty under the following circumstances: when deciding where future research efforts will result in the maximum benefit, when expert judgement is used due to a lack of data, or when uncertain information from multiple sources must be merged (Morgan and Henrion, 1990; EPA, 1997a).

Uncertainty analysis may lead to a reduction in the scope of the analysis by identifying the variables of concern. This may assist in determining where to focus future efforts and money (McKone and Bogen, 1991; EPA, 1992, 1994).

Sensitivity is the simplest type of uncertainty analysis (IAEA, 1989; Morgan and Henrion, 1990; EPA, 1997a). A sensitivity analysis determines how changes in individual input variables influence the outcome. Thus, the sensitivity analysis identifies the main contributors to the variation and uncertainty in the outcome. The most elementary measure of sensitivity is formed by noting how the output changes when a single input variable is changed from the minimum value to the maximum value while holding all other input variables constant at their nominal values (IAEA, 1989; Morgan and Henrion, 1990; EPA, 1992). The nominal value is the "best guess" for an input variable. Frequently the mean, median, or mode is used as the nominal value. Similarly, another common sensitivity measure is formed by noting how the output changes when a single input variable is varied a certain percentage while holding all other input variables constant at their nominal values (Morgan and Henrion, 1990; Thompson *et al.*, 1992; Finley and Paustenbach, 1994). The relationship between uncertainty and sensitivity is displayed in Figure 3–1.

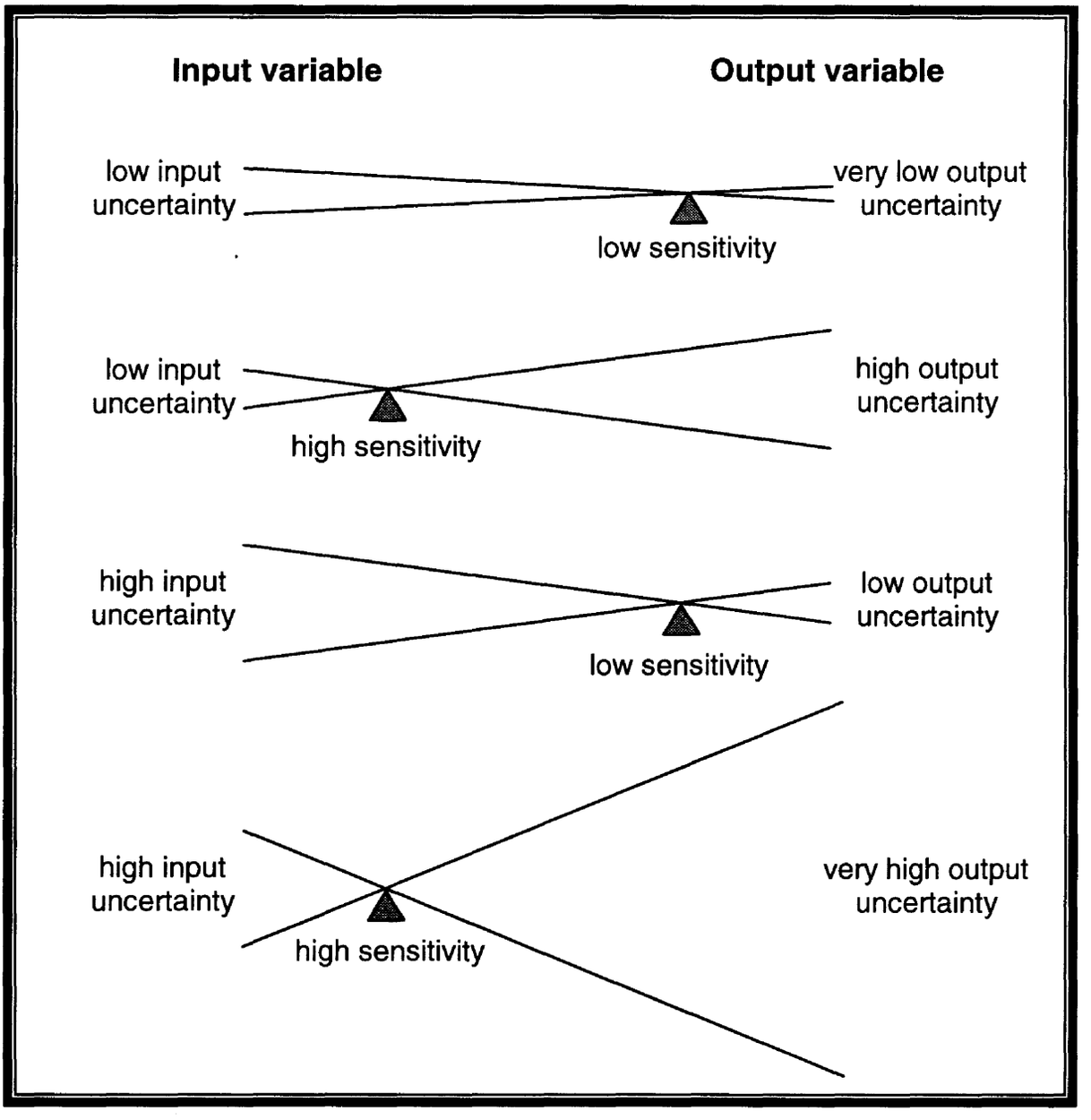

Figure 3–1. A Simple Illustration of the Relationship Between Uncertainty and Sensitivity

These approaches are most useful as screening techniques to determine those input variables that have the greatest effect on the outcome (IAEA, 1989; Morgan and Henrion, 1990; EPA, 1992). In fact, in many cases a small number of input variables account for the bulk of the variation in the output (Morgan and Henrion, 1990; Iman and Helton, 1991). Non–sensitive input variables can be considered as constants in the modeling equation; less–sensitive input variables may be estimated from less precise data, while highly–sensitive input variables require the most precise and reliable data (Morgan and Henrion, 1990; Finley

and Paustenbach, 1994; EPA, 1997a). Thus, confidence in the results would be high if the most sensitive input variables are characterized by dependable data and low if the most sensitive input variables are based on limited or uncertain data.

Unfortunately these two sensitivity measures do not consider dependencies between input variables. These techniques are also somewhere between a local and a global approach. Where a *local* approach evaluates the response of the function only in the proximity of the nominal scenario, a *global* approach makes use of the entire input and output data sets.

More sophisticated methods of ranking uncertainty use a truly global approach. Global techniques may be applied to determine the contribution to overall uncertainty from individual input variables.

The simplest global method to rank contributions to overall uncertainty is to compute the sample (Pearson's) correlation coefficient between each input variable and the outcome (IAEA, 1989; Morgan and Henrion, 1990; Iman and Helton, 1991; EPA, 1997a). The sample correlation coefficient (r) measures the degree of linear relationship between two variables; thus r provides a meaningful measure of the degree to which an input variable and the output variable change together. If the absolute value of the correlation coefficient for an input variable and the output variable is high (close to one), then the uncertainty and variability for this input variable have a significant impact on the outcome variable. Unfortunately the correlation coefficient only considers the linear relationship between two variables, without considering effects from other variables. For

example, two highly correlated input variables could both have similar sample correlation coefficients with the output, even though only one of the two input variables is primarily responsible for the uncertainty.

The partial correlation coefficient measures the degree of linear relationship between the output and an input variable that cannot be explained by linear relationships between the remaining input variables (Iman and Helton, 1988, 1991; IAEA, 1989; Morgan and Henrion, 1990; EPA, 1997a). Thus, the partial correlation coefficient determines the portion of the output uncertainty that is *uniquely* accounted for by uncertainty from a single input variable. Both the correlation coefficient and partial correlation coefficient measure linear relationships; if the relationship is not linear then these methods will underestimate the predictability of the output from an input variable.

Spearman's rank–order correlation coefficient measures any monotonic, rather than just linear, relationship (Iman and Helton, 1988, 1991; IAEA, 1989; Morgan and Henrion, 1990; Sargent and Wainwright, 1996; EPA, 1997a). Spearman's rank–order correlation coefficient is basically Pearson's correlation coefficient calculated using rankings of values rather than the actual values. Rank values are determined for the variable of interest by ordering the data from lowest to highest and replacing the lowest value with a rank of 1, the second lowest with a rank of 2, and so on. This process is repeated for the values of each variable where a correlation is desired.

Benefits analogous to those obtained from using the partial correlation coefficient rather than Pearson's correlation coefficient lead to using the partial

rank–order correlation coefficient rather than Spearman's rank–order correlation coefficient (IAEA, 1989; Iman and Helton, 1988, 1991). The partial rank–order correlation coefficient is basically the partial correlation coefficient calculated using rank values rather than actual values.

These approaches characterize the uncertainty associated with linear or non–linear, monotonic relationships quite well, yet one caveat is the failure to deal with non–monotonic relationships. Uncertainty analyses where relationships are non–monotonic may be inaccurate and should be regarded with suspicion.

Methods of Exposure Estimation

Exposure is defined as contact between a contaminant and one or more outer boundaries (e.g., mouth nose, skin) of an individual (EPA, 1992). Several methods are available to estimate exposure. The ideal situation is to use as simple a method as possible without oversimplifying the problem, as significant components of the problem may be neglected.

Point estimation is the simplest method used to estimate exposure. The point estimate is calculated by assigning a single value (e.g., the mean, 95th percentile, or maximum value) to each input variable (IAEA, 1989; Morgan and Henrion, 1990; McKone and Bogen, 1991; Ryan, 1991). Many researchers use the mean or median values of the input variables to produce a central estimate for the output. The upper percentiles such as the 95th percentile or the

theoretical maximum are frequently used as input values to obtain an upper estimate of the output.

Point estimation is useful as a screening technique (IAEA, 1989; Morgan and Henrion, 1990; Finley and Paustenbach, 1994). Potentially important sources of exposure may be identified by choosing conservative values to overpredict exposure. Maximum values or 95th percentiles are frequently used as inputs values; if the maximum values or 95th percentiles reveal no appreciable risk of deleterious effects, then more sophisticated methods of estimation would waste both time and money (Hattis and Burmaster, 1994; EPA, 1997a). More advanced techniques are also unnecessary when the cost of remediation is low (Hattis and Burmaster, 1994; EPA, 1997a).

The primary weakness of point estimation is that no information is provided as to where the estimate lies on the output distribution. The mean or median values do not necessarily produce good estimates of central tendency; likewise the 95th percentiles or maximum values often greatly overestimate the upper percentiles of the output variable (Burmaster and von Stackelberg, 1991; EPA, 1992; Thompson *et al.*, 1992; Finley and Paustenbach, 1994; Hattis and Burmaster, 1994; Keenan *et al.*, 1994; Cohen *et al.*, 1996; Thompson and Graham, 1996).

It is becoming evident that risk assessment techniques need to evolve from point estimates to probabilistic methods (Burmaster and von Stackelberg, 1991; EPA, 1992, 1997a; Finley and Paustenbach, 1994; Keenan *et al.*, 1994; Thompson and Graham, 1996). Unlike point estimation, probabilistic methods

account for variability by characterizing each input variable as a probability density function (PDF) or cumulative distribution function (CDF). These techniques yield a PDF or CDF for the output variable. The output probability distribution supplies a complete picture of potential outcomes. This is a tremendous elaboration on the point estimation method because the probability density function shows the relative likelihood of occurrence for each outcome value or even ranges of outcome values. Probabilistic methods may be advantageous when conservative point estimates reveal a potential problem, when an uncertainty analysis is necessary, or when remediation is expensive (Finley and Paustenbach, 1994; EPA, 1997a).

One of the principal probabilistic methods is called *Monte Carlo* simulation. The technique was developed in 1946 by Stanislaw Ulam, who first applied the method to assist the U.S. government with the development of the hydrogen bomb (Rugen and Callahan, 1996). Monte Carlo methods are used to simulate output distributions based on input distributions (Sargent and Wainwright, 1996; Palisade Corporation, 1997a). Using commercial software, e.g., Crystal Ball (Decisioneering, Inc., Denver, CO), @Risk (Palisade Corporation, Newfield, NY), or Analytica (Decisioneering, Inc., Denver, CO), a value is randomly selected from each of the input distributions, which provides a single estimate of the output (Metzger *et al.*, 1998). This constitutes a single iteration. Iterations are run in large batches, typically with 1,000 iterations per batch. By convention, a sufficient number of iterations is achieved when the upper percentiles of the distribution do not change significantly (e.g., <3%) from

one batch to the next (Palisade Corporation, 1997a). After a sufficient number of iterations, typically between 1,000 to 15,000, all of the output estimates form the output distribution. This method of simulation is here referred to as *traditional Monte Carlo* or *Monte Carlo* simulation. An illustration of the procedure is given in Figure 3–2.

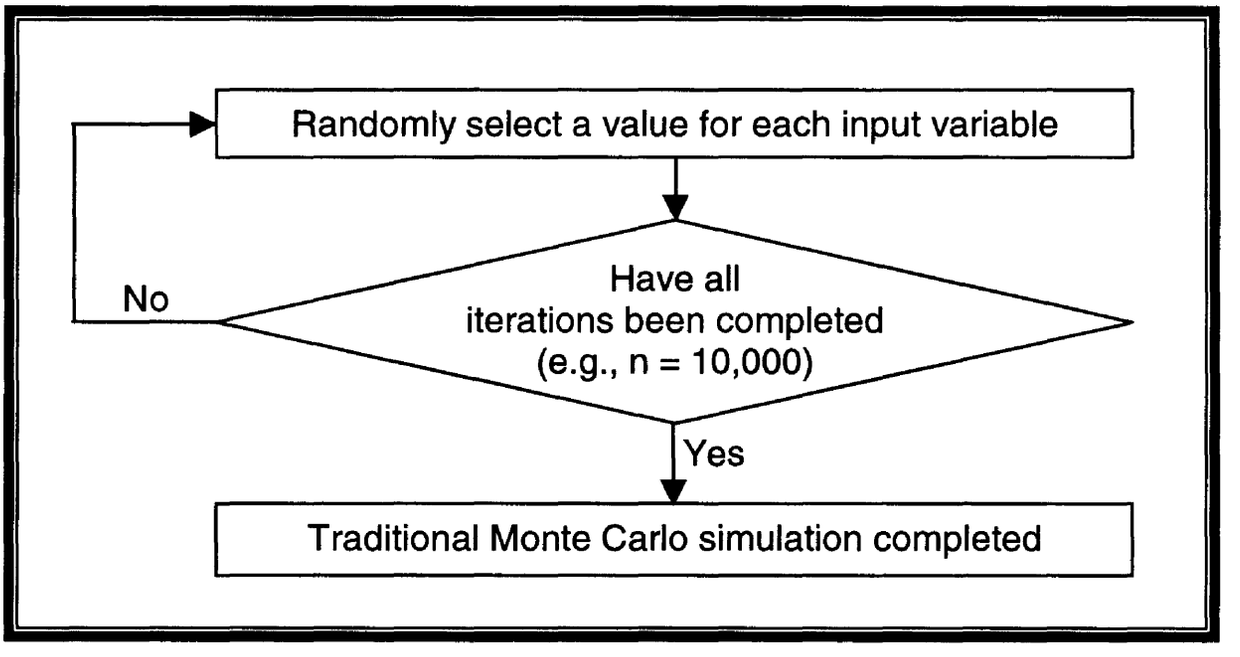

Figure 3–2. Traditional Monte Carlo Simulation Procedure

Models involving input variables that have either variability or uncertainty, but not both, are appropriate for traditional Monte Carlo simulations. The traditional Monte Carlo has also been shown to be the appropriate method for modeling averages of the output (Frey and Rhodes, 1996). Under these conditions, results from the traditional analysis and from more sophisticated methods that account for both variability and uncertainty are similar; thus the extra effort required to distinguish variability and uncertainty is essentially wasted under these circumstances. This is because the variability in an average is less than the variability in individual measurements. Thus, variability is so small

compared to uncertainty that the input distribution essentially reduces to one involving only uncertainty.

Traditional Monte Carlo simulations are typically less sensitive than point estimates to changes in a single input value; consequently, errors in input values for point estimates generally result in greater changes to the output than errors in input distributions for Monte Carlo simulations.

The traditional Monte Carlo method does require more time and resources than point estimation. Another deficiency is the independent selection of input values, as dependencies exist among input variables in most models.

Many researchers recognize the need to account for dependencies among input variables (IAEA, 1989; Morgan and Henrion, 1990; Smith *et al.*, 1992; Burmaster and Anderson, 1994; Bukowski *et al.*, 1995; Frey and Rhodes, 1996; EPA, 1997a). Several Monte Carlo simulation software products currently employ techniques for assigning correlation between input variables by using rank–order correlation (Morgan and Henrion, 1990). The random values for the input variables will approximately have the desired correlation. An estimated correlation between input variables is required prior to running the simulation.

A more exact approach of resolving this problem uses hierarchical simulations. Hierarchical Monte Carlo simulations are similar to traditional Monte Carlo simulations, except that *hierarchical simulations* account for dependencies among input variables by selecting input values in a sequential fashion (Voit *et al.*, 1993, 1995; Finley and Paustenbach, 1994; Balthis *et al.*, 1996; Balthis, 1998).

To execute a hierarchical Monte Carlo simulation, dependent distributions are assigned to input variables. For example, human body weight and human seafood consumption are both dependent on age; thus age–specific distributions for body weight and consumption are developed. For each iteration of the example above, an age would first be randomly selected, then random values from the corresponding age–specific distributions for body weight and consumption would be selected. This eliminates potential problems such as selecting an individual with a low body weight and a high consumption rate. The hierarchical Monte Carlo steps are displayed in Figure 3–3.

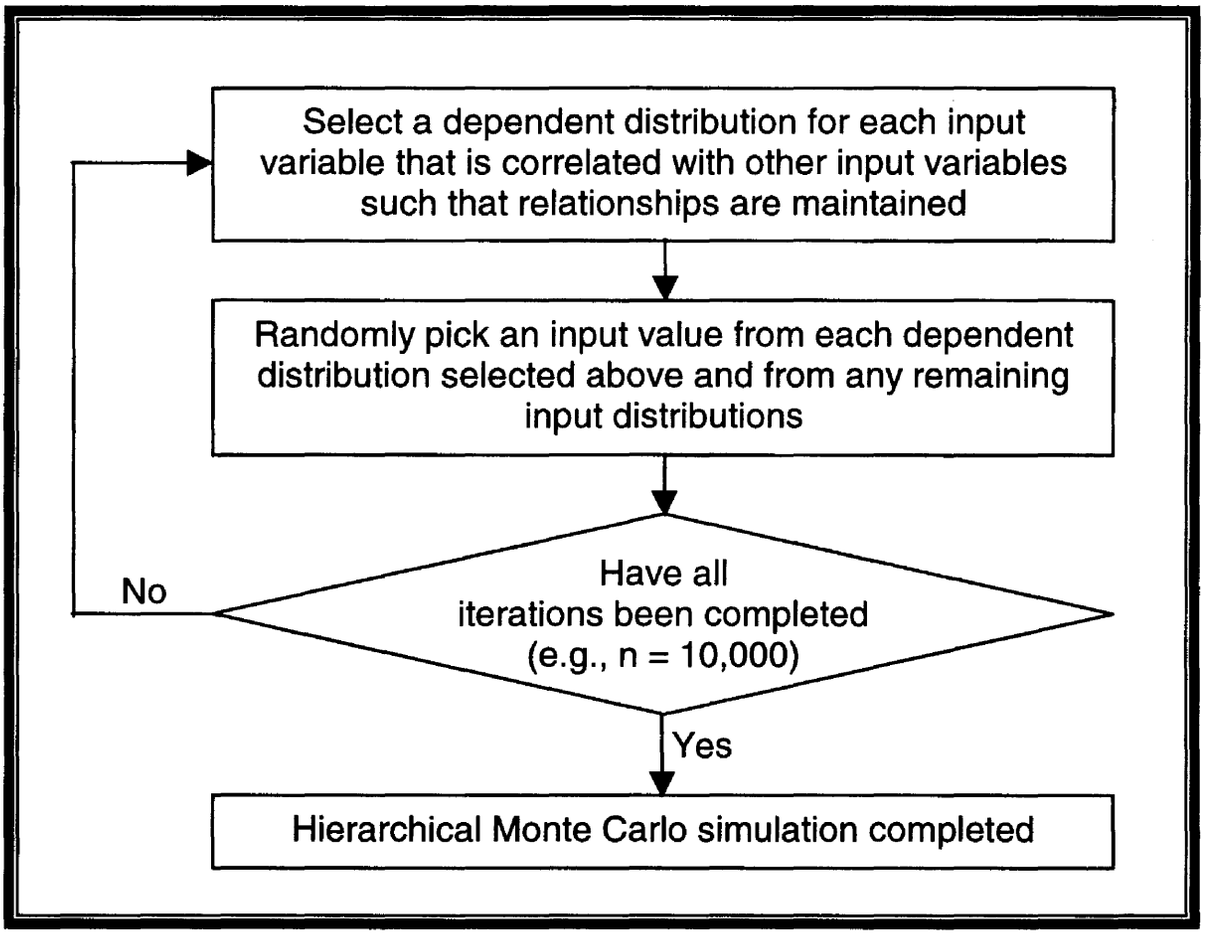

Figure 3–3. Hierarchical Monte Carlo Simulation Procedure

In the same way that the traditional Monte Carlo simulation is generally better than point estimates for showing the true probability of risk, a hierarchical

Monte Carlo simulation typically characterizes risk more accurately than a traditional Monte Carlo simulation.

Hierarchical methods are particularly appropriate when dependencies among input variables are strong and/or non–linear.

Unfortunately hierarchical Monte Carlo methods require considerably more data points than traditional Monte Carlo methods because several dependent distributions, rather than just a single distribution, must be modeled for each input variable. Hierarchical Monte Carlo techniques also fail to distinguish between variability and uncertainty.

It is becoming apparent that variability and uncertainty need to be differentiated, and Monte Carlo simulations are a suitable statistical tool for this purpose (IAEA, 1989; Morgan and Henrion, 1990; Burmaster and Anderson, 1994; Hoffman and Hammonds, 1994; McKone, 1994; Rowe, 1994; Bogen, 1995; Bukowski *et al.*, 1995; Cronin *et al.*, 1995; EPA, 1997a; Murphy, 1998; Werckman and Wainwright, 1998). Techniques called *two–dimensional Monte Carlo* (2DMC) are currently emerging that account for both variability and uncertainty (Hoffman and Hammonds, 1994; MacIntosh *et al.*, 1994; Burmaster and Wilson, 1996; Cohen *et al.*, 1996; Frey and Rhodes, 1996; Price *et al.*, 1996; Murphy, 1998; Werckman and Wainwright, 1998). The original two–dimensional technique was developed by Frey in 1992 as a tool for environmental policy decisions (Cohen *et al.*, 1996; Frey and Rhodes, 1996).

Since this time, two–dimensional simulations have been used to study cancer risks, exposure, emission characterization, and effects of remediation

(MacIntosh *et al.*, 1994; Bogen, 1995; Cohen *et al.*, 1996; Frey and Rhodes, 1996; Price *et al.*, 1996).

Input variables with only variability or uncertainty are simply characterized by PDFs similar to input variables in traditional Monte Carlo simulations, while input variables with both variability and uncertainty are represented as "distributions of distributions". The variability is characterized by depicting input variables using PDFs, while certain PDF parameters are also assigned PDFs to account for uncertainty.

The sampling scheme is now two–dimensional. First, an *outer loop* is run to select the uncertainty values (PDF parameters). Next, the uncertainty values, or PDF parameters, are now frozen while an *inner loop* is run to account for variability. Thus, the inner loop consists of running several iterations of the whole model using the selected PDF parameters. The whole process is repeated for a specified number of outer iterations in order to provide a portrait of how uncertainty varies the output distribution, where each set of PDF parameters represents uncertainty. Typically an inner loop has between 1,000 and 15,000 iterations, while an outer loop has between 50 and 2,500 iterations. The two–dimensional simulation scheme is presented in Figure 3–4.

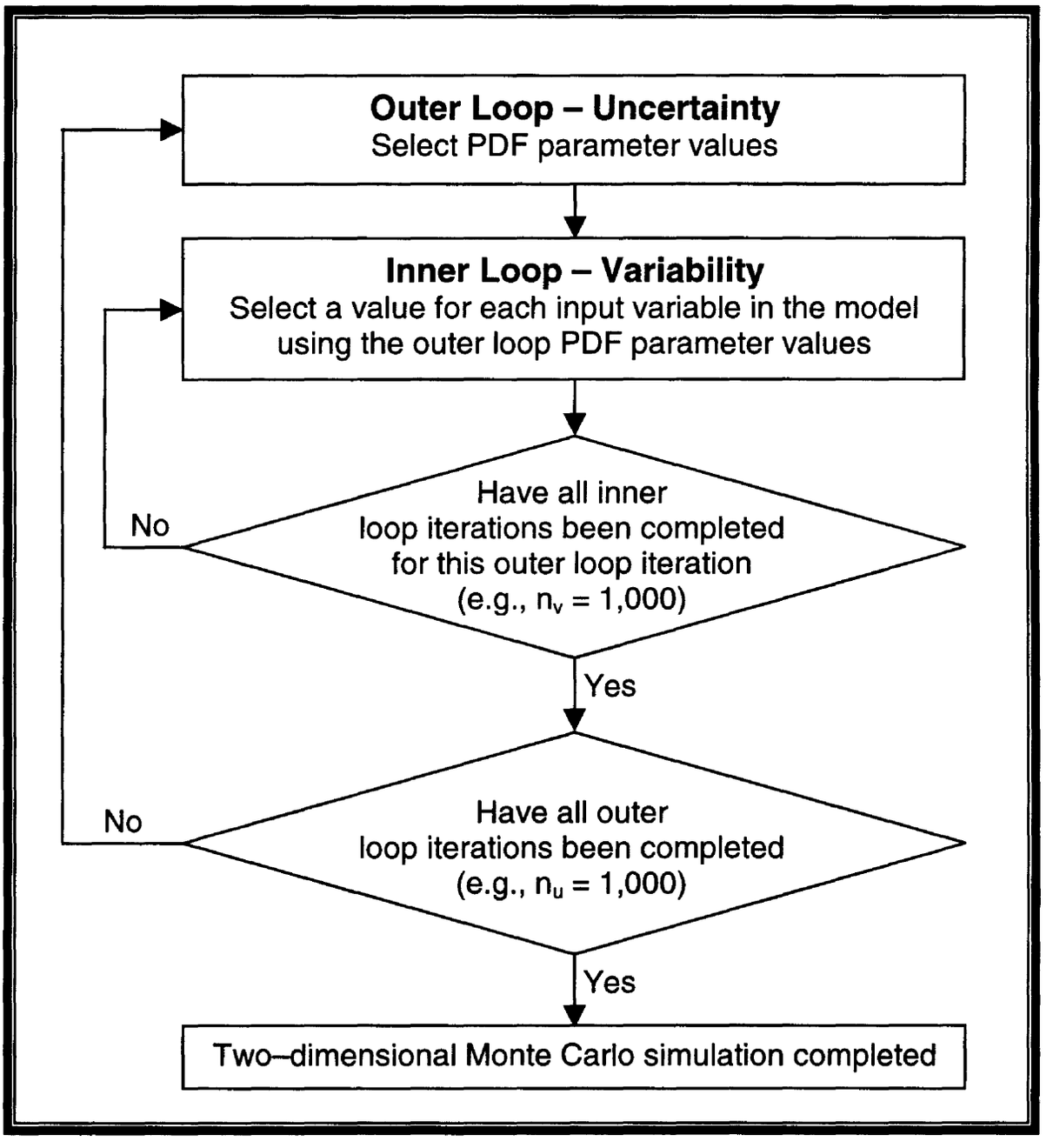

Figure 3–4. Two–Dimensional Monte Carlo Simulation Procedure

In the literature, variables with only variability or uncertainty are referred to as first–order random variables, while variables with both variability and uncertainty are referred to as second–order random variables.

Two–dimensional Monte Carlo simulations are appropriate in the following situations: when input variables exhibit both variability and uncertainty, when future research efforts must be determined in order to reduce the maximum amount of uncertainty, or when risk managers desire that uncertainty be

addressed in the risk assessment (EPA, 1992; Haimes *et al.*, 1994; MacIntosh *et al.*, 1994). Monte Carlo guidelines from EPA (1997a) suggest that an analysis of uncertainty and variability is only necessary if the differentiation could improve the results, if time and recourses are available for a complex analysis, or if the project warrants this level of effort.

Neither hierarchical nor two–dimensional Monte Carlo simulations account for dependencies among input variables while distinguishing between variability and uncertainty. A new approach called the *hierarchical two–dimensional Monte Carlo* accounts for dependencies among input variables and separates the effects from variability and uncertainty.

As with hierarchical simulations, it is first necessary to model dependent distributions for the input variables in hierarchical two–dimensional simulations. Next, an *outer loop* is run to select the uncertainty values (PDF parameters), and then the uncertainty values are frozen while an *inner loop* is run to account for variability. The initial step of each inner loop iteration is to select dependent distributions for the input variables. A specified number of inner loop iterations is performed, and then the whole process is repeated until a specified number of outer loop iterations have been completed. The outer loop values are used to characterize how uncertainty varies the output distribution. The hierarchical two–dimensional simulation steps are displayed in Figure 3–5.

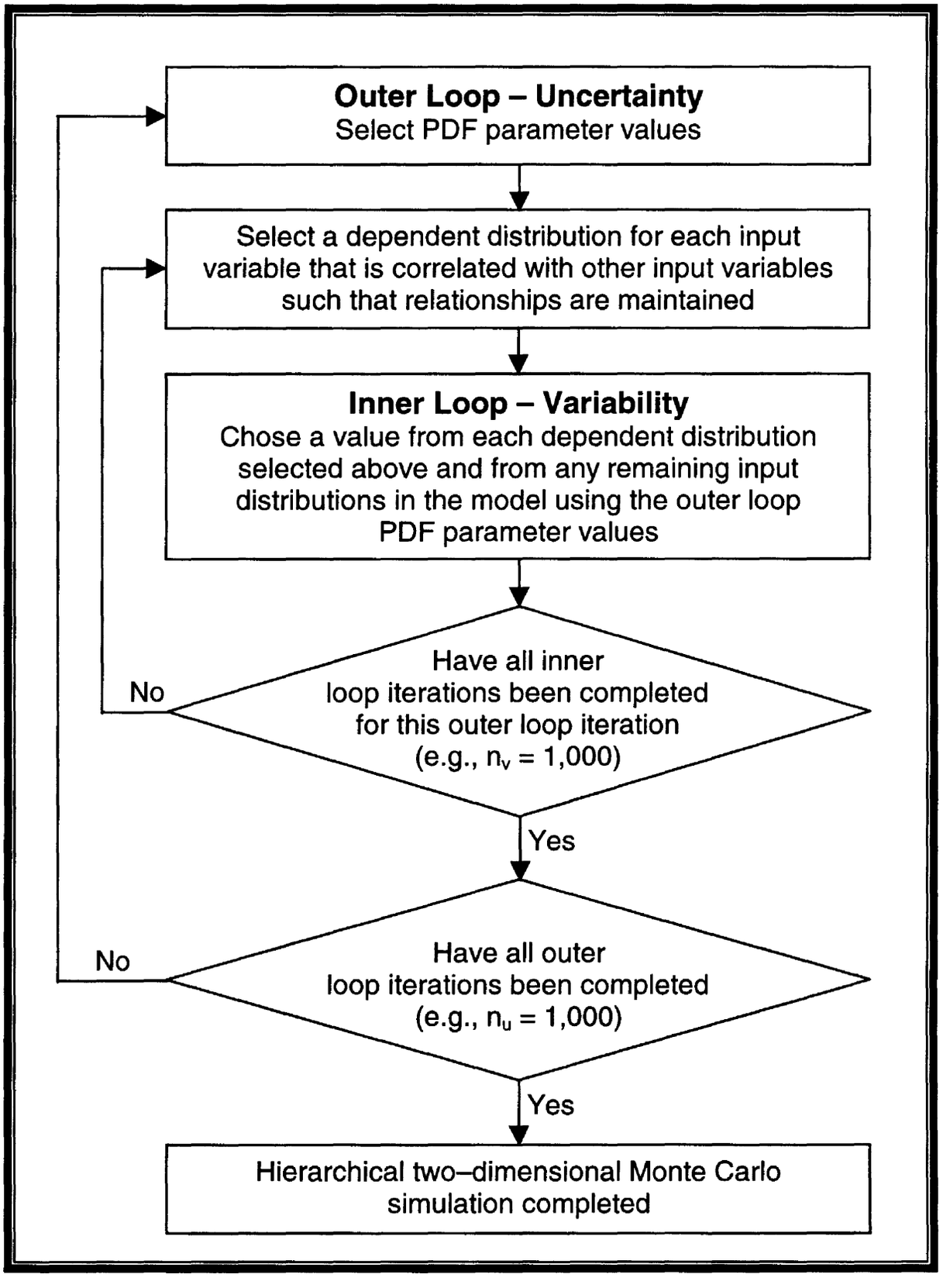

Figure 3–5. Hierarchical Two–Dimensional Monte Carlo Simulation Procedure

Probabilistic methods other than Monte Carlo simulations may be used to account for uncertainty while estimating exposure. Fuzzy number theory and Bayesian procedures are two alternate methods. Fuzzy number theory is

principally used with data that rely on opinion or interpretation (Yager, 1982; Morgan and Henrion, 1990; Burmaster and Wilson, 1996). For example, if individuals were asked to recall the number of seafood servings they had consumed in the last year, then the answers obtained would be "fuzzy" due to both recall capabilities and the interpretation of "serving". Fuzzy set theory defines the process for simple mathematical techniques (e.g., addition, subtraction, multiplication, and division) that can be applied to standard statistical techniques (Dubois and Prade, 1978).

Bayesian methods are used to define input distributions (Morgan and Henrion, 1990; Brand and Small, 1995). Bayesian procedures start with a *prior* distribution that is based on any available information, including expert opinion. Each time new information becomes available a *posterior* distribution is formed, based on all previous information and the new information. The posterior distributions can then be used with the Monte Carlo simulation methods described above. Morgan and Henrion (1990) point out that Bayesian methods often yield final results comparable to classical statistical approaches. Bayesian methods are most useful when data are continually monitored or updated (Morgan and Henrion, 1990).

Distribution Approximation

The input distribution represents both uncertainty in the estimate and biological variation in the human or fish populations.

It has been suggested that the reduction of uncertainty may currently be more important than the development of more sophisticated models (McKone and Ryan, 1989; McKone and Bogen, 1991). One way to reduce uncertainty is by accurately depicting input distributions (Bukowski, 1995; Seiler and Alvarez, 1996). It is critical to characterize input variables correctly when using Monte Carlo simulations as even slight errors can propagate into radically biased results (Seiler and Alvarez, 1996).

Traditionally, the normal and lognormal distributions have been used to model fish consumption (Hattis and Burmaster, 1992; Ruffle *et al.*, 1994). But Rupp *et al.* (1980) reported that the NPD seafood consumption data were found to be neither normally nor lognormally distributed because of the long right tails; thus, increased flexibility is required to model consumption distributions.

Input distributions, particularly for hierarchical methods, may be symmetric or skewed to the right or left. Several classic statistical distributions are available to model input distributions of varying shape, although a single statistical distribution is typically not flexible enough to model symmetric, left skewed, and right skewed distributions. A relatively new distribution, the S–distribution, has been shown to be capable of modeling distributions that are symmetric or skewed in either direction (Voit, 1992, 1996; Voit and Rust, 1992; Voit and Yu, 1994; Voit *et al.*, 1995; Yu and Voit, 1995; Balthis *et al.*, 1996; Balthis, 1998; Voit and Schwacke, 1998). In fact, S–distributions have already successfully modeled seafood consumption, mercury concentrations in seafood, and body weights (Voit *et al.*, 1995; Balthis *et al.*, 1996; Balthis, 1998); consequently, the

S–distribution is appropriate to model distributions for this project due to its high degree of flexibility.

The *S–distribution* uses the ordinary differential equation

$$\frac{dF}{dX} = \alpha\left(F^g - F^h\right), \qquad F_o = F(X_o) \qquad \textbf{(3.3)}$$

where:

F = cumulative distribution function (dependent variable) and

X = random variable (independent variable).

The S–distribution is characterized by four parameters that need to be estimated. The spread of the distribution is determined by α, which is always greater than zero. The shape of the distribution is determined by g and h, where g is always less than h. And the location of the distribution is determined by the initial value of the differential equation, F_o, which is between zero and one. Typically X_o has been selected such that $F(X_o)=0.5$, or, in other words, the initial value is at the median, X_o (Voit, 1992; Voit and Yu, 1994; Voit *et al.*, 1995; Balthis *et al.*, 1996; Balthis, 1998; Voit and Schwacke, 1998).

The *standard S–distribution* is a special case where $\alpha=1$ and $X_o=0$. With a median at zero, the standard S–distribution is characterized exclusively by the shape parameters g and h. L.H. Schwacke from the Medical University of South Carolina developed Equation (3.4) to approximate quantile t for the standard S-distribution. This equation is based on the rational approximation for quantiles of the normal distribution as published by Hastings (1955). The parameter values for a_1, a_2, a_3, b_1, b_2, and b_3 are listed in Appendix A.

$$sQ(t) = \tau - \frac{a_1 + a_2\tau + a_3\tau^2}{1 + b_1\tau + b_2\tau^2 + b_3\tau^3}, \qquad \text{where } \tau = \sqrt{\ln\left(\frac{1}{t^2}\right)} \qquad \textbf{(3.4)}$$

Quantiles from the standard S–distribution are easily converted to quantiles of the four parameter S–distribution using Equation (3.5) (Voit and Schwacke, 1998).

$$Q(t) = \frac{sQ(t)}{\alpha} + X_o, \qquad \text{where } X_o = \text{Median} \qquad \textbf{(3.5)}$$

The four S–distribution parameter values were estimated using a Mathcad (Mathsoft, Inc., Cambridge, MA) program developed by Schwacke (see Appendix A). The data to be fit to an S–distribution were read into the program; then the program systematically tested different combinations of the four parameters searching for the combination that produced the minimum difference between the actual data values and the S–distribution.

The majority of the distributions in this dissertation are modeled with the S-distribution, yet the methods presented here are independent of the distributions selected to model the input and output variables. The National Ocean Service preferred to have some of the distributions modeled with classic statistical distributions, and some were modeled with classic distributions because of computational limitations or a superior fit.

Chapter 4

ANALYTICAL SOLUTIONS

Monte Carlo simulations are used because an exact solution is unobtainable for many problems, although an exact solution may be obtained under special circumstances. The exact solutions and hierarchical two–dimensional Monte Carlo simulation results were compared for hypothetical problems in this chapter.

In this report point values are denoted without an underscore, first–order random variables with a single underscore, and second–order random variables with a double underscore.

If the variable $\underline{\underline{X}}$ is a normally distributed random variable dependent upon the PDF parameters $\underline{\mu}$ and $\underline{\sigma}$, then the expected value of $\underline{\underline{X}}$ can be obtained using conventional methods for computing the expected value of a conditional random variable as shown in Equation (4.1) (Hogg and Craig, 1978; Burmaster and Wilson, 1996). The expected value of $\underline{\underline{X}}^2$ is given in Equation (4.2).

$$E[\underline{\underline{X}}] = \int_{-\infty}^{\infty}\int_{-\infty}^{\infty}\left[\int_{-\infty}^{\infty} x \cdot f_{x|\mu,\sigma}(x|\mu,\sigma)dx\right] f_{\mu,\sigma}(\mu,\sigma)d\mu\, d\sigma \qquad \textbf{(4.1)}$$

$$E\left[\underline{\underline{X}}^2\right] = \int_{-\infty}^{\infty}\int_{-\infty}^{\infty}\left[\int_{-\infty}^{\infty} x^2 \cdot f_{x|\mu,\sigma}(x|\mu,\sigma)\,dx\right] f_{\mu,\sigma}(\mu,\sigma)\,d\mu\,d\sigma \qquad (4.2)$$

For this exercise it was assumed that the PDF parameters $\underline{\mu}$ and $\underline{\sigma}$ were independent, consequently $f_{\mu,\sigma}(\mu,\sigma) = f_{\mu}(\mu)\cdot f_{\sigma}(\sigma)$.

Example 1

For the first illustration suppose the outcome is equal to a single hierarchical two–dimensional variable, $\underline{\underline{X}}$. Suppose $\underline{\underline{X}}$ ~ Normal Distribution ($\underline{\mu}$, $\underline{\sigma}$), where half the time $\underline{\mu}$ ~ Triangular Distribution (a=100, b=10) and $\underline{\sigma}$ ~ Triangular Distribution (a=3, b=0.3) and half the time $\underline{\mu}$ ~ Triangular Distribution (a=103, b=10) and $\underline{\sigma}$ ~ Triangular Distribution (a=3, b=0.3). In each of these triangular distributions, the parameter 'a' represents the peak of the distribution, and the endpoints are given by a ± b. The Triangular Distribution(a=100, b=10) is displayed in Figure 4–1 as an example.

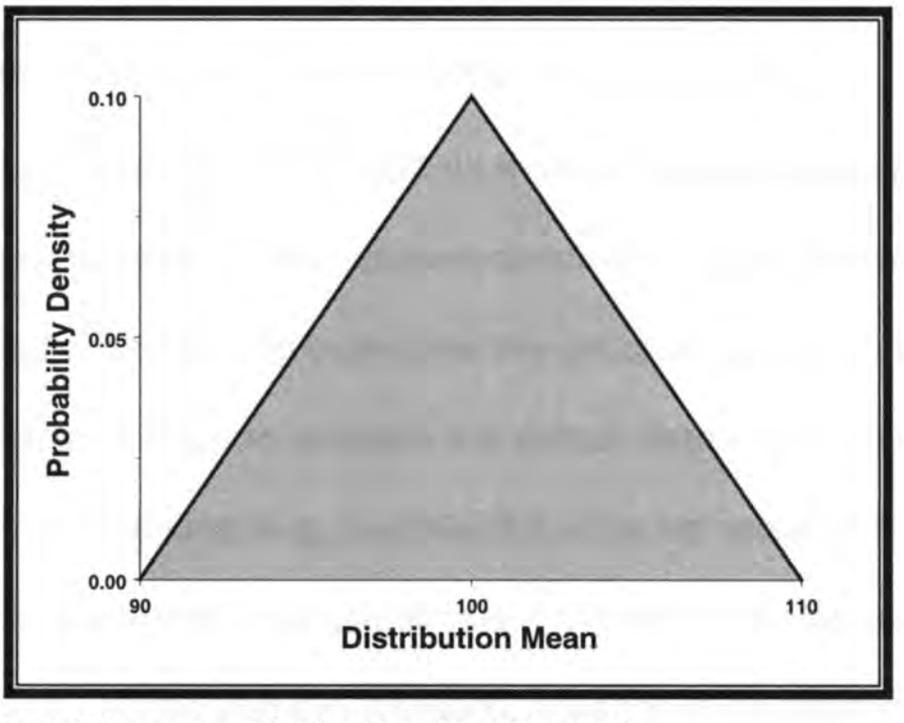

Figure 4–1. Triangular Distribution (a=100, b=10)

The outcome distribution was obtained by solving each two–dimensional part of the hierarchical two–dimensional problem; thus, the outcome distribution in this illustration was characterized using the different distributions for the PDF parameters $\underline{\mu}$ and $\underline{\sigma}$. After obtaining the two–dimensional solutions, the hierarchical two–dimensional problem was reduced to a simple hierarchical problem, or in other words, the two–dimensional analytical solutions reduced the problem from one involving second–order random variables to one with only single–order random variables. The mean of the outcome distribution was calculated using the means from the two–dimensional analytical solutions in Equation (4.3).

$$E[\underline{\underline{X}}] = \sum_{i=1}^{k} p_i \cdot \mu_i \qquad \textbf{(4.3)}$$

where:

p_i = The proportion of the outcome distribution from the i^{th} two–dimensional component and

μ_i = The mean of the i^{th} two–dimensional component.

Unfortunately, there was no mathematical means of calculating the standard deviation of the outcome distribution given the two–dimensional analytical solutions. To overcome this problem, the two–dimensinal analytical solutions were used to simulate the output distribution using an extremely high number of iterations (e.g., n=250,000). The sample standard deviation from the simulation was used to approximate the standard deviation of the outcome distribution, as the sample standard deviation is an asymptotically unbiased

estimator of the population standard deviation. Decisioneering's Crystal Ball Version 4.0c was used to perform the simulations and then to fit the simulated output to classic statistical distributions. Distribution parameters were calculated using maximum–likelihood estimators (Sargent and Wainwright, 1996). Potential distributions were compared using standard goodness–of–fit tests such as the Kolmogorov–Smirnov test and the Anderson–Darling test, which compared the fit between a distribution and the actual data values (Sargent and Wainwright, 1996; Palisade Corporation, 1997b). The Kolmogorov–Smirnov test put more weight on the fit in the mid–range of the distribution, whereas the Anderson–Darling test placed more importance on the fit in the tails of the distribution (Sargent and Wainwright, 1996; Palisade Corporation, 1997b). Graphs of the actual values superimposed with the fitted distributions, such as those seen in Figure 5–8 through Figure 5–16, were also used to compare potential distributions.

The two–dimensional problem using $\underline{\mu}$ ~ Triangular (a=100, b=10) and $\underline{\sigma}$ ~ Triangular Distribution (a=3, b=0.3) was first solved.

The probability density function for a symmetrical triangular distribution is given in Equation (4.4).

$$f(x) = \frac{b - |x - a|}{b^2}, \qquad \text{where } a-b \le x \le a+b \qquad \textbf{(4.4)}$$

Inserting Equation (4.4) in Equation (4.1) resulted in Equation (4.5), noting that the portion of Equation (4.1) enclosed in brackets is equal to $E[X] = \mu$ for a normal distribution.

$$E[\underline{X}] = \int_{90}^{110} \int_{2.7}^{3.3} \mu \cdot \frac{10 - |\mu - 100|}{10^2} \cdot \frac{0.3 - |\sigma - 3|}{0.3^2} \, d\sigma \, d\mu \qquad \textbf{(4.5)}$$

Equation (4.5) rendered the solution $E[\underline{X}] = 100$.

Inserting Equation (4.4) in Equation (4.2) resulted in Equation (4.6), noting that the portion of Equation (4.2) enclosed in brackets is equal to $E[X^2] = (\mu^2 + \sigma^2)$ for a normal distribution.

$$E[\underline{X}^2] = \int_{90}^{110} \int_{2.7}^{3.3} (\mu^2 + \sigma^2) \cdot \frac{10 - |\mu - 100|}{10^2} \cdot \frac{0.3 - |\sigma - 3|}{0.3^2} \, d\sigma \, d\mu \qquad \textbf{(4.6)}$$

Equation (4.6) produced $E[\underline{X}^2] = 10025.68$. Using the above two solutions and the fact that $Var[X] = E[X^2] - (E[X])^2$, it was determined that $\underline{X}$ ~ Normal Distribution (μ=100.00, σ=5.07).

The analytical two–dimensional solution was next compared with simulated results from Crystal Ball. First, it was necessary to decide how many iterations were required for the two–dimensional Monte Carlo simulations. Twenty preliminary simulations were run using a normal distribution (μ=100, σ=3.33) (see Appendix B for additional distribution information). Seventy–five percent of the preliminary simulations stabilized by 200 iterations, 90% by 250 iterations, and all simulations by 300 iterations, where stabilization was defined as the mean, median, standard deviation, and every fifth percentile changing less than 5% from one batch of 50 to the next. Based on these results, it was decided that the inner loop and the outer loop of the two–dimensional Monte Carlo simulations would contain 250 iterations.

A two–dimensional simulation was performed for $\underline{\underline{X}}$ using $\underline{\mu}$ ~ Triangular Distribution (a=100, b=10) and $\underline{\sigma}$ ~ Triangular Distribution (a=3, b=0.3). The simulated results were fit to a normal distribution as previously described. The fitted normal distribution (μ=99.98, σ=5.02) was very similar to the analytical solution (μ=100.00, σ=5.07); thus, the two–dimensional simulation results appeared to be consistent with the analytical solution.

The same procedure was followed using $\underline{\mu}$ ~ Triangular Distribution (a=103, b=10) and $\underline{\sigma}$ ~ Triangular Distribution (a=3, b=0.3). The resulting analytical solution was $\underline{\underline{X}}$ ~ Normal Distribution (μ=103, σ=5.07). The two–dimensional simulation produced a Normal (μ=102.96, σ=5.13). Once again, the analytical solutions compared well with the two–dimensional simulation results.

The mean of the output distribution, 101.50, was calculated using the two–dimensional analytical solutions and Equation (4.3). To estimate the standard deviation of the output distribution, 200,000 hierarchical iterations were run assuming that $\underline{X}$ was distributed normally with a mean of 100.00 and a standard deviation of 5.07 half the time and with a mean of 103.00 and a standard deviation of 5.07 the other half of the time. The hierarchical output was best fit by a Normal Distribution (μ=101.50, σ=5.28).

The hierarchical two–dimensional simulation was obtained by combining the two–dimensional simulation results. A normal distribution with a mean of 101.47 and a standard deviation of 5.29 provided the most accurate fit. Thus, the analytical solutions and the simulated results were remarkably similar.

Example 2

For the second illustration $\underline{\underline{Z}} = \underline{\underline{X}} \cdot \underline{\underline{Y}}$, where $\underline{\underline{X}}$ and $\underline{\underline{Y}}$, were normally distributed. $\underline{\underline{X}}$ was defined as in Example 1 and $\underline{\underline{Y}}$ ~ Normal Distribution ($\underline{\mu}$, $\underline{\sigma}$), where one–third of the time $\underline{\mu}$ ~ Normal Distribution (μ=100, σ=3) and $\underline{\sigma}$ ~ Uniform Distribution (min=2.9, max=3.1) and two–thirds of the time $\underline{\mu}$ ~ Lognormal Distribution (μ=104, σ=4) and $\underline{\sigma}$ ~ Uniform Distribution (min=2.5, max=3.0).

The two–dimensional solutions were obtained for $\underline{\underline{Y}}$ in the same manner as those for $\underline{\underline{X}}$ in Example 1. The two–dimensional problem for $\underline{\mu}$ ~ Normal Distribution (μ=100, σ=3) and $\underline{\sigma}$ ~ Uniform Distribution (min=2.9, max=3.1) was solved first.

Equations (4.7) and (4.8) contain the probability density function for the normal distribution and the uniform distribution respectively (see Appendix B for additional distribution information).

$$f(y) = \frac{1}{\sqrt{2\pi} \cdot \sigma} \cdot e^{\frac{-(y-\mu)^2}{2\sigma^2}}, \qquad \text{where } -\infty \le y \le \infty \qquad \textbf{(4.7)}$$

$$g(y) = \frac{1}{\max - \min}, \qquad \text{where } \min \le y \le \max \qquad \textbf{(4.8)}$$

Inserting Equations (4.7) and (4.8) into Equation (4.1) resulted in Equation (4.9), noting that the portion of Equation (4.1) enclosed in brackets is equal to $E[Y] = \mu$ for a normal distribution.

$$E[\underline{Y}] = \int_{-\infty}^{\infty} \int_{2.9}^{3.1} (\mu) \left(\frac{1}{\sqrt{2\pi} \cdot 3} e^{-\frac{(\mu-100)^2}{2 \cdot 3^2}} \right) \left(\frac{1}{3.1-2.9} \right) d\sigma \, d\mu \qquad \textbf{(4.9)}$$

Equation (4.9) rendered the solution $E[\underline{Y}] = 100$.

Inserting Equations (4.7) and (4.8) in Equation (4.2) resulted in Equation (4.10), noting that the portion of Equation (4.2) enclosed in brackets is equal to $E[Y^2] = (\mu^2 + \sigma^2)$ for a normal distribution.

$$E[\underline{Y}^2] = \int_{-\infty}^{\infty} \int_{2.9}^{3.1} (\mu^2 + \sigma^2) \left(\frac{1}{\sqrt{2\pi} \cdot 3} e^{-\frac{(\mu-100)^2}{2 \cdot 3^2}} \right) \left(\frac{1}{3.1-2.9} \right) d\sigma \, d\mu \qquad \textbf{(4.10)}$$

Equation (4.10) produced $E[\underline{Y}^2] = 10018.00$. Using the above two solutions and the fact that $Var[Y] = E[Y^2] - (E[Y])^2$, it was determined that $\underline{Y}$ ~ Normal Distribution (μ=100.00, σ=4.24).

The analytical two–dimensional solution was again compared with simulated results from Crystal Ball. The inner loop and the outer loop of the two–dimensional Monte Carlo simulations had 250 iterations. The simulated results were accurately fit by a normal distribution (μ=99.97, σ=4.34). The analytical solution appeared to be consistent with the two–dimensional simulation results as both distributions were similar.

The same procedure was followed $\underline{Y}$ ~ ($\underline{\mu}$,$\underline{\sigma}$), where $\underline{\mu}$ ~ Lognormal Distribution (μ=104, σ=4) and $\underline{\sigma}$ ~ Uniform Distribution (min=2.5, max=3.0).

Equation (4.11) contains the probability density function for the lognormal distribution. The equations for μ_{LN} and σ_{LN} are given in Appendix B under the Lognormal Distribution.

$$f(y)=\frac{1}{\sqrt{2\pi}\cdot\sigma_{LN}\cdot x}\cdot e^{\frac{-(\ln(y)-\mu_{LN})^2}{2\sigma_{LN}^2}}, \qquad \text{where } 0\le y\le\infty \qquad \textbf{(4.11)}$$

Inserting Equations (4.11) and (4.8) into Equation (4.1) resulted in Equation (4.12).

$$E[\underline{Y}]=\int_0^{\infty}\int_{2.5}^{3.0}(\mu)\left(\frac{1}{\sqrt{2\pi}\cdot 0.0384\cdot\mu}e^{-\frac{(\mu-4.644)^2}{2\cdot 0.0384^2}}\right)\left(\frac{1}{3.0-2.5}\right)d\sigma\, d\mu \qquad \textbf{(4.12)}$$

Equation (4.12) rendered the solution $E[\underline{Y}] = 104$.

Inserting Equations (4.11) and (4.8) in Equation (4.2) resulted in Equation (4.13).

$$E[\underline{Y}^2]=\int_0^{\infty}\int_{2.5}^{3.0}(\mu^2+\sigma^2)\left(\frac{1}{\sqrt{2\pi}\cdot 0.0384\cdot\mu}e^{-\frac{(\mu-4.644)^2}{2\cdot 0.0384^2}}\right)\left(\frac{1}{3.0-2.5}\right)d\sigma\, d\mu \qquad \textbf{(4.13)}$$

Equation (4.13) produced $E[\underline{Y}^2] = 10839.58$. Using the above two solutions and the fact that $Var[Y] = E[Y^2] - (E[Y])^2$, it was determined that $\underline{Y}$ ~ Normal Distribution (μ=104.00, σ=4.86).

The two–dimensional simulation was accurately fit by a Normal (μ=103.81, σ=4.82). Once again, the analytical solutions compared well with the two–dimensional simulation results.

The analytical solutions now reduced the second–order problem to a first–order problem. In other words, $\underline{Z}$ was now characterized by four potential combinations of the PDF parameters for $\underline{X}$ and $\underline{Y}$. Assuming that $\underline{X}$ and $\underline{Y}$ were stochastically independent and employing the relationship

$E[Z^2] = Var[Z] + (E[Z])^2$, the $E[\underline{Z}]$ was computed using Equation (4.14) and the $Var[\underline{Z}]$ using Equation (4.15).

$$\begin{aligned} E[\underline{Z}] &= E[\underline{X}\,\underline{Y}] \\ &= E[\underline{X}] \cdot E[\underline{Y}] \\ &= \mu_x \cdot \mu_y \end{aligned} \qquad \textbf{(4.14)}$$

$$\begin{aligned} Var[\underline{Z}] &= E\left[\underline{X}^2\,\underline{Y}^2\right] - (E[\underline{X}\,\underline{Y}])^2 \\ &= E\left[\underline{X}^2\right] \cdot E\left[\underline{Y}^2\right] - \mu_x^2 \cdot \mu_y^2 \\ &= \left(Var[\underline{X}] + E[\underline{X}]^2\right) \cdot \left(Var[\underline{Y}] + E[\underline{Y}]^2\right) - \mu_x^2 \cdot \mu_y^2 \\ &= \left(\sigma_x^2 + \mu_x^2\right) \cdot \left(\sigma_y^2 + \mu_y^2\right) - \mu_x^2 \cdot \mu_y^2 \\ &= \sigma_x^2 \cdot \sigma_y^2 + \mu_y^2 \cdot \sigma_x^2 + \mu_x^2 \cdot \sigma_y^2 \end{aligned} \qquad \textbf{(4.15)}$$

Equations (4.14) and (4.15) were used to obtain the hierarchical distributions for potential combinations of $\underline{X}$ and $\underline{Y}$. For each of these combinations, simulated data were fit to classic statistical distributions in Crystal Ball; in each situation the normal distribution fit the data well. The hierarchical distributions are given in Table 4–1.

Combination of $\underline{X}^*$ and $\underline{Y}^{**}$	Distribution
$\underline{X}_1$ and $\underline{Y}_1$	Normal Distribution (μ=10,000, σ=661.32)
$\underline{X}_1$ and $\underline{Y}_2$	Normal Distribution (μ=10,400, σ=717.09)
$\underline{X}_2$ and $\underline{Y}_1$	Normal Distribution (μ=10,300, σ=669.55)
$\underline{X}_2$ and $\underline{Y}_2$	Normal Distribution (μ=10,712, σ=727.03)
* X_1 ~ Normal Distribution(μ=100, σ=5.07), X_2 ~ Normal Distribution(μ=103, σ=5.07) ** Y_1 ~ Normal Distribution(μ=100, σ=4.24), Y_2 ~ Normal Distribution(μ=104, σ=4.86)	

Table 4–1. Hierarchical Distributions for Potential Combinations of $\underline{X}$ and $\underline{Y}$

The mean of the output distribution, 10420.67, was calculated using means from Table 4–1 and Equation (4.3). To estimate the standard deviation of the output distribution, 600,000 hierarchical iterations were run using the distributions in Table 4–1. The hierarchical output was accurately fit by a Lognormal Distribution (μ=10,420.67, σ=746.27).

A hierarchical two–dimensional Monte Carlo simulation was run using 250 iterations for both the inner and outer loop. A lognormal distribution with a mean of 10,421.93 and a standard deviation of 746.54 provided the most accurate fit; thus the analytical solutions and the simulated results were again remarkably similar.

Chapter 5

DESCRIPTION OF DATA

Body Weight Data

Many researchers use point estimates for body weight, such as those in Table 5–1 obtained from EPA's *Exposure Factors Handbook* (1990). The averages presented in Table 5–1 are derived from the second National Health and Nutrition Examination Survey (NHANES II) conducted from 1976 to 1980.

Age Group (yrs)	Average Male Body Weight (kg)	Average Female Body Weight (kg)	Average Body Weight for Males and Females Combined (kg)
< 3	11.9	11.2	11.6
3 to 6	17.6	17.1	17.4
0 to 6	14.8	14.2	14.5
6 to 9	25.3	24.6	25.0
9 to 12	35.7	36.2	36.0
12 to 15	50.5	50.7	50.6
15 to 18	64.9	57.4	61.2
18 to 25	73.7	60.6	67.2
25 to 35	78.7	64.2	71.5
35 to 45	80.8	67.1	74.0
45 to 55	81.0	67.9	74.5
55 to 65	78.8	67.9	73.4
65 to 75	74.8	66.6	70.7
18 to 45	–	64	–
18 to 75	78.1	65.4	71.8

Table 5–1. Body Weights Presented in EPA's Exposure Factor Handbook

The third National Health and Nutrition Examination Survey (NHANES III) has since been completed. NHANES III included the examination of 30,818 individuals from 1988 to 1994 (NCHS, 1994, 1996). The participants ranged from 2 months to 90 years of age.

Although NHANES III is more recent, several risk assessors continue to use body weights from NHANES II (Brainard and Burmaster, 1992; Finley *et al.*, 1994; Burmaster and Crouch, 1997; Balthis, 1998). Based on a 1994 review by Finley *et al.* the NHANES II study represents the most complete and reliable body weight data for the U.S. Figure 5–1 presents a comparison of body weight distributions between NHANES II and III by age class. These comparisons were limited to ages 12–69 because NHANES II had a more limited age range than NHANES III and National Ocean Service lacked infant data from NHANES II. Body weight distributions are fairly constant, as demonstrated in Figure 5–1, with a low level of uncertainty (EPA, 1994; Finley *et al.*, 1994; Cohen *et al.*, 1996; Rai *et al.*, 1996). This research will use NHANES III because it is more recent, larger in scope, and doesn't seem to differ significantly from NHANES II.

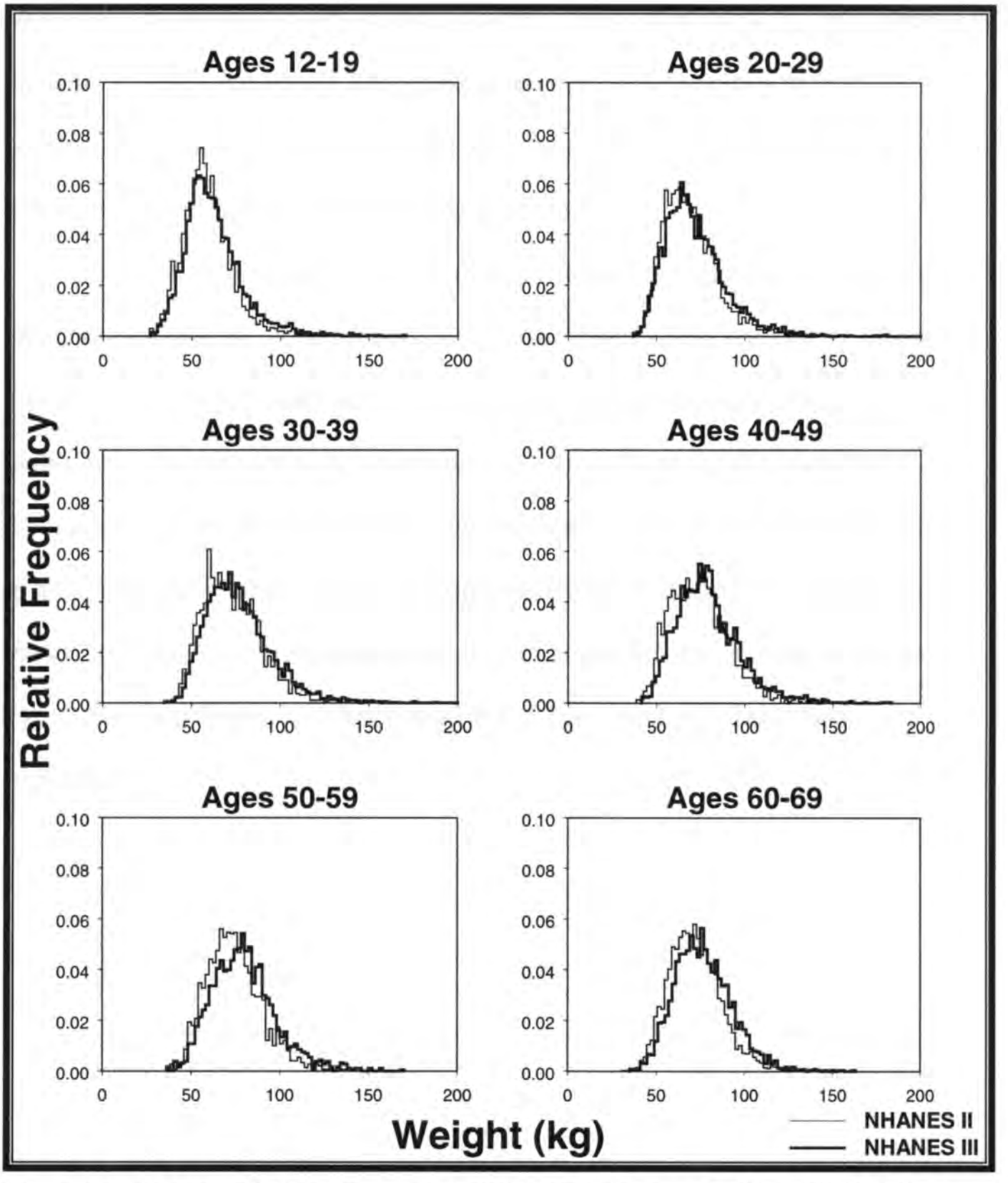

Figure 5–1. Observed Relative Frequency Distributions Comparing Body Weights from NHANES II (thin line) and NHANES III (thick line) by Age Class

The following subgroups of the U.S. populations were oversampled during NHANES III in order to better understand their nutritional status: infants from two months to five years old, adults over 60 years old, black Americans, and

Mexican–Americans (NCHS, 1994). To account for this oversampling, a random sample of 7,500 individuals was selected based on proportions of the U.S. population in each race, gender, and age class. This subgroup was used to model a single distribution for all body weights.

In addition, a random sample of over 14,000 individuals was selected to be representative of racial proportions in each gender and age class. These 14,000 body weights were used to model age and gender–specific body weight distributions for hierarchical simulations. The age–specific body weight distributions for females and males can be seen in Figure 5–2 and Figure 5–3, respectively. S–distributions have been superimposed upon each histogram in these figures. The parameter values that characterize the S-distributions in Figure 5–2 and Figure 5–3 are contained in Table 5–2 and Table 5–3 respectively.

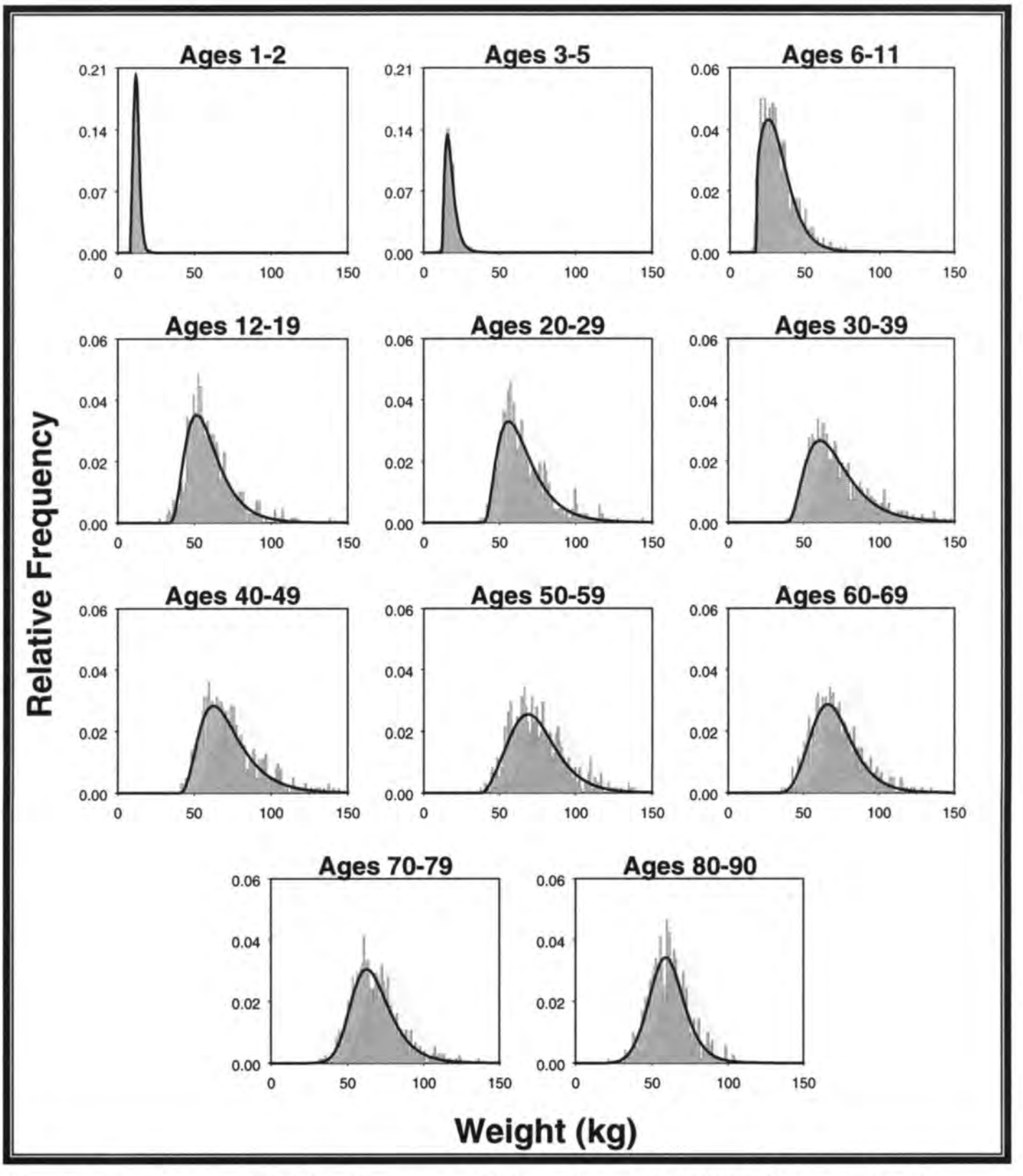

Figure 5–2. Observed Relative Frequency Distributions of NHANES III Female Body Weights by Age Class with Fitted S–Distributions Superimposed (see Table 5–2 for parameter values)

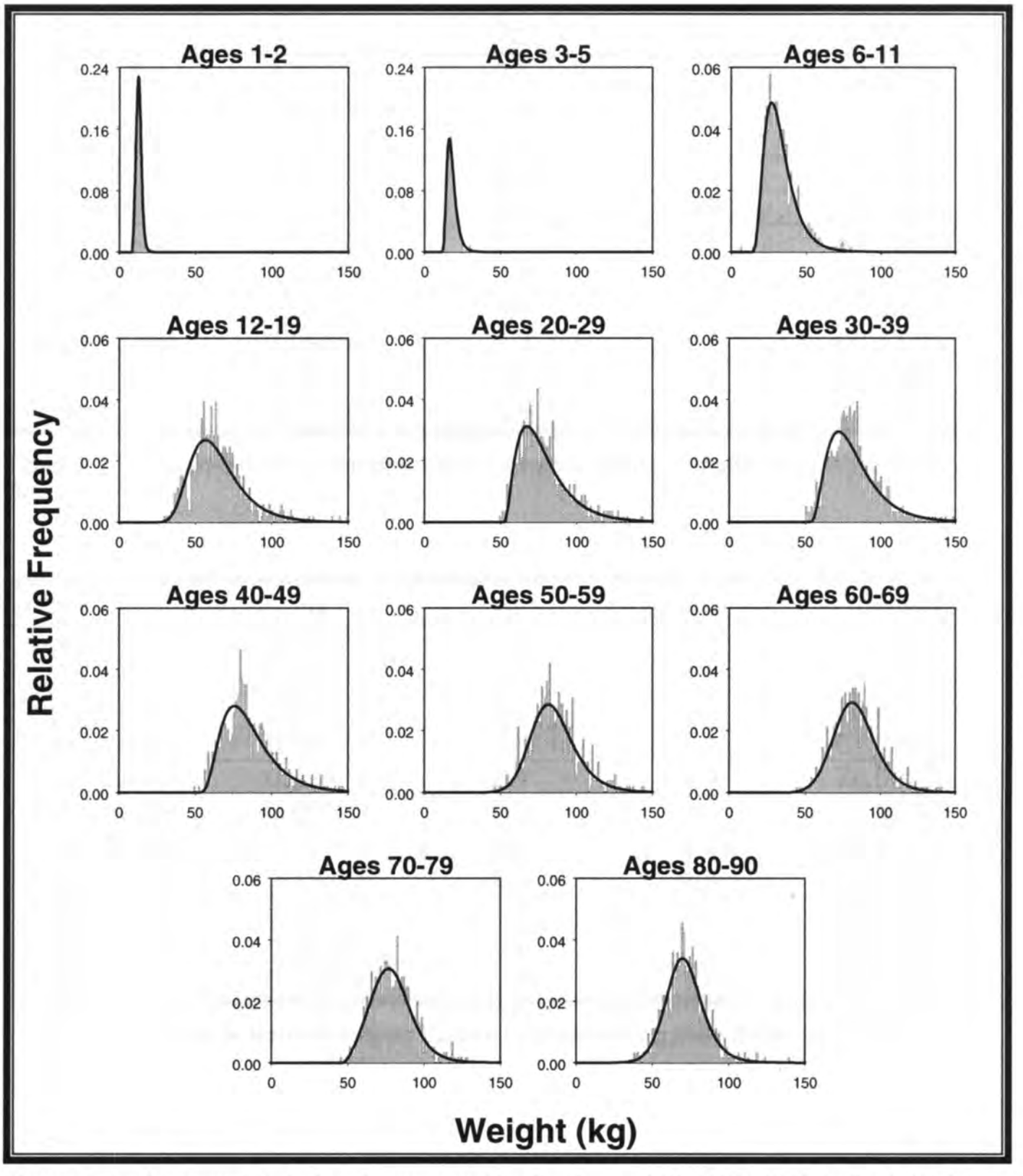

Figure 5–3. Observed Relative Frequency Distributions of NHANES III Male Body Weights by Age Class with Fitted S–Distributions Superimposed (see Table 5–3 for parameter values)

Class	α	g	h	Median
Ages 1–2	0.37573	0.5	2.5	12.03760
Ages 3–5	3.09031	0.8	0.9	17.16166
Ages 6–11	0.06033	0.2	2.2	30.38003
Ages 12–19	0.42865	0.8	1.0	56.56892
Ages 20–29	0.75949	0.8	0.9	62.12824
Ages 30–39	0.16128	0.7	1.1	67.65988
Ages 40–49	0.34464	0.8	1.0	68.75156
Ages 50–59	0.06321	0.6	1.9	72.20282
Ages 60–69	0.09037	0.7	1.7	69.11739
Ages 70–79	0.45518	1.0	1.2	65.73622
Ages 80+	0.10536	0.8	2.0	59.83721

Table 5–2. S–Distribution Parameter Values Characterizing Female Body Weights by Age Class

Class	α	g	h	Median
Ages 1–2	0.45927	0.6	2.6	12.56484
Ages 3–5	1.26019	0.8	1.1	17.33495
Ages 6–11	0.59251	0.8	1.0	30.43149
Ages 12–19	0.36377	0.9	1.1	61.70202
Ages 20–29	0.33824	0.7	0.9	74.59208
Ages 30–39	0.68023	0.8	0.9	78.92429
Ages 40–49	0.34207	0.8	1.0	81.99774
Ages 50–59	0.15322	0.9	1.5	84.06716
Ages 60–69	0.09441	0.8	1.9	82.68983
Ages 70–79	0.06477	0.6	2.4	77.93952
Ages 80+	0.13576	0.9	1.8	70.93637

Table 5–3. S–Distribution Parameter Values Characterizing Male Body Weights by Age Class

Consumption Data

Estimating seafood consumption can be a difficult task due to interindividual variability, age–dependent consumption rates, and the infrequent consumption of seafood (Rupp, 1980; EPA, 1997c). In the early 1970s the Tuna Research Institute and the National Marine Fisheries Service commissioned

NPD Research, Inc., to conduct a seafood consumption survey with these problems in mind (Rupp *et al.*, 1980; Stanford Research Institute, 1980; Ruffle *et al.*, 1994). According to a 1980 Stanford Research Institute (SRI) review and two 1994 reviews, the 1973–1974 survey conducted by NPD Research is the most reliable source of data on U.S. fish consumption (Stanford Research Institute, 1980; Finley *et al.*, 1994; Ruffle *et al.*, 1994). EPA (1997c) used NPD data in the Report to Congress as a major long–term study characterizing dietary intake of seafood. Over 7,650 families (23,213 individuals), from the 9,950 families originally contacted, completed the survey. Each month from September 1973 to August 1974 fish consumption data were collected from one–twelfth of the participants for a one month period. The survey collected demographic information, consumption date, species consumed, amount consumed, and whether the seafood was recreationally caught or commercially purchased.

SRI (1980) determined that the survey was conducted appropriately, but an absence of documentation concerning the questionnaire, coding, and quality control procedures makes it difficult to confirm this claim. Two possible sources of bias in the NPD database are that no one member households were surveyed and data were only retained for individuals who consumed fish (94% of population) (Stanford Research Institute, 1980).

Seafood consumption seems to be more correctly recalled than most other food consumption (EPA, 1997c). It is particularly advantageous to be studying lobster consumption because most individuals remember eating lobster, as opposed to their recollection of other seafood consumption.

Seafood consumption rates are dependent upon gender and body weight, and body weight is dependent on age (EPA, 1994). Previous studies using the NPD data have adopted the following three age classes to characterize seafood consumption: infants (1–11 years old), teens (12–18 years old), and adults (19–98 years old) (Rupp, 1980; Rupp *et al.*, 1980; Ruffle *et al.*, 1994). Ruffle *et al.* (1994) regard the NPD data as appropriate for use in Monte Carlo simulations. One potential use is the development of age and gender–specific consumption rate distributions for hierarchical simulations.

Both the infant and teen lobster consumption patterns were comparable between genders. Thus, neither infant nor teen distributions were gender–specific. Adult lobster consumption patterns did differ between genders; consequently, gender–specific consumption distributions were obtained for adults. During the observation period, 641 individuals in the NPD survey consumed Northern lobster (see Appendix C). Age and gender–specific lobster consumption is displayed in Figure 5–4. S-distributions have been superimposed upon each histogram in this figure. The parameter values that characterize the S–distributions in Figure 5–4 are contained in Table 5–4. Distributions were modeled using grams of lobster consumed per month due to a superior fit. Thus, the random values obtained from these distributions were multiplied by the appropriate constant to obtain grams of lobster consumed per day.

The teen, adult female, and adult male data did have one flaw in that large proportions of each data set consisted of identical values. It is highly

suspicious that the majority of individuals in each age and gender class consumed equivalent amounts of lobster. For example, 60% of the adult females consumed exactly 150 g of lobster with each lobster meal. Using the fact that approximately four and a half pounds of live lobster yield one pound of edible meat, this corresponds to consuming a one and a half pound lobster for adult female meals. This is most likely the result of NPD participants reporting that they consumed a particular size lobster (e.g., small, average, or large) with a meal. To help account for this lack of variability each teen and adult lobster consumption rate was replaced by randomly selecting a value from a uniform distribution centered at the reported consumption rate. The uniform distribution for teen consumption rates extended half an ounce above and below each reported value, and the uniform distribution for adult consumption rates extended one ounce above and below each reported value. The consumption rates with the added variation are plotted in Figure 5–4.

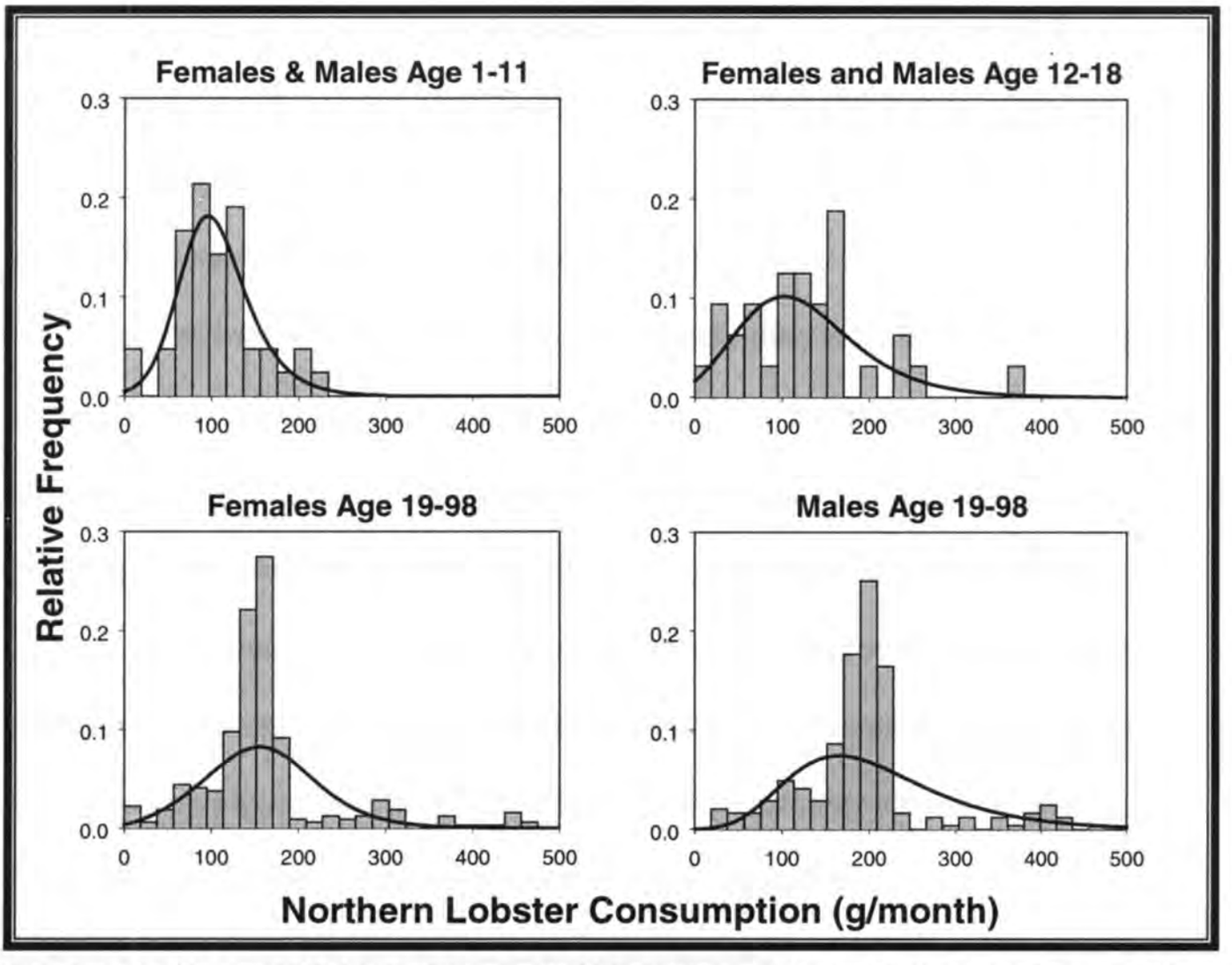

Figure 5–4. Observed Relative Frequency Distributions of Northern Lobster Consumption by Consumer Gender and Age Class with Fitted S–Distributions Superimposed (see Table 5–4 for parameter values)

Class	α	g	h	Median
Females & Males Age 1–11	0.16405	1.1	1.3	102.15685
Females & Males Age 12–18	0.01890	0.7	1.7	117.56379
Females Age 19–98	0.01419	0.7	2.5	156.85875
Males Age 19–98	0.06519	0.9	1.1	193.94634

Table 5–4. S–Distribution Parameter Values Characterizing Northern Lobster Consumption by Gender and Age Class

The infant and teen distributions seem to fit the data reasonably well, but the adult female and male distributions lack the extreme peak seen in the data. Eleven classic distributions were fit to the data using Decisioneering's Crystal

Ball Version 4.0c. Crystal Ball calculated distribution parameters using maximum–likelihood estimators (Sargent and Wainwright, 1996). The classic statistical distributions resulted in adult female and male consumption distributions similar to those observed in Figure 5–4.

The distribution fit may be improved by dividing both the adult female and the adult male consumption rates into two separate components. Consumption rates for adult females were separated into those above and those below 180 g/month. The adult male consumption rates were divided at 250 g/month. Each of these groups was fit to a distribution, and the resulting distributions more accurately resembled the adult female and adult male consumption data as evidenced by Figure 5–5 and Figure 5–6. The parameter values for the S-distributions in these figures are provided in Table 5–5.

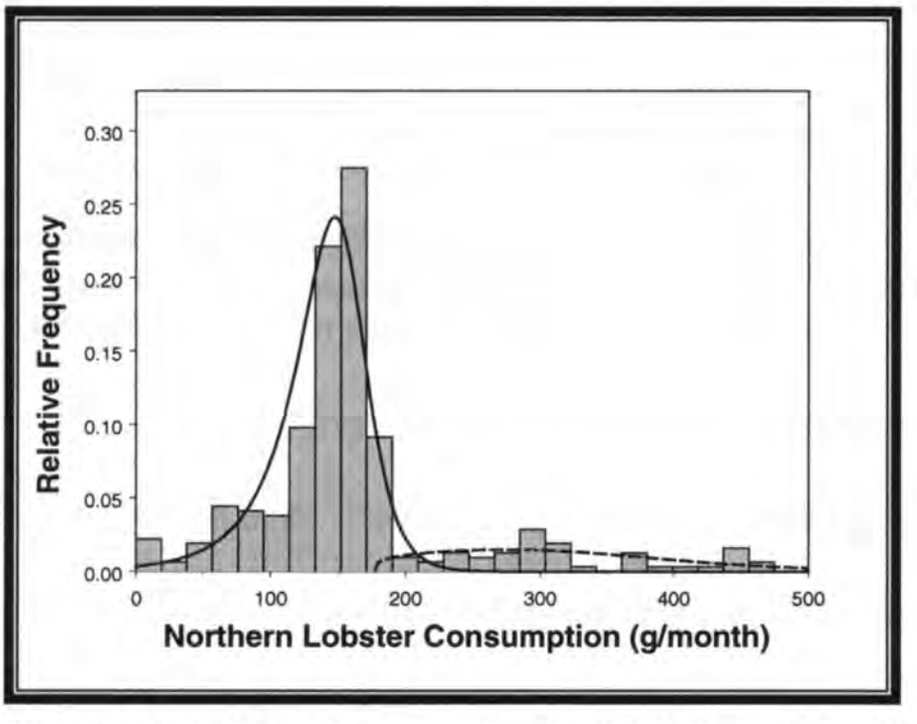

Figure 5–5. Lobster Consumption for Adult Females modeled with two S–Distributions (see Table 5–5 for parameter values)

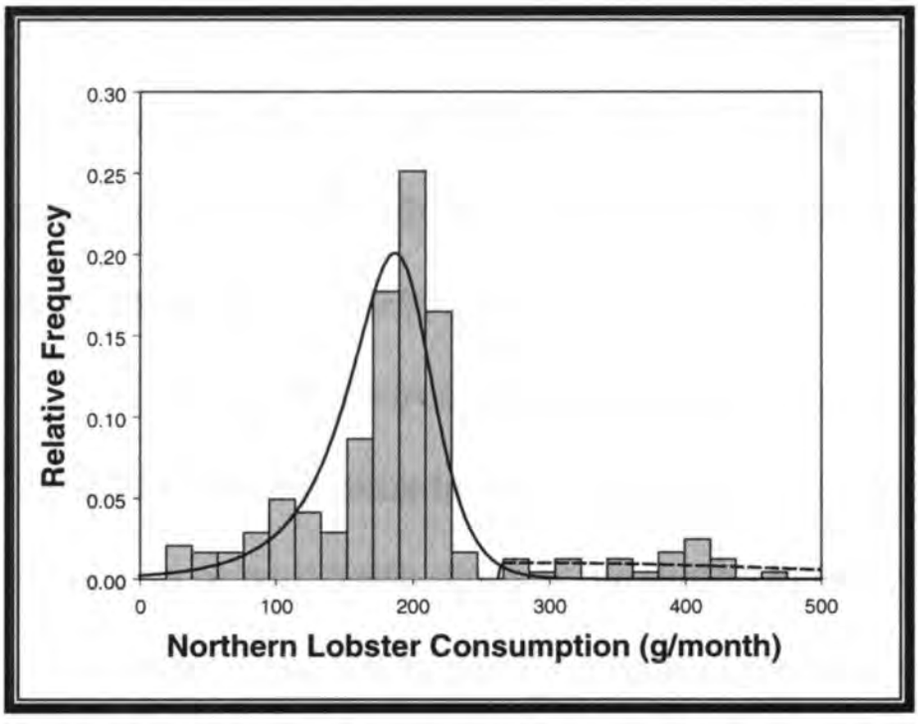

Figure 5–6. Lobster Consumption for Adult Males modeled with two S–Distributions (see Table 5–5 for parameter values)

Class	α	g	h	Median
Adult Females consuming under 180 g/month	0.04000	1.1	3.0	141.15835
Adult Females consuming over 180 g/month	0.00580	0.2	2.8	307.08436
Adult Males consuming under 250 g/month	0.03294	1.1	3.0	179.17789
Adult Males consuming over 250 g/month	0.00353	0.0	2.5	413.48989

Table 5–5. S–Distribution Parameter Values Characterizing Lobster Consumption Using Two Distributions for Adult Females and Adult Males

It is noted that the tails of the two S–distributions overlap in both Figure 5–5 and Figure 5–6. The tails are simply a characteristic of the distributions. The problem was considered to be negligible as the overlap is for such a small portion of the curves.

When an adult female or adult male was selected in a hierarchical Monte Carlo iteration, then the proportion of consumption values in each of the two

groups was used to select one of the two distributions to characterize age and gender–dependent consumption rates. Eighty–four percent of the adult females consumed less than 180 g of lobster per month, and 86% of the adult males consumed less than 250 g/month.

The difference in exposure from hierarchical Monte Carlo simulations as a result of modeling adult female consumption and adult male consumption with either one or two distributions is presented in Figure 5–7. A more in depth explanation of the hierarchical simulation process is found in Chapters 3 and 6. Although the distributions in Figure 5–5 and Figure 5–6 fit the adult consumption data more accurately, the distributions in Figure 5–4 were used to characterize consumption for adult females and adult males in all subsequent simulations as negligible differences are seen in Figure 5–7. In addition, the single distribution in Figure 5–4 most likely depicts true lobster consumption more correctly, as lobsters vary in weight and individuals consume different lobster parts and portions.

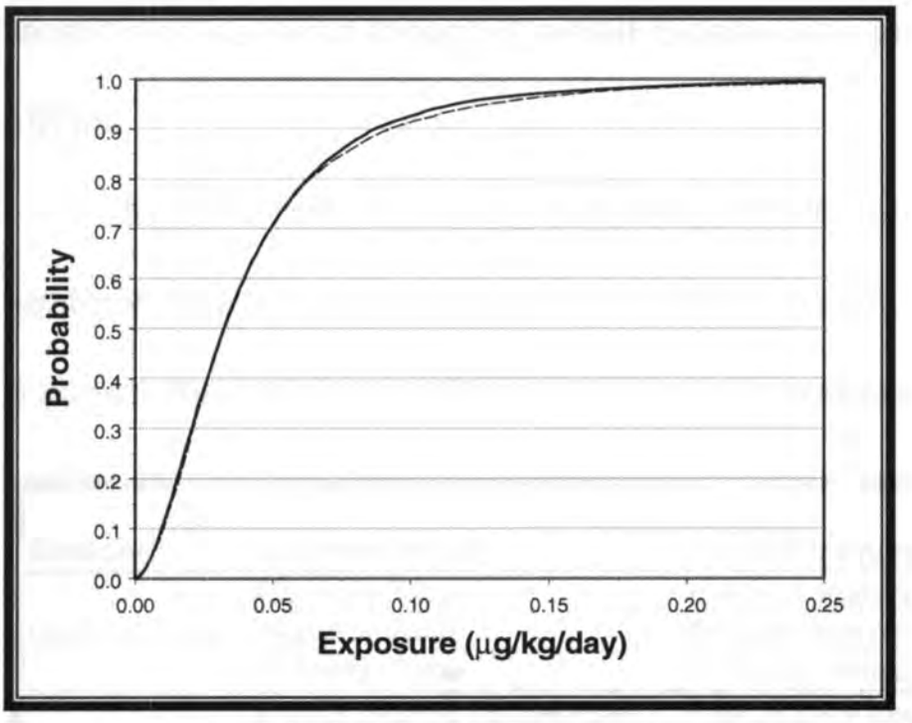

Figure 5–7. Empirical Distributions from Hierarchical Monte Carlo Simulations Using a Single Distribution (solid line) and Two Distributions (dashed line) to Characterize Lobster Consumption for Both Adult Females and Adult Males

Contaminant Data

The contaminant data to be used for this dissertation are from a comprehensive survey of trace elements in seafood (Hall *et al.*, 1978). The National Marine Fisheries Service collected tissues for 204 species of finfish, Mollusca, and Crustacea from numerous U.S. coastal locations for this survey. At the time of the survey, these 204 species constituted approximately 95% of the total volume of consumed seafood. Each sample was analyzed for 15 contaminants, including mercury.

The Environmental Protection Agency used the NMFS trace element data to characterize mercury concentrations for marine species in the *Mercury Study Report to Congress* (1997c). EPA (1997c) concluded that mercury concentrations in the database were comparable to levels obtained in more

recent studies, even though the NMFS data were primarily collected in the 1970s.

Distributions of mercury concentrations in the most frequently consumed seafood may be developed using the NMFS survey of trace elements. Table 5–6 shows some of the most commonly consumed species (EPA, 1997b, 1997c).

Seafood	Common Name	Scientific Name	Number Sampled	Mean (ppm)
Canned Tuna	Albacore Tuna	*Thunnus alalunga*	131	0.264
	Skipjack Tuna	*Katsuwonus pelamis*	70	0.136
	Yellowfin Tuna	*Thunnus albacares*	115	0.218
Shrimp	Alaska Shrimp (Sidestripe)	*Pandalopsis dispar*	26	0.042
	Brown Shrimp	*Penaeus aztecus*	63	0.048
	Ocean Shrimp	*Pandalus jordani*	12	0.053
	Pink Shrimp	*Penaeus duorarum*	48	0.031
	Pink Shrimp (Northern)	*Pandalus borealis*	76	0.024
	White Shrimp	*Penaeus setiferus*	99	0.054
Pollock	Alaska Pollock	*Theragra chalcogramma*	145	0.066
Salmon	Chinook Salmon (King)	*Oncorhynchus tshawytscha*	265	0.063
	Chum Salmon (Keta)	*Oncorhynchus keta*	138	0.030
	Coho Salmon (Silver)	*Oncorhynchus kisutch*	173	0.038
	Pink Salmon	*Oncorhynchus gorbuscha*	94	0.019
	Sockeye Salmon (Red)	*Oncorhynchus nerka*	148	0.027
Cod	Atlantic Cod	*Gadus marhua*	134	0.114
	Pacific Cod	*Gadus macrocephalus*	122	0.127
Clams	Hard Clam	*Mercenaria mercenaria*	157	0.034
	Soft Clam	*Mya arenaria*	33	0.027
Flounder	Fourspot Flounder	*Paralichthys oblongus*	72	0.090
	Gulf Flounder	*Paralichthys albigutta*	40	0.147
	Southern Flounder	*Paralichthys lethostigma*	42	0.078
	Summer Flounder	*Paralichthys dentatus*	59	0.127
	Windowpane Flounder	*Scophthalmus aquosus*	59	0.151
	Winter Flounder	*Pleuronectes americanus*	172	0.066
	Witch Flounder	*Glyptocephalus cynoglossus*	71	0.083
	Yellowtail Flounder	*Pleuronectes ferrugineus*	114	0.067
Crab	Blue Crab	*Callinectes sapidus*	57	0.123
	Dungeness Crab	*Cancer magister*	51	0.173
	King Crab	*Paralithodes camtschaticus*	62	0.071
	Tanner Crab	*Chionoecetes bairdi*	49	0.102
Scallops	Sea Scallop (Smooth)	*Placopecten magellanicus*	104	0.101

Table 5–6. Number Sampled and Mean Mercury Concentration for the Most Frequently Consumed Marine Species in the NMFS Survey of Trace Elements

The individual species were combined into the general seafood groups listed in the first column of Table 5–6, as most consumers are not familiar with the particular species of fish and shellfish. EPA (1997b, 1997c) combined species in a similar manner. Histograms of the mercury concentrations for these groups are presented in Figure 5–8 through Figure 5–16. Each histogram has been superimposed with a classic statistical distribution which characterizes the mercury concentrations. The statistical distributions and parameter values associated with each seafood group are displayed in Table 5–7.

These distributions were obtained by entering the actual contaminant data into Decisioneering's Crystal Ball Version 4.0c. Crystal Ball calculated distribution parameters using maximum–likelihood estimators (Sargent and Wainwright, 1996). Eleven classic statistical distributions were compared using standard goodness–of–fit tests such as the Kolmogorov–Smirnov test and the Anderson–Darling test, which assess the fit between a distribution and the actual data values (Sargent and Wainwright, 1996; Palisade Corporation, 1997b). The Kolmogorov–Smirnov test put more weight on the fit in the mid–range of the distribution, whereas the Anderson–Darling test placed more importance on the fit in the tails of the distribution (Sargent and Wainwright, 1996; Palisade Corporation, 1997b). Graphs of the actual contaminant values superimposed with the fitted distributions were also used to compare potential distributions.

Figure 5–8 demonstrates that S–distributions could have been used to model mercury concentrations, but classic statistical distributions were fit to the data at the request of NOS. In addition, the classic distributions more accurately

fit data where most of the values were at or near a concentration of zero (i.e., shrimp, pollock, clams, flounder, and crab).

The Extreme Value, Logistic, and Weibull distributions were truncated in the left tail at zero to prevent negative concentrations. The probability density functions and parameters that characterize each statistical distribution are provided in Appendix B.

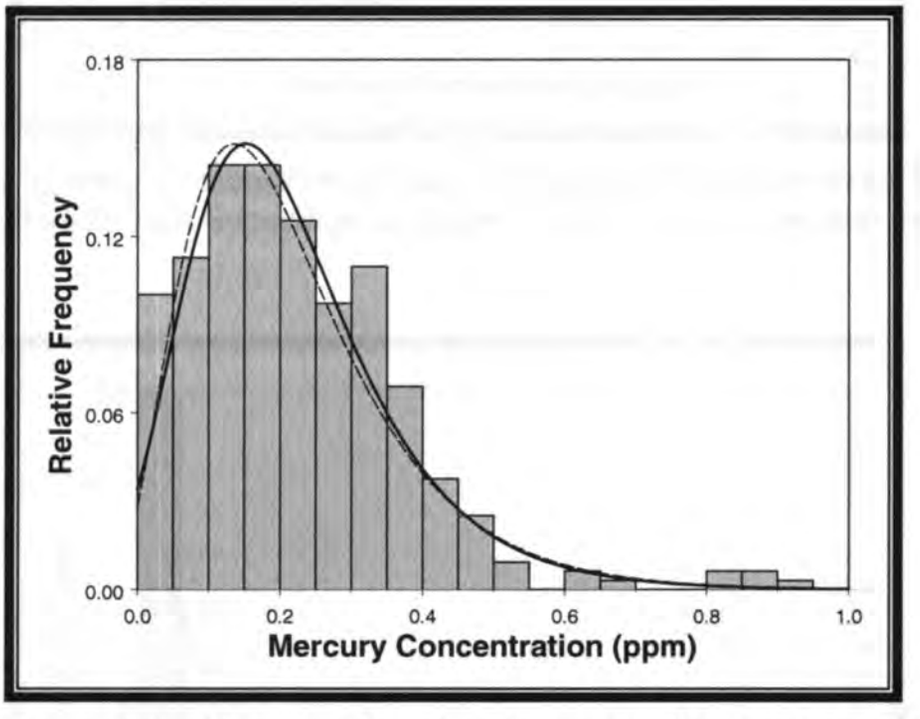

Figure 5–8. Observed Relative Frequency Distribution of Tuna with Fitted Extreme Value Distribution (solid line) and S–Distribution (dashed line) Superimposed (see Table 5–7 for parameter values)

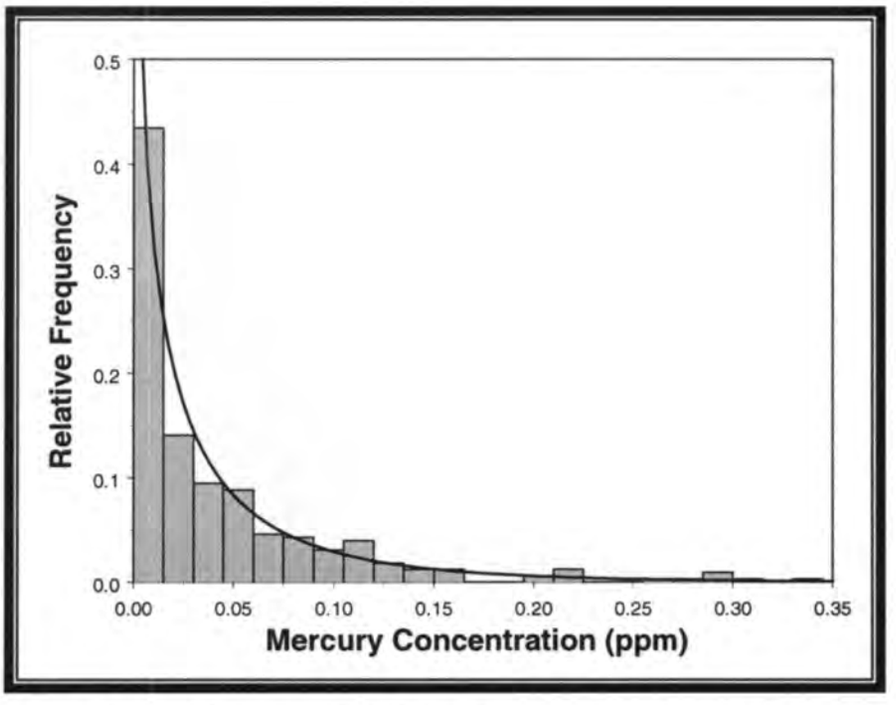

Figure 5–9. Observed Relative Frequency Distribution of Shrimp with Fitted Weibull Distribution Superimposed (see Table 5–7 for parameter values)

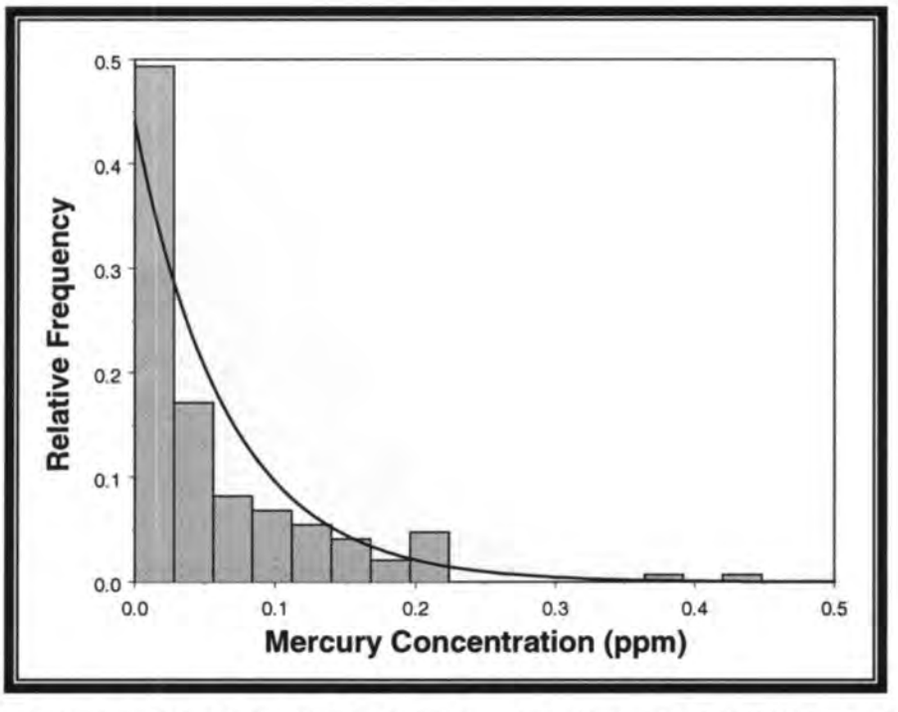

Figure 5–10. Observed Relative Frequency Distribution of Pollock with Fitted Exponential Distribution Superimposed (see Table 5–7 for parameter values)

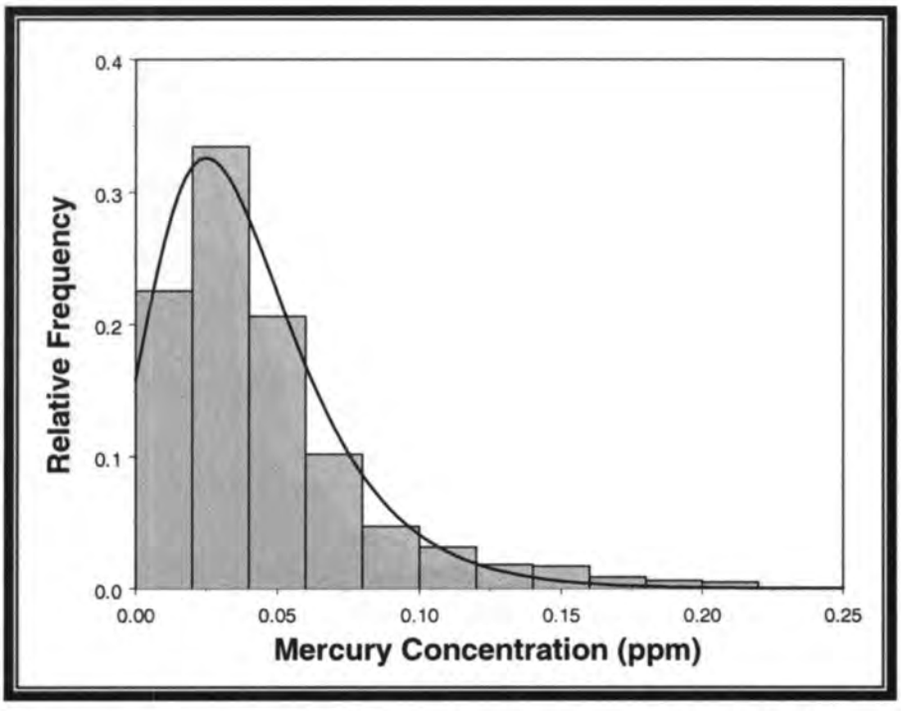

Figure 5–11. Observed Relative Frequency Distribution of Salmon with Fitted Extreme Value Distribution Superimposed (see Table 5–7 for parameter values)

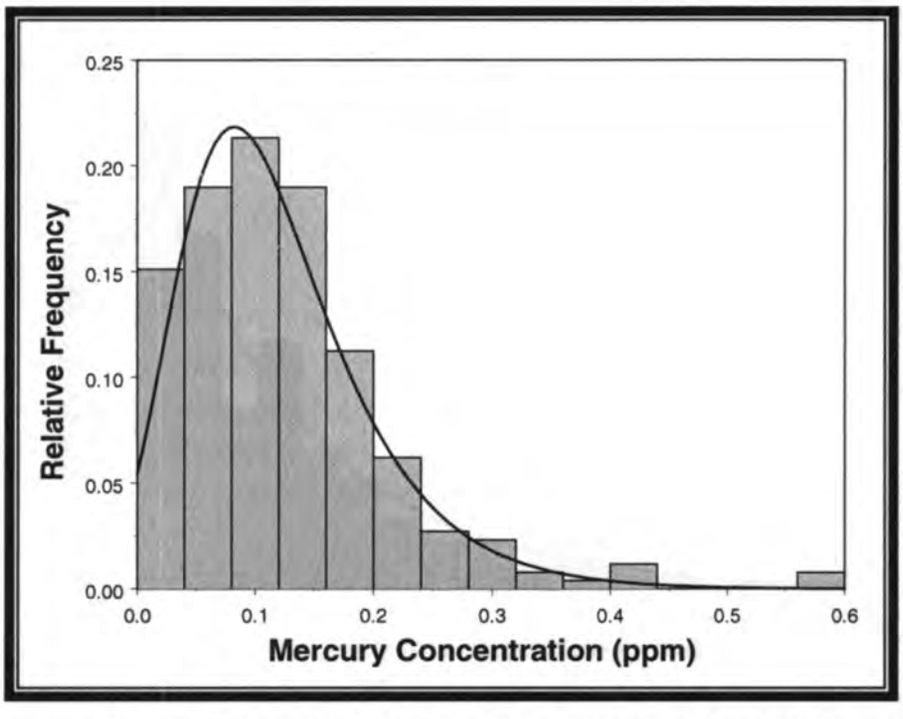

Figure 5–12. Observed Relative Frequency Distribution of Cod with Fitted Extreme Value Distribution Superimposed (see Table 5–7 for parameter values)

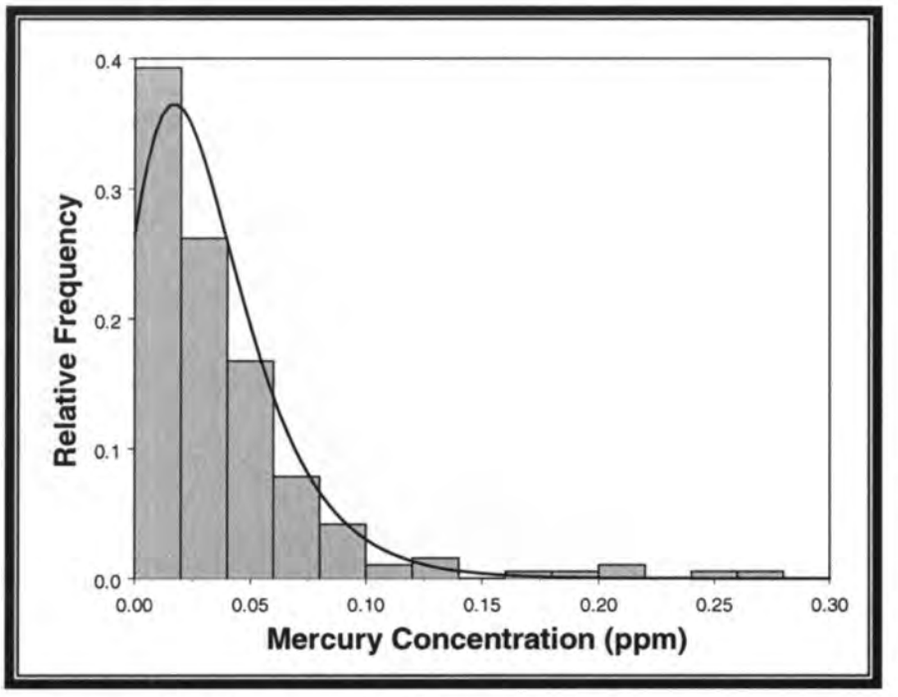

Figure 5–13. Observed Relative Frequency Distribution of Clams with Fitted Extreme Value Distribution Superimposed (see Table 5–7 for parameter values)

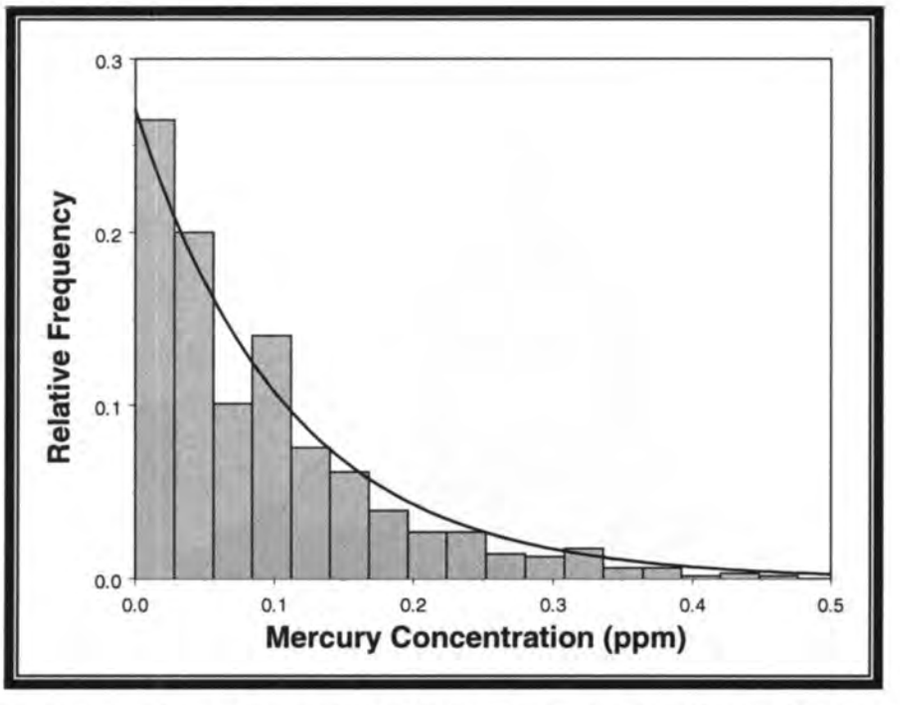

Figure 5–14. Observed Relative Frequency Distribution of Flounder with Fitted Exponential Distribution Superimposed (see Table 5–7 for parameter values)

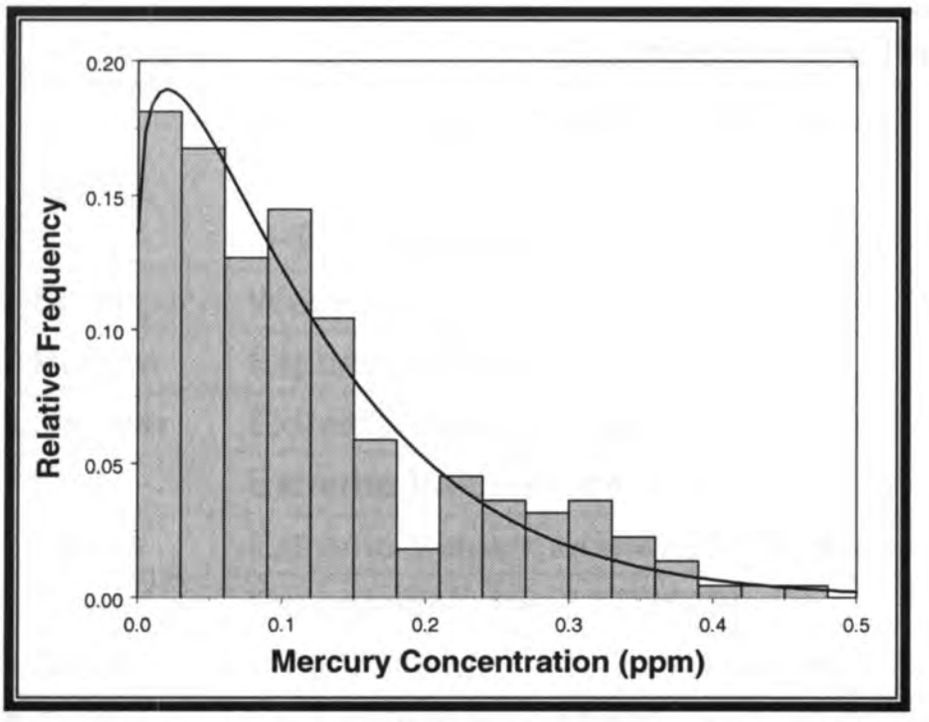

Figure 5–15. Observed Relative Frequency Distribution of Crab with Fitted Weibull Distribution Superimposed (see Table 5–7 for parameter values)

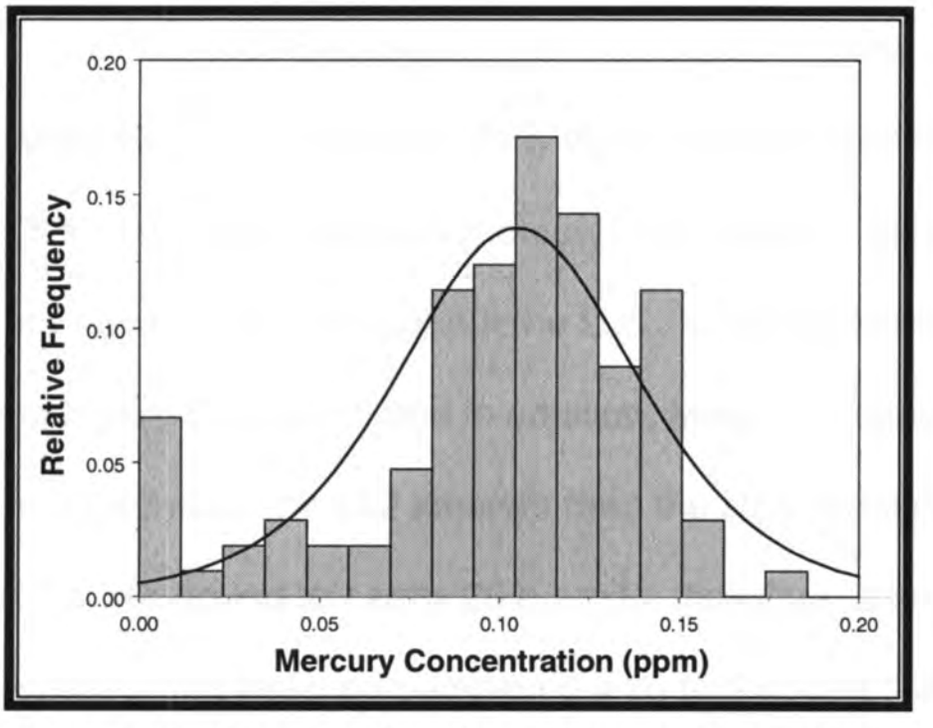

Figure 5–16. Observed Relative Frequency Distribution of Scallops with Fitted Logistic Distribution Superimposed (see Table 5–7 for parameter values)

Group	Distribution and Parameters
Tuna	Extreme Value(mode=0.15191, scale=0.11288) or S–Distribution(α=40.53566, g=0.8, h=1.0, median=0.18934)
Shrimp	Weibull(location=-0.00013, scale=0.03373, shape=0.71878851)
Pollock	Exponential(rate=15.15789)
Salmon	Extreme Value(mode=0.02486, scale=0.02482)
Cod	Extreme Value(mode=0.08223, scale=0.06286)
Clams	Extreme Value(mode=0.01698, scale=0.02397)
Flounder	Exponential(rate=11.03533)
Crabs	Weibull(location=-0.00099, scale=0.12235, shape=1.15059144)
Scallops	Logistic(mean=0.10486, scale=0.02240)

Table 5–7. Distributions and Parameter Values Characterizing Mercury Concentrations in the Most Frequently Consumed Seafood Groups

The NMFS survey of trace elements includes 642 Northern lobsters (see Appendix D) sampled primarily from the eight sites displayed in Figure 5–17. The association between mercury concentration and lobster weight is displayed in Figure 5–18. Throughout the U.S., a lobster must weigh at least one pound to be legally harvested, and in addition, Maine imposes an upper harvest limit of four pounds. The 642 lobsters from the NMFS data range in weight from less than one pound to nearly 20 pounds, therefore to be practical only the 507 lobsters that weighed between 0.4 kg (0.9 pounds) and 1.8 kg (4.0 pounds) were used for these research analyses. Figure 5–19 displays the lobster weight versus the mercury concentration for the 507 lobsters studied.

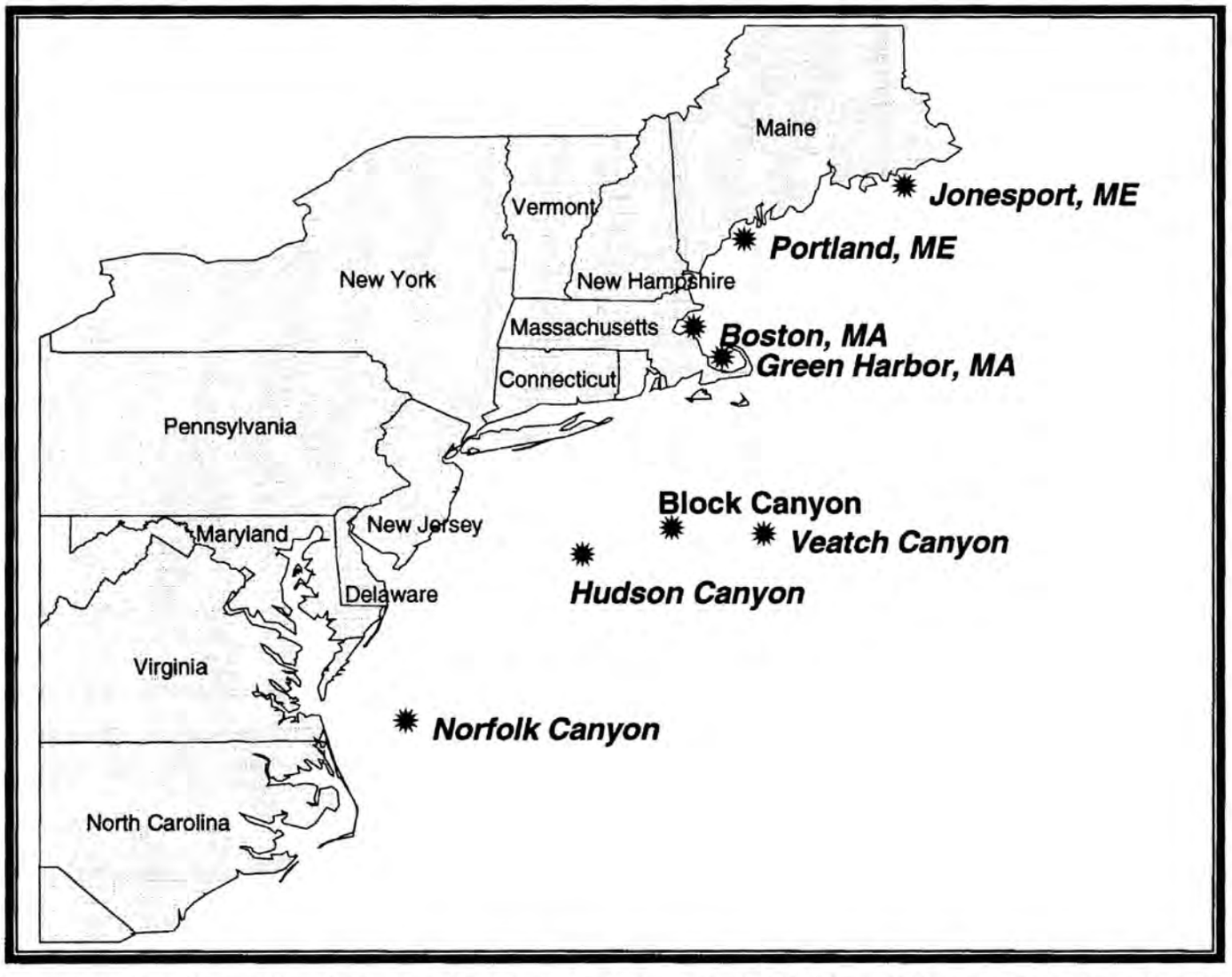

Figure 5–17. Sampling Sites for Northern Lobsters in the National Marine Fisheries Service Survey of Trace Elements

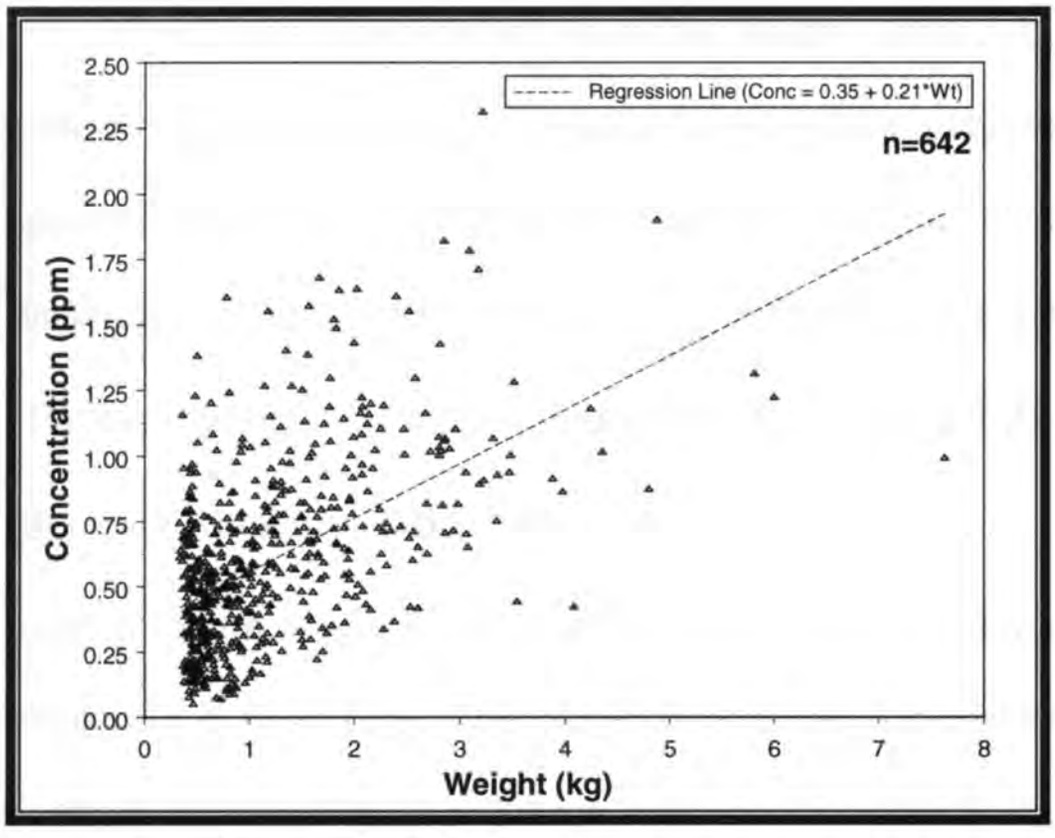

Figure 5–18. Association Between Northern Lobster Weight and Tail Meat Mercury Concentration with the Associated Linear Regression Line

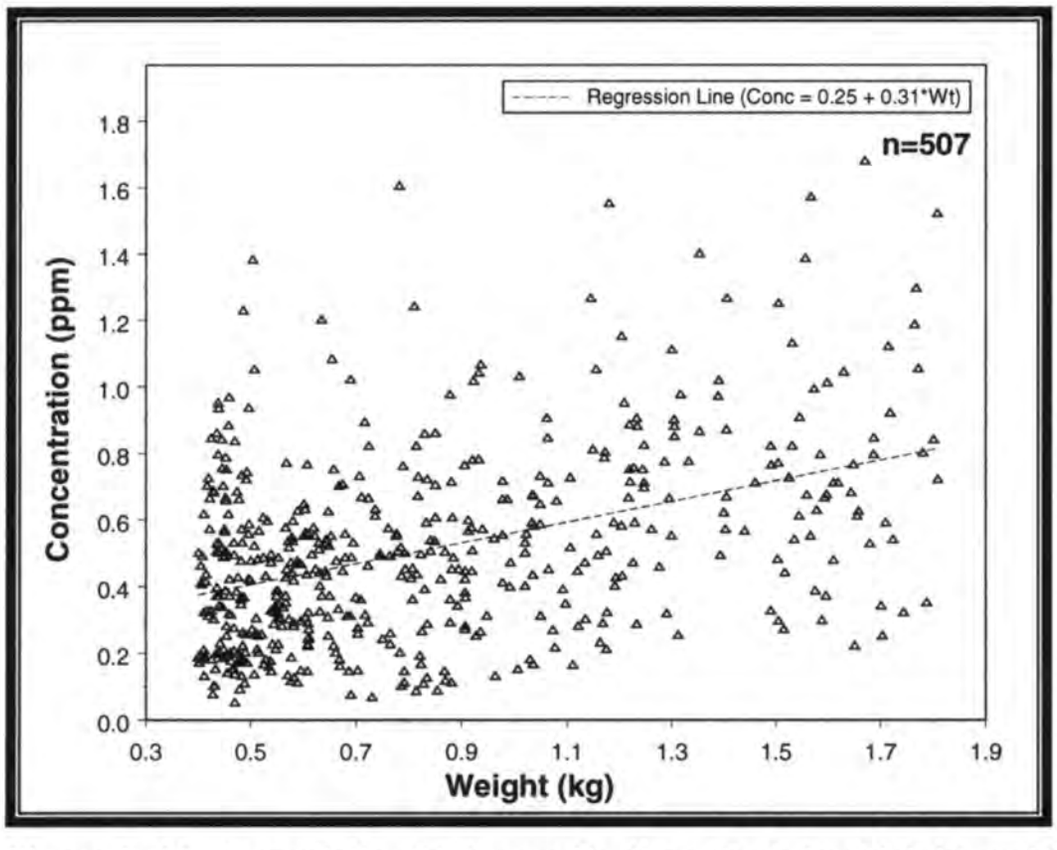

***Figure 5–19. Association Between Northern Lobster Weight and Tail Meat Mercury* Concentration for Lobsters Weighing Between 0.4 and 1.8 kg with the Associated Linear Regression Line**

For these research analyses four weight classes, based on the weight classes typically used in commercial sales, will be adopted to form weight–specific mercury concentration distributions. The four classes will be distinguished as follows: small (0.9 lbs. ≤ Weight < 1¼ lbs.), regular (1¼ lbs. ≤ Weight < 1¾ lbs.), large (1¾ lbs. ≤ Weight < 2½ lbs.), and jumbo (2½ lbs. ≤ Weight < 4 lbs.). The weight–specific mercury concentrations can be seen in Figure 5–20. S–distributions have been superimposed upon each histogram in this figure. The parameter values that characterize the S-distributions in Figure 5–20 are contained in Table 5–8.

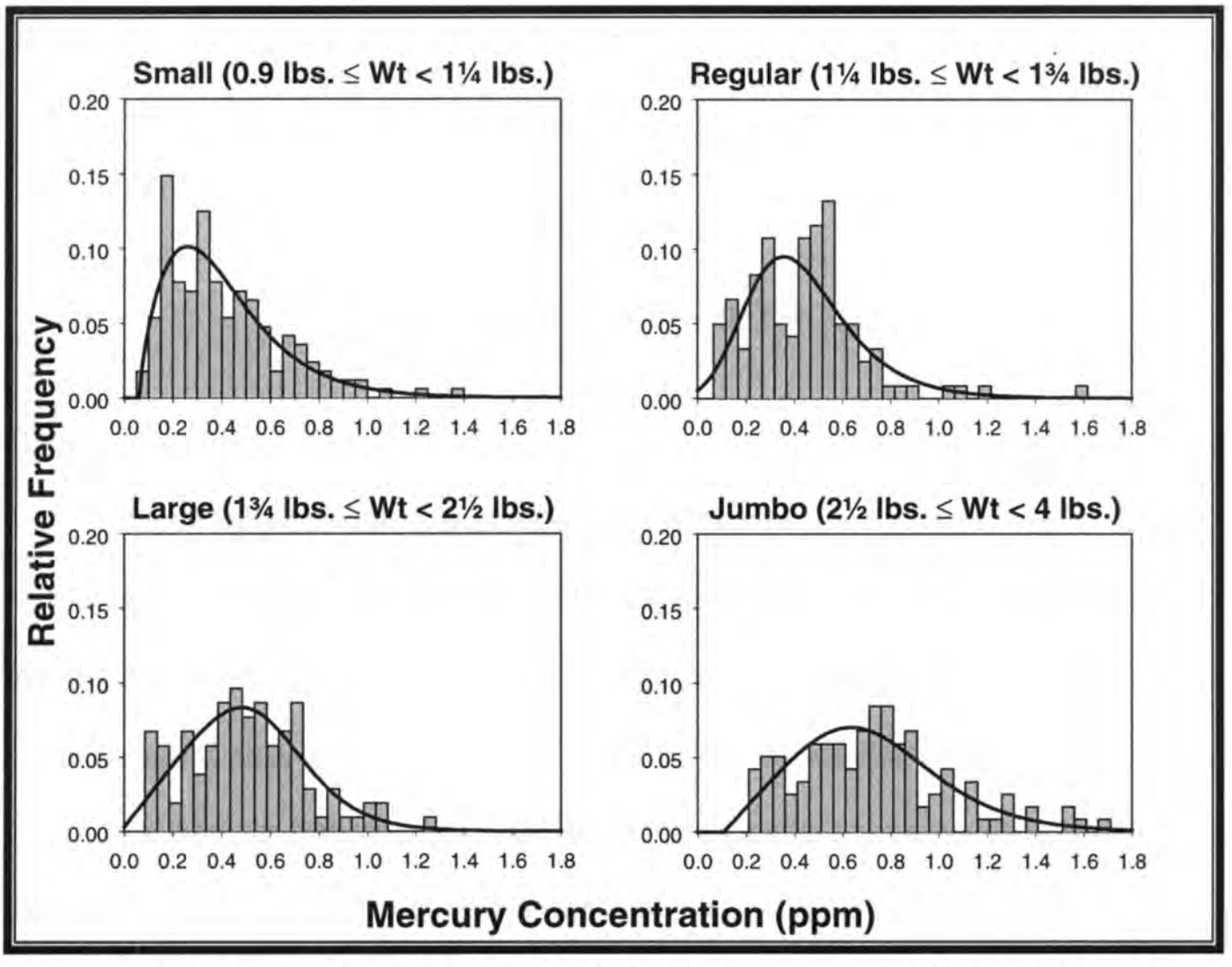

Figure 5–20. Observed Relative Frequency Distributions of Mercury Concentrations by Northern Lobster Weight Class with Fitted S–Distributions Superimposed (see Table 5–8 for parameter values)

Class	α	g	h	Median
Small	4.56876	0.4	1.5	0.36062
Regular	9.59494	0.8	1.4	0.41088
Large	2.87699	0.5	2.9	0.48445
Jumbo	2.61099	0.5	2.3	0.68915

Table 5–8. S–Distribution Parameter Values Characterizing Mercury Concentration by Northern Lobster Weight Class

Chapter 6

COMPARISON OF METHODS

Chapter Overview

This chapter contains a comparison of the five methods used to characterize mercury exposure from the consumption of Northern lobster. All of the exposures in this chapter apply to the general population; some additional scenarios and sub–groups of the general population are discussed in Chapter 7.

It is easy to become confused when comparing so many methods; therefore, a brief outline of this chapter is provided below for the benefit of the reader.

Point Estimates

Two point estimates of Equation (3.1) were performed as a part of this research; one estimated the central tendency and one the upper percentiles. The central tendency was estimated using the median values (0.478 μg/g for mercury concentration, 4.932 g/day for consumption rate, and 66.85 kg for body weight). The resulting exposure was 0.035 μg/kg/day.

The upper tail of exposure was estimated using the 95th percentile for mercury concentration and consumption rate because they appear in the numerator of Equation (3.1) and the 5th percentile for body weight because it appears in the denominator. Thus, the following values were used: 1.042 μg/g for mercury concentration, 12.712 g/day for consumption rate, and 16.4 kg for body weight. The resulting exposure was 0.808 μg/kg/day.

Just as point estimates only use a few values to characterize exposure, the sensitivity measure applied here simply uses a few values to characterize uncertainty and ignores all of the additional sample information.

A *Sensitivity Index* was formed using Equation (6.1), where E_{min} is the minimum exposure and E_{max} is the maximum exposure using the 1st and the 99th percentiles of the actual data for a variable of interest and the median values for all remaining variables (Hoffman and Gardner, 1983). It takes the form:

$$\text{Sensitivity Index} = 1 - \frac{E_{min}}{E_{max}} \qquad \textbf{(6.1)}$$

The 1st and 99th percentiles were used in place of the minimum and maximum values because Equation (6.1) is very sensitive to extreme values. With the large size of the data sets that were used to characterize the input distributions, it was more likely to have extreme minimum and maximum values. The 1st and 99th percentiles removed the effect of extreme outliers while still accounting for nearly all of a variable's range. The most sensitive variables will have a Sensitivity Index near one, while less sensitive variables have an Index value closer to zero.

The most sensitive variable was consumption rate with a Sensitivity Index of 0.98, then mercury concentration with a Sensitivity Index of 0.94, and finally body weight with a Sensitivity Index of 0.91. Although the sensitivity of the variables was ranked, the Sensitivity Indices did not differ too much for all three input variables. Thus all of the input variables seemed to evoke a significant effect on exposure.

The Sensitivity Index does lend a rough idea of uncertainty, but the correlation coefficients will provide a more accurate characterization of uncertainty as discussed earlier. Before the correlation coefficients can be computed, it is necessary to obtain the simulated data; thus, the other measures of uncertainty will be discussed after the simulations.

Traditional Monte Carlo Simulations

First, it was necessary to decide how many iterations were required for the traditional Monte Carlo simulation. Preliminary simulations were run using the

gamma distribution (location=0.0, scale=0.17, shape=3.06) to model mercury concentration, the logistic distribution (mean=5.42, scale=1.59) to model lobster consumption, and the logistic distribution (mean=62.36, scale=12.80) to model body weight (see Appendix B for additional distribution information). These distributions were obtained by entering the actual data values into Palisade's BestFit Version 2.0d. BestFit generates and compares 22 classic statistical distributions in a manner similar to that described for Crystal Ball in the *Contaminant Data* section of Chapter 5 (Palisade Corporation, 1997b). Distribution parameters were calculated using maximum–likelihood estimators, and then potential distributions were compared using the Kolmogorov–Smirnov test, the Anderson–Darling test, and graphs of the actual values superimposed with the fitted distribution (Palisade Corporation, 1997b). Fifty preliminary simulations using the selected distributions were carried out using Palisade's @Risk Version 3.5. All preliminary simulations stabilized by 3,500 iterations, where stabilization was defined as the mean, median, standard deviation, and every fifth percentile changing less than 3% from one batch of 100 to the next. Based on these results, it was decided that 10,000 iterations would be used for the traditional Monte Carlo simulation because the additional time and computer memory requirements associated with a few thousand iterations were negligible. A diagram of the traditional Monte Carlo process specific to this problem is given in Figure 6–1.

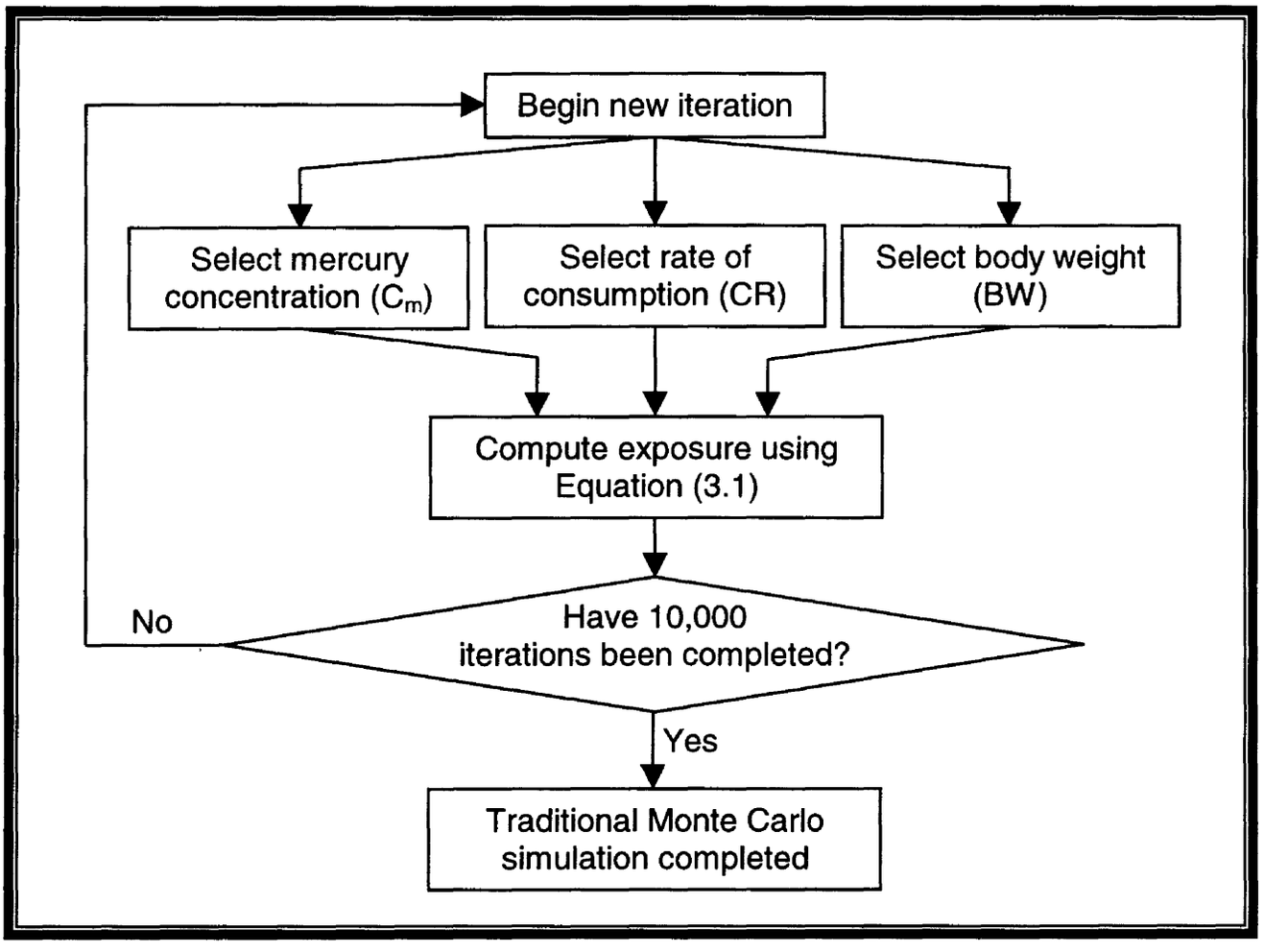

Figure 6–1. Traditional Monte Carlo Simulation Procedure Specific to This Research Problem

The traditional Monte Carlo simulation resulted in 0.038, 0.161, 0.351, and 0.498 μg/kg/day for the 50th, 95th, 99th, and 99.5th percentiles respectively. The central tendency point estimate is comparable to the median (50th percentile), yet the upper percentile point estimate is over five times greater than the 95th percentile from the traditional simulation. The distribution of simulated exposures is given in Figure 6–2. The simulated exposures were fit to classic statistical distributions using Crystal Ball and SAS (SAS Institute, Inc., Cary, NC). SAS became necessary with the large number of exposures from the two–dimensional and hierarchical two–dimensional simulations. Using Crystal Ball, a lognormal distribution (μ=0.0587, σ=0.0759) most accurately fit the data. This is

logical as the multiplication of several input variables tends to produce an output variable with lognormal characteristics, regardless of the input variable distributions (Burmaster and Hull, 1997). The empirical distribution of the exposure data is provided in Figure 6–3, where the probability associated with an exposure represents the percent of simulated exposures below the referenced exposure.

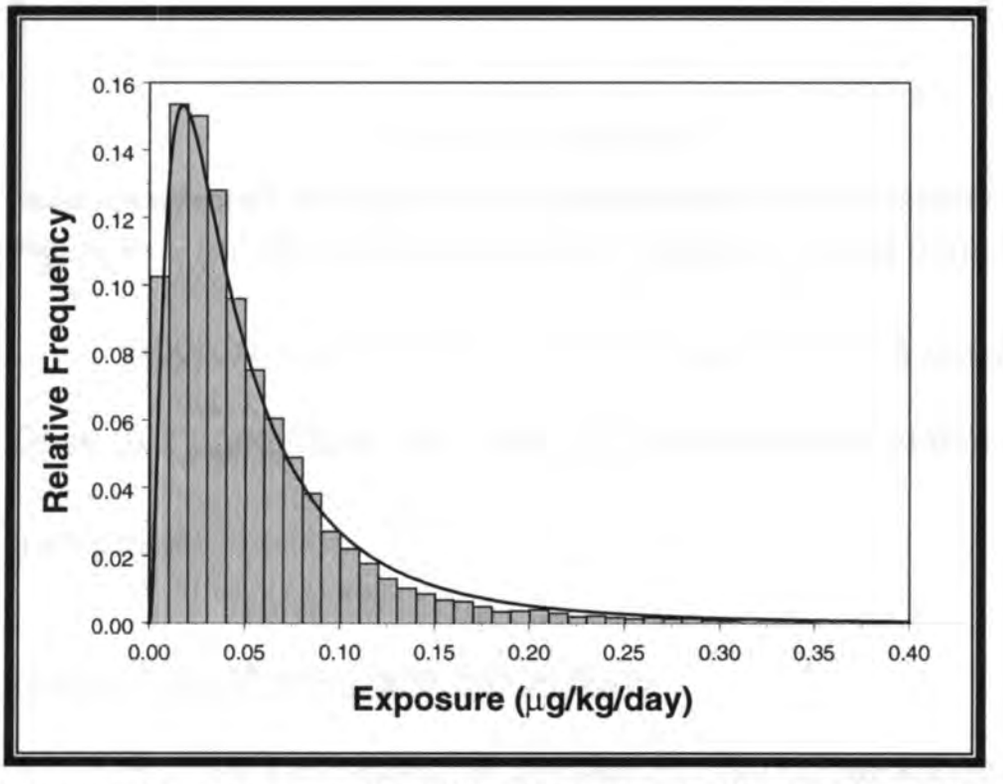

Figure 6–2. Exposures Resulting from the Traditional Monte Carlo Simulation Superimposed with a Lognormal PDF

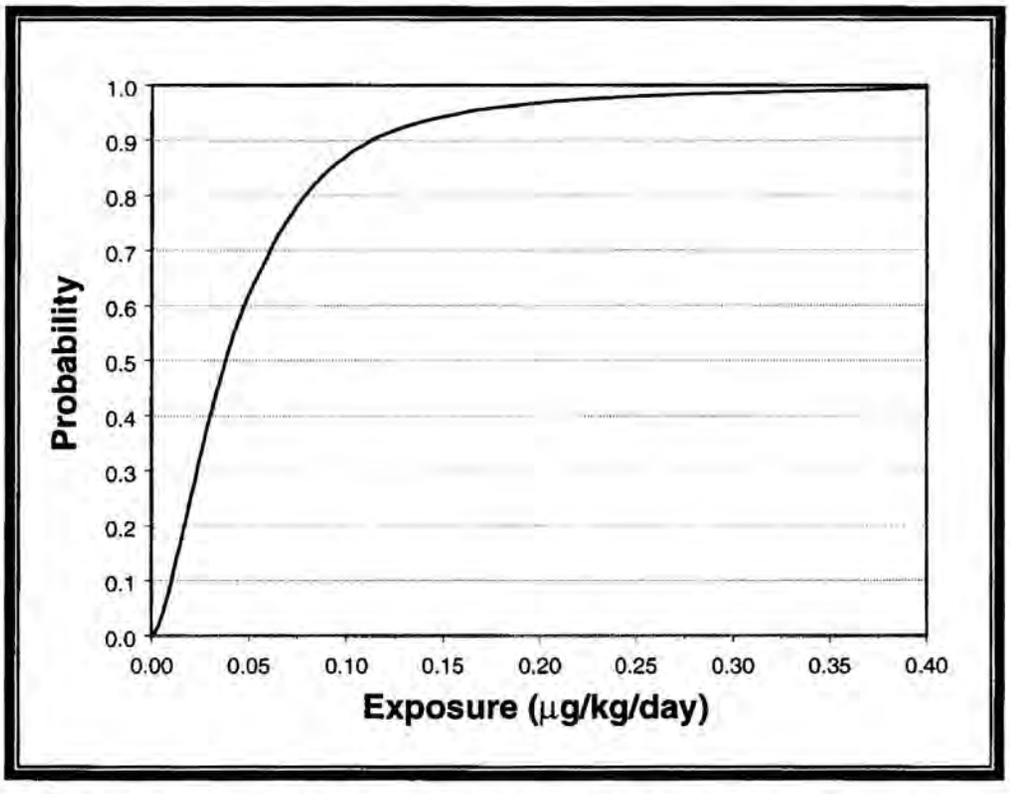

Figure 6–3. Empirical Distribution from Traditional Monte Carlo Simulation Data

Approximately 12.8% of the simulated results surpassed EPA's Reference Dose (0.1 µg/kg/day), yet only 0.5% surpassed ATSDR's Minimal Risk Level (0.5 µg/kg/day).

Hierarchical Monte Carlo Simulations

As with the traditional simulation, 10,000 iterations were performed for the hierarchical Monte Carlo simulation. Again, this is a bit conservative, but the additional time and computer memory requirements were negligible for the additional iterations.

A consumer age class and gender along with a lobster weight class had to be selected at the beginning of each hierarchical simulation iteration. The age was chosen based on the proportion of individuals in each age class from the 1993 Current Population Survey (NCHS, 1996), and each gender had an equal

probability of selection. The probability of selecting a lobster weight class was based on the proportion of lobsters from each weight class that were caught in Maine waters during 1997 as reported by the Maine Lobster Institute at the University of Maine (personal communication).

A diagram of the hierarchical Monte Carlo process specific to this problem is given in Figure 6–4.

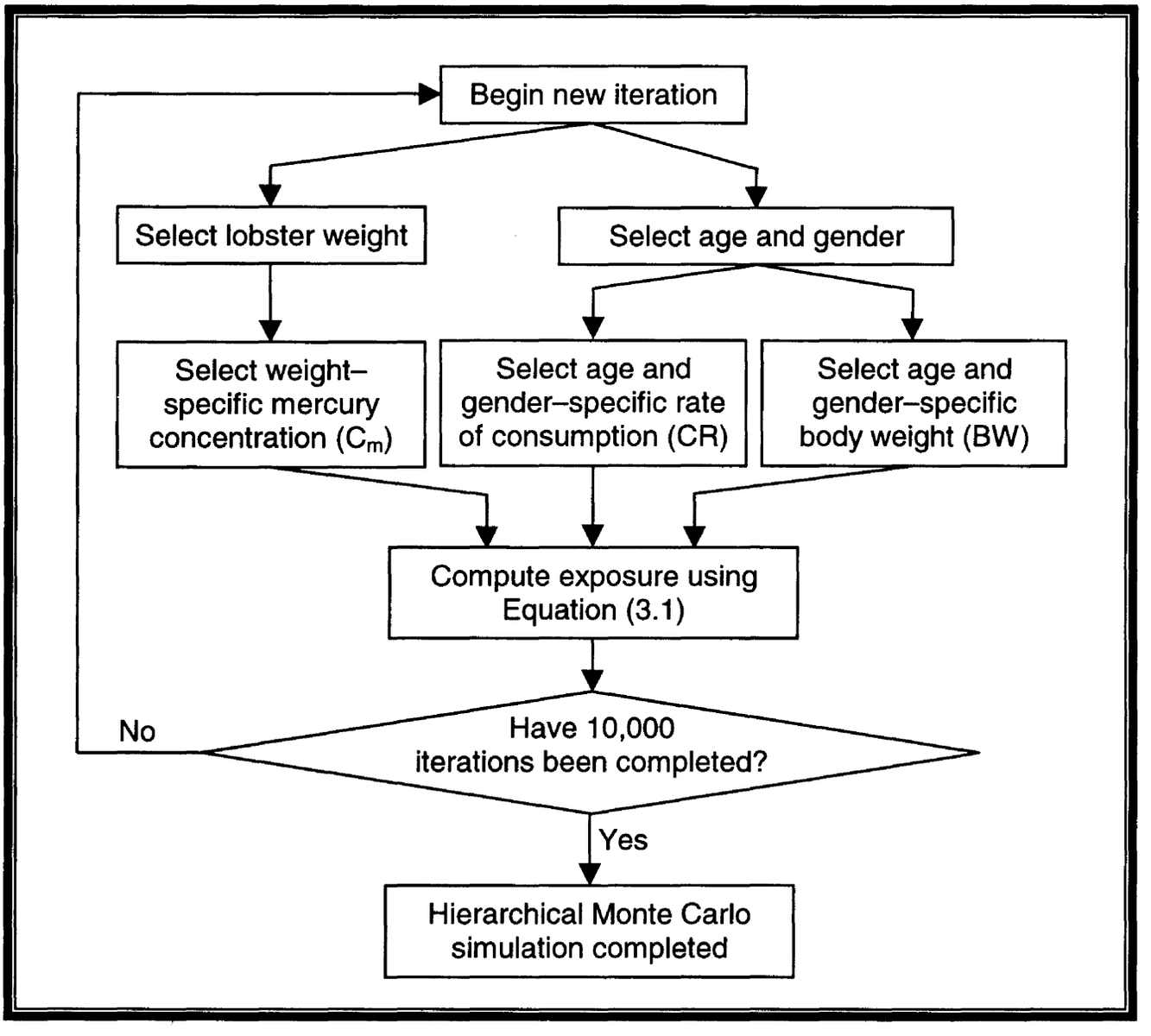

Figure 6–4. Hierarchical Monte Carlo Simulation Procedure Specific to This Research Problem

The hierarchical Monte Carlo simulation resulted in 0.032, 0.117, 0.213, and 0.256 μg/kg/day for the 50^{th}, 95^{th}, 99^{th}, and 99.5^{th} percentiles respectively.

The central tendency point estimate is comparable to the median (50th percentile), yet the upper percentile point estimate is almost seven times greater than the 95th percentile from the hierarchical simulation. The distribution of exposures from the simulation is given in Figure 6–5. Using Crystal Ball, a lognormal distribution (μ=0.0454, σ=0.0503) most accurately fit the data. The empirical distribution of the exposure data is provided in Figure 6–6.

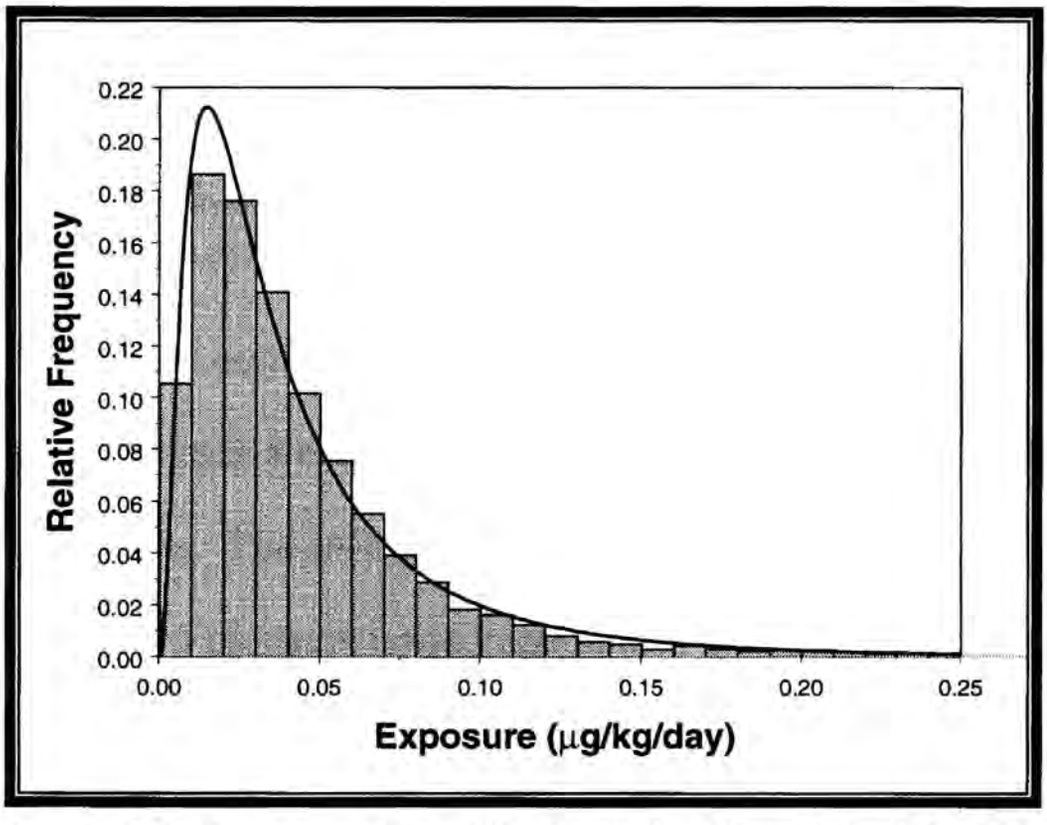

Figure 6–5. Exposures Resulting from the Hierarchical Monte Carlo Simulation Superimposed with a Lognormal PDF

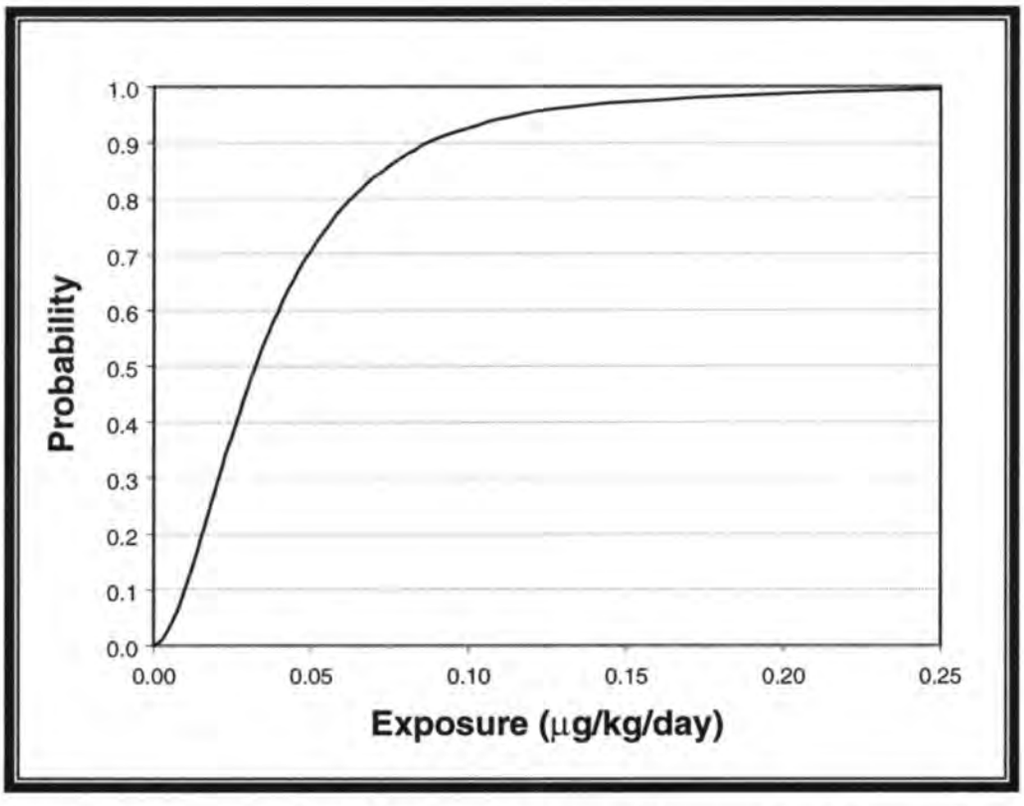

Figure 6–6. Empirical Distribution from Hierarchical Monte Carlo Simulation Data

The correlation between lobster consumption rate and consumer body weight should be stronger with the hierarchical simulation than the traditional simulation. The utility of the hierarchical method is evident as the correlation coefficient between consumption rate and body weight was 0.32 using the hierarchical simulation data, yet only –0.01 using the traditional simulation data. The relationship between consumption rate and body weight from both the traditional and hierarchical simulations is displayed in Figure 6–7 and Figure 6–8, respectively.

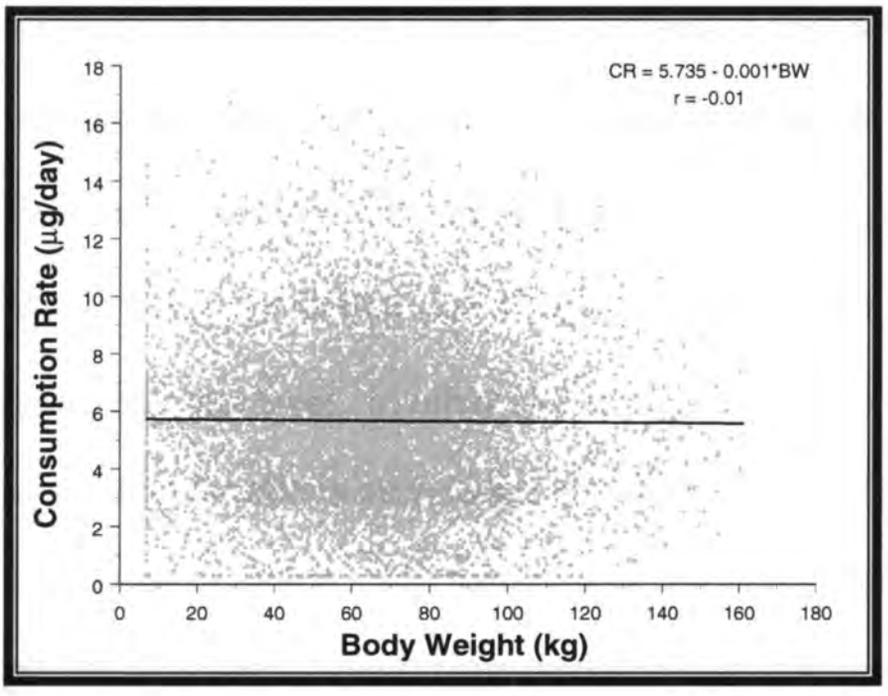

Figure 6–7. Association Between Northern Lobster Consumption Rate and Consumer Body Weight using Traditional Monte Carlo Simulation Data with the Linear Regression Line Superimposed

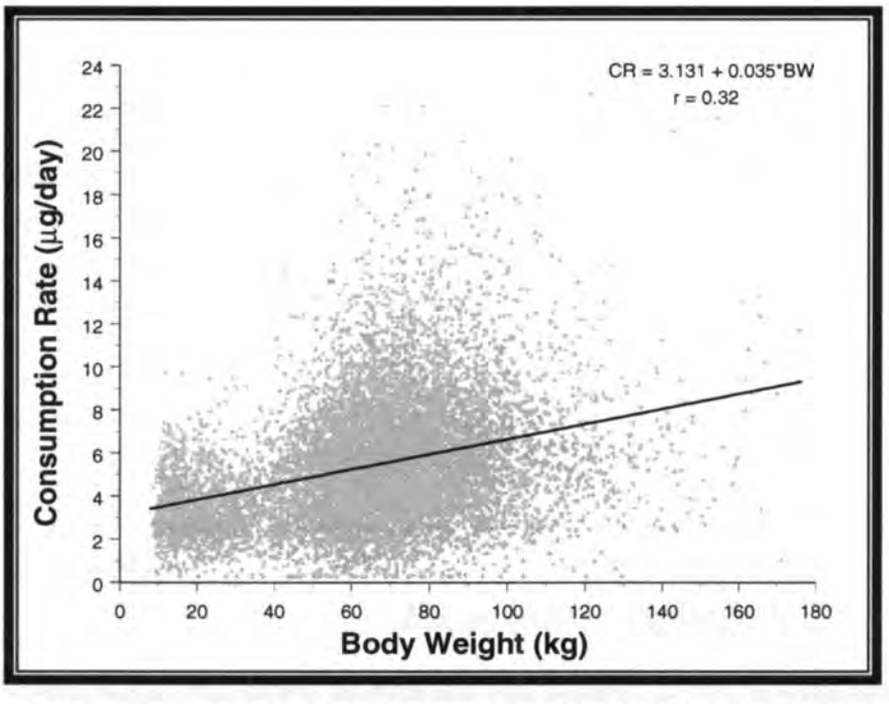

Figure 6–8. Association Between Northern Lobster Consumption Rate and Consumer Body Weight using Hierarchical Monte Carlo Simulation Data with the Linear Regression Line Superimposed

The distribution of exposures from the hierarchical simulation has less probability in the higher exposures than the distribution from the traditional simulation, as evidenced by Figure 6–9. For example, only 7.5% of the

hierarchical simulation exposures exceeded EPA's Reference Dose (0.1 μg/kg/day), whereas 12.8% of the traditional simulation exposures did. And fewer than 0.1% of the hierarchical simulation results surpassed ATSDR's Minimal Risk Level (0.5 μg/kg/day), yet 0.5% of the traditional simulation results exceeded this level. In other words, approximately one of every 200 traditional simulation iterations surpassed ATSDR's Minimal Risk Level, whereas only about one of every 3,500 hierarchical simulation iterations did.

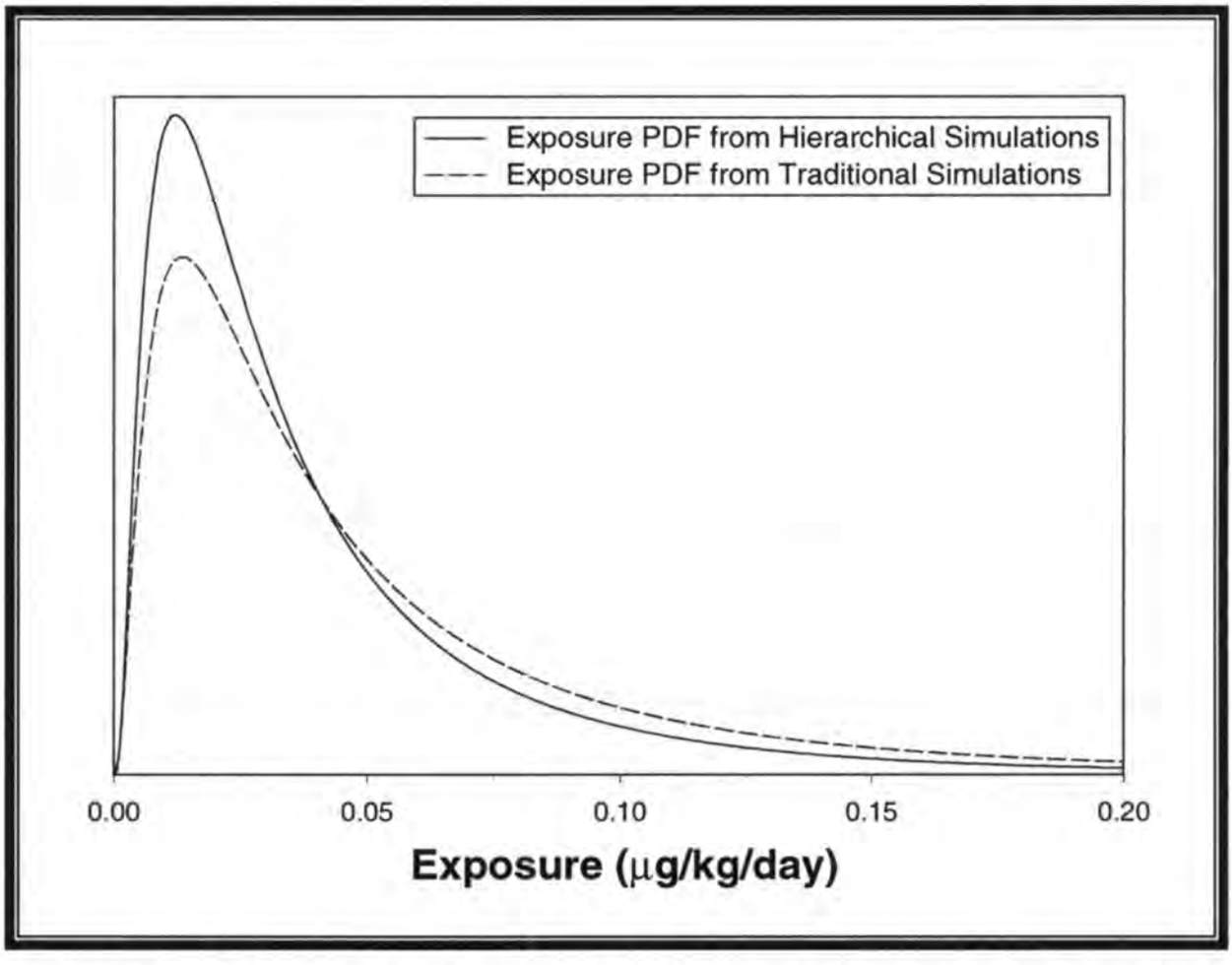

Figure 6–9. A Comparison of Exposure PDFs from Traditional and Hierarchical Simulation Data

Two–Dimensional Monte Carlo Simulations

Again it was first necessary to first decide how many iterations were required for the two–dimensional simulation. The preliminary simulations

previously described in the *Traditional Monte Carlo Simulations* section were used to estimate the required number of inner loop iterations. Fifty–eight percent of the preliminary simulations stabilized by 1,700 iterations and 88% by 1,800 iterations. Thus based on these results, it was decided that the inner loop of the two–dimensional Monte Carlo simulation would contain 1,800 iterations.

Estimating the number of iterations required for the outer loop was more involved. First, it was decided that only mercury concentration and lobster consumption rate would have uncertainty, as uncertainty associated with body weight is negligible (EPA, 1994; Finley *et al.*, 1994; Cohen *et al.*, 1996; Rai *et al.*, 1996).

It was also assumed that the uncertainty due to limited sample sizes was manifest in the location, rather than the shape, of the input distribution. Thus, the S–distribution would have uncertainty associated only with the initial value of the differential equation, where the median was used for the initial value in this research.

A parametric bootstrap technique was employed to estimate the uncertainty associated with the median (Frey and Rhodes, 1996, 1998; Werckman and Wainwright, 1998). The parametric bootstrap quantifies the sampling error introduced by calculating a statistic from a limited sample size. The n sample data points, $\boldsymbol{x} = \{x_1, x_2, \ldots, x_n\}$, are assumed to be a random sample from some unknown probability distribution that will be referred to as the

parent distribution or simply P. λ, the parameter of interest, is some function or characteristic of the parent distribution such that $\lambda = f(P)$.

The unknown parent distribution, P, is estimated by $\hat{P}$, the distribution that best characterizes the sample data points, **x**. The sample data points may also be used to calculate the statistic $\hat{\lambda}$, an estimate of the parameter λ.

The parametric bootstrap determines the effect if **x** were n different random samples from $\hat{P}$. Thus, each bootstrap consists of drawing n random samples from the parent distribution, $\hat{P}$, and computing $\hat{\lambda}$ from the sample. A large number, n_b, of bootstrap samples are selected, and the statistic of interest is calculated from each bootstrap sample. The n_b estimates are then used to characterize the uncertainty introduced by calculating the statistic from a limited sample size of n.

For this research, the parent distribution was obtained by fitting the n data values to the most appropriate classical distribution. One thousand bootstraps of n random samples were then drawn from this parent distribution, and the median was computed from each bootstrap sample. The combined bootstrap samples thus resulted in 1,000 median estimates, all of which were combined to form a distribution of medians. The normal distribution accurately modeled the median values each time. Each distribution of medians was used to characterize the location uncertainty associated with limited sample sizes in the two–dimensional simulation. The process is reviewed in Figure 6–10. The bootstrap technique

was performed using the complete data set for the two–dimensional simulation and also subsets of the data for the hierarchical two–dimensional simulation.

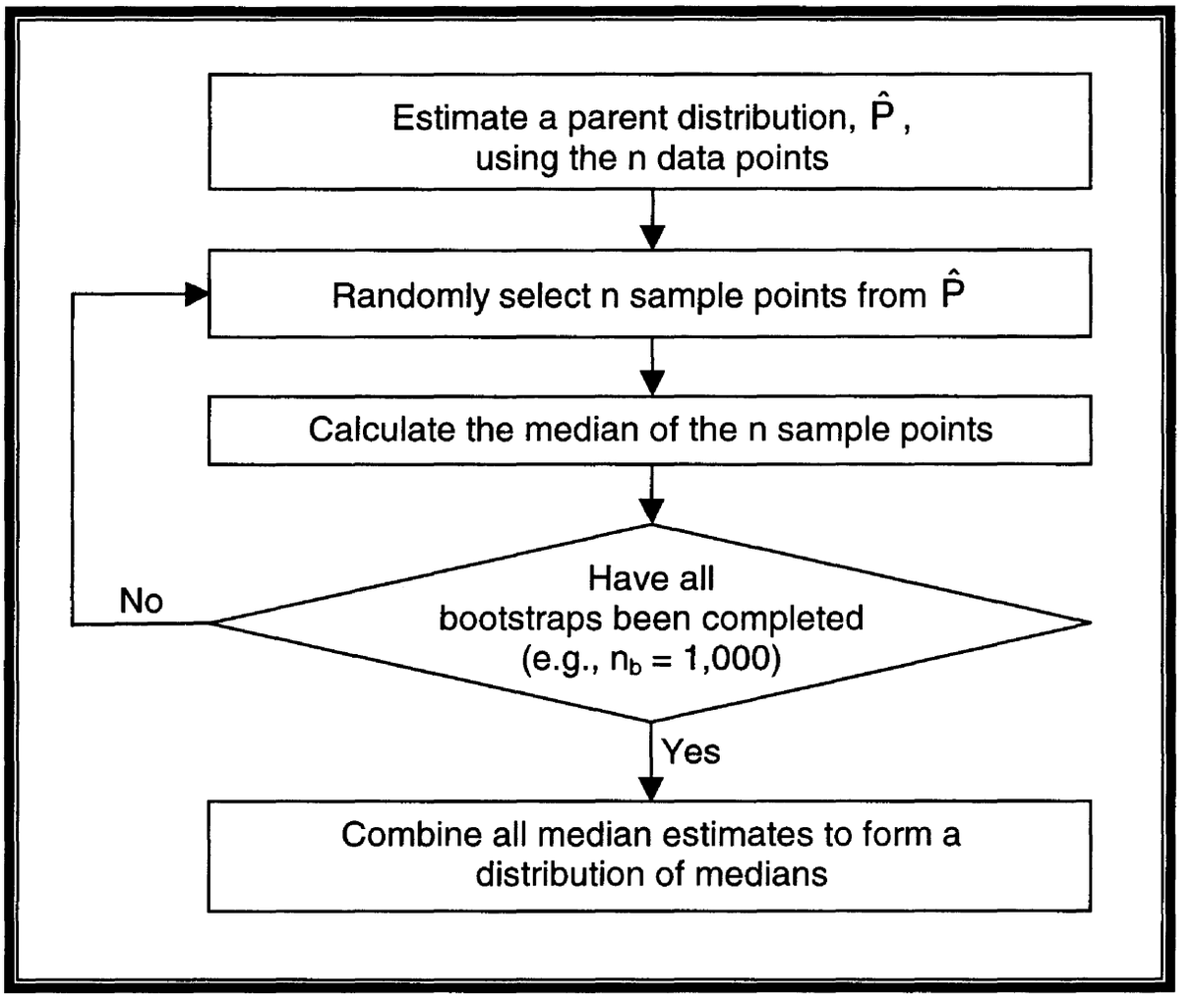

Figure 6–10. The Bootstrap Procedure Used to Characterize Uncertainty in the Median

The parent distributions, trials per sample, and the resulting distributions used to represent median uncertainty for mercury concentration and lobster consumption rate are listed in Table 6–1 (see Appendix B for additional distribution information). Both the parent and median uncertainty distributions were obtained using Crystal Ball in the same manner described in the *Contaminant Data* section of Chapter 5.

	Parent Distribution	Trials per Sample	Median Uncertainty
Mercury Concentration	Weibull (0.039, 0.526, 1.68)	507	Normal (0.462, 0.00239)
Lobster Consumption Rate	Logistic (164.88, 48.22)	638	Normal (164.700, 0.828)

Table 6–1. Median Uncertainty Distributions Resulting from Bootstrapping Mercury Concentration and Consumption Rate Distributions

The number of trials necessary for stabilization in the outer loop of the two–dimensional simulation was now estimated using the median uncertainty distributions. The distribution of medians for teen consumption had the most variability with a standard deviation and mean of approximately 13 and 124 g/month respectively. Consequently, fifty simulations using a normal distribution (mean=124, standard deviation=13) were performed with @Risk (see Appendix B for additional distribution information). Stabilization was defined as the mean, median, standard deviation, and every fifth percentile changing less than 1.5% from one batch of 100 to the next. Stabilization was defined more conservatively here than for the estimation of the inner loop sample size because only one distribution was used to estimate the outer loop sample size. Sixty percent of the simulations stabilized by 600 iterations, 84% by 700 iterations, and 92% by 800 iterations. Based on these results, it was decided that the outer loop of the two–dimensional Monte Carlo simulation would contain 800 iterations.

Each two–dimensional Monte Carlo simulation now resulted in 1,440,000 total iterations. Due to computational limitations, each two–dimensional and hierarchical two–dimensional simulation had to be performed in 16 batches with

an outer loop sample size of 50 and the full inner loop sample size of 1,800. Every batch required approximately 30–45 minutes to run, extract, and save the results. Over 200 megabytes were necessary to store the data and simulation information from each two–dimensional Monte Carlo simulation. A diagram of the two–dimensional Monte Carlo process specific to this problem is given in Figure 6–11.

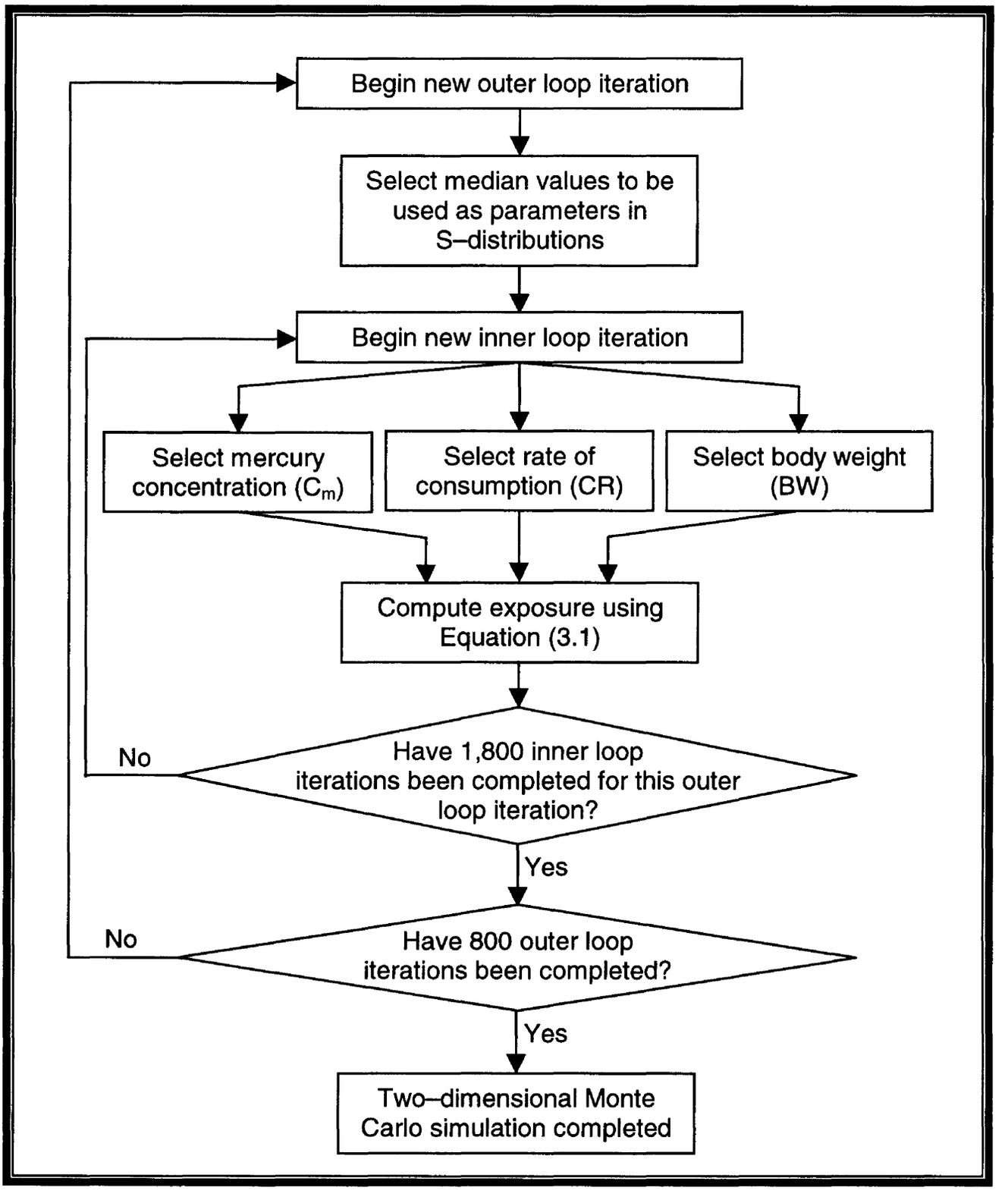

Figure 6–11. Two–Dimensional Monte Carlo Simulation Procedure Specific to This Research Problem

Each inner loop in a two–dimensional simulation produced a distribution of exposures. In the literature, the different inner loop distributions are often referred to as *alternate realizations*. Figure 6–12 contains a sample of ten alternate realizations of exposure from the two–dimensional simulation. The

uncertainty is evident as the curves are not identical. Exposures at every fifth percentile (i.e., 0.00, 0.05, 0.10, ..., 1.00), called *icosatiles*, were calculated and stored for each inner loop. This resulted in 800 exposure estimates at each icosatile. In Figure 6–13, the median exposure at each icosatile is given as a solid line, and ninety–five percent of the exposures at each icosatile lie between the dashed lines. Thus 95 percent of the realizations fall within the 95^{th} percentile boundaries. Figure 6–13 may be interpreted in one of the following two ways: 95 percent of the alternate realizations had somewhere between 12 and 14% of the individuals exceeding an exposure of 0.10 μg/kg/day, or 95 percent of the alternate realizations resulted in a 90^{th} percentile somewhere between 0.11 and 0.12 μg/kg/day. The maximum exposures (probability=1.00 in Figure 6–13) were not graphed as the values were too large. The median of the maximum exposures was 1.15 μg/kg/day, and the upper and lower 95^{th} percentiles were 1.97 and 0.71 μg/kg/day respectively.

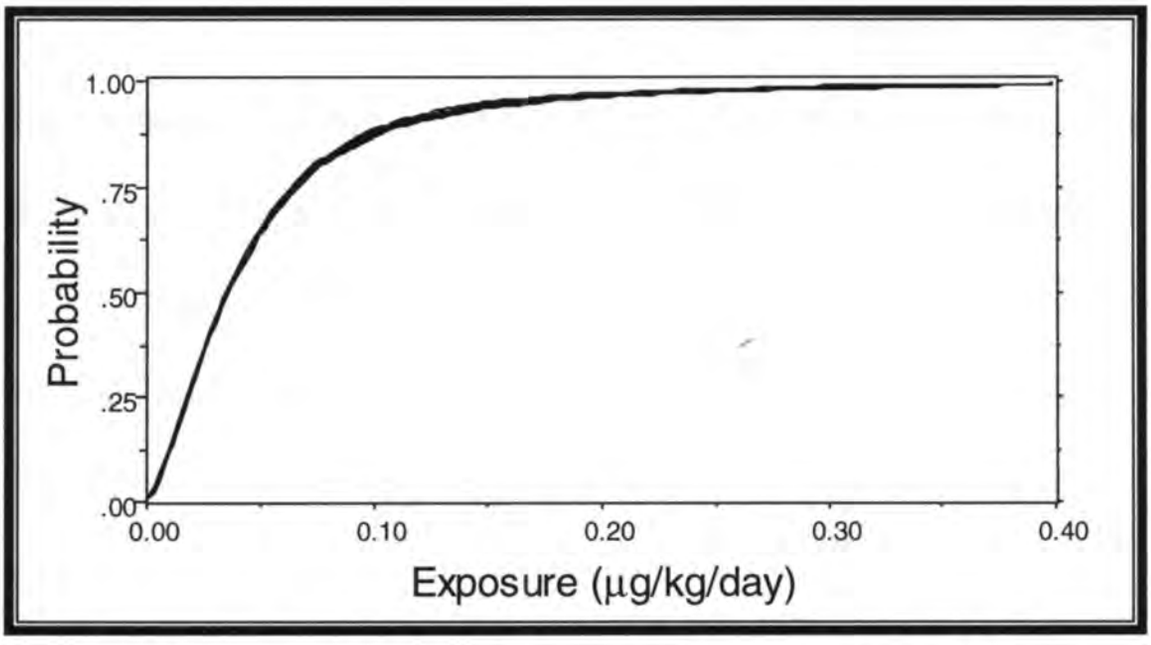

Figure 6–12. A Sample of Ten Alternate Realizations from the Two–Dimensional Monte Carlo Simulation

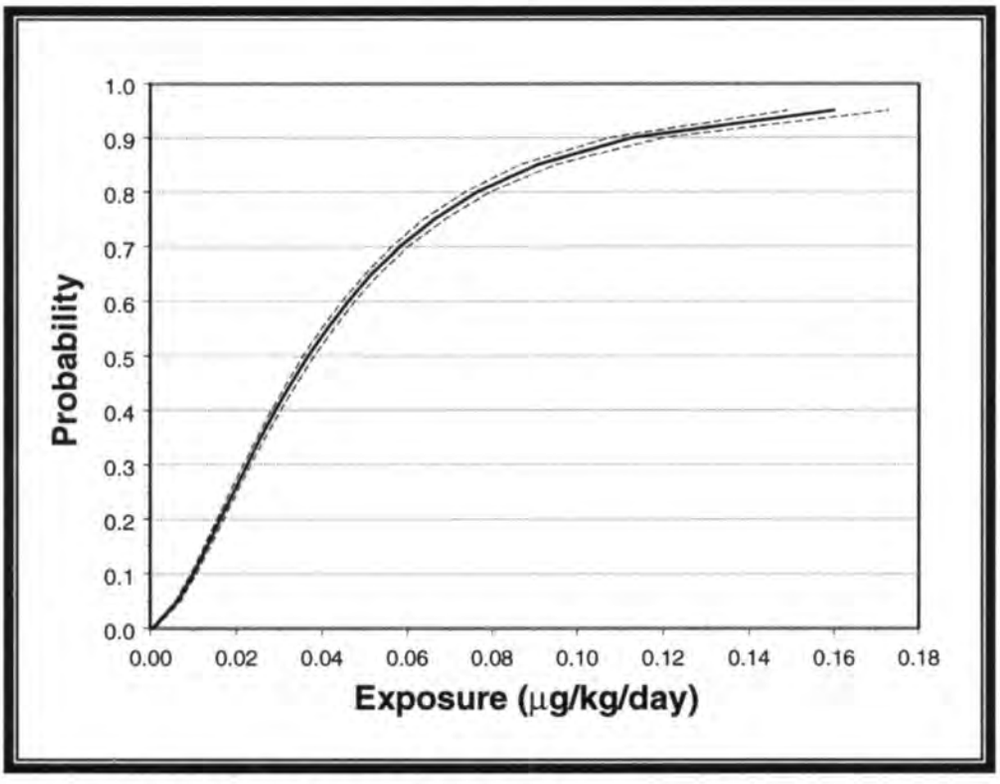

Figure 6–13. The Median Empirical Distribution (solid line) with 95th Percentiles (dashed lines) for the Two–Dimensional Monte Carlo Simulation

The two–dimensional simulation resulted in 0.037, 0.161, 0.362, and 0.497 µg/kg/day for the 50th, 95th, 99th, and 99.5th percentiles respectively. It is interesting that these exposure percentiles are nearly identical to those obtained

from the traditional Monte Carlo simulation. In addition to the percentiles, the distribution of exposures from this simulation was essentially identical to the distribution of exposures from the traditional simulation, which is logical since the two–dimensional simulation method only differs from the traditional method by distinguishing between variability and uncertainty. Using SAS, it was determined that the two–dimensional exposures were most accurately fit by a lognormal distribution (μ=0.0574, σ=0.0747).

Approximately 12.6% of the simulated results surpassed EPA's Reference Dose (0.1 μg/kg/day), yet only 0.5% exceeded ATSDR's Minimal Risk Level (0.5 μg/kg/day).

The uncertainty associated with limited sample sizes was not great in the two–dimensional simulation as evidenced by the close fit of the 95th percentile bands in Figure 6–13. This is not surprising as the sample sizes were very large. Over 500 mercury concentrations were used, with an analytical cost of $75 per lobster and additional costs for collecting the lobsters. Over 600 individuals who consumed Northern lobster were located, but recall that these 600 individuals came from a sample of 23,213 seafood consumers.

In order to see how the two–dimensional simulation performs with more uncertainty, a second two–dimensional simulation was run using reduced sample sizes. The entire process was repeated assuming that only 25 mercury concentrations were obtained and only 50 lobster consumers were located. The

distributions of medians used to characterize uncertainty associated with the limited sample sizes in this simulation are given in Table 6–2.

	Data Distribution	Trials per Sample	Median Uncertainty
Reduced Mercury Concentration Data Set	Weibull (0.039, 0.526, 1.68)	25	Normal (0.462, 0.0592)
Reduced Consumption Rate Data Set	Logistic (164.88, 48.22)	50	Normal (163.187, 9.477)

Table 6–2. Median Uncertainty Distributions Resulting from Bootstrapping the Reduced Data Sets for Mercury Concentration and Consumption Rate

Figure 6–14 contains a sample of ten alternate realizations of exposure from this two–dimensional simulation. The uncertainty from the reduced sample sizes is evident as the curves are considerably different. Once again, exposures at the icosatiles were calculated and stored for each inner loop. In Figure 6–15, the median exposure at each icosatile is given as a solid line, and ninety–five percent of the exposures at each icosatile lie between the dashed lines. Thus 95 percent of the realizations fall within the 95th percentile boundaries. Figure 6–15 may be interpreted in one of the following two ways: 95 percent of the alternate realizations had somewhere between 8 and 17% of the individuals exceeding an exposure of 0.10 μg/kg/day, or 95% of the alternate realizations resulted in a 90th percentile somewhere between 0.09 and 0.14 μg/kg/day. The maximum exposures (probability=1.00 in Figure 6–15) were not graphed as the values were too large. The median of the maximum exposures was 1.12 μg/kg/day, and the upper and lower 95th percentiles were 2.08 and 0.65 μg/kg/day respectively.

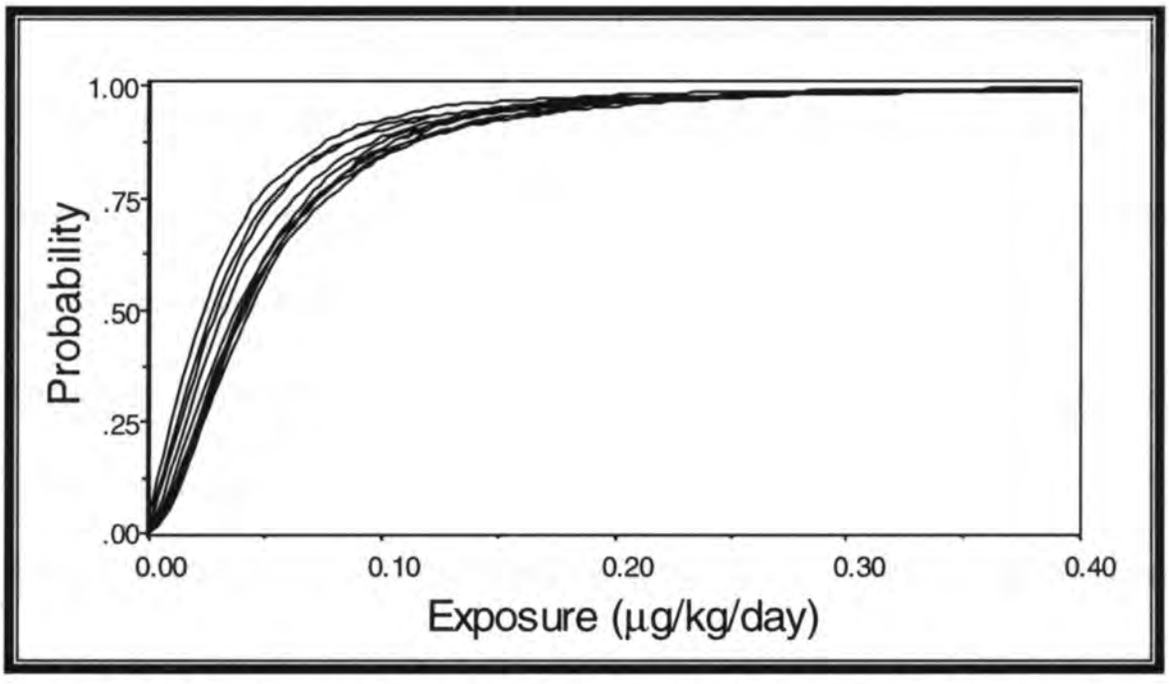

Figure 6–14. A Sample of Ten Alternate Realizations from the Two–Dimensional Monte Carlo Simulation Using Reduced Sample Sizes

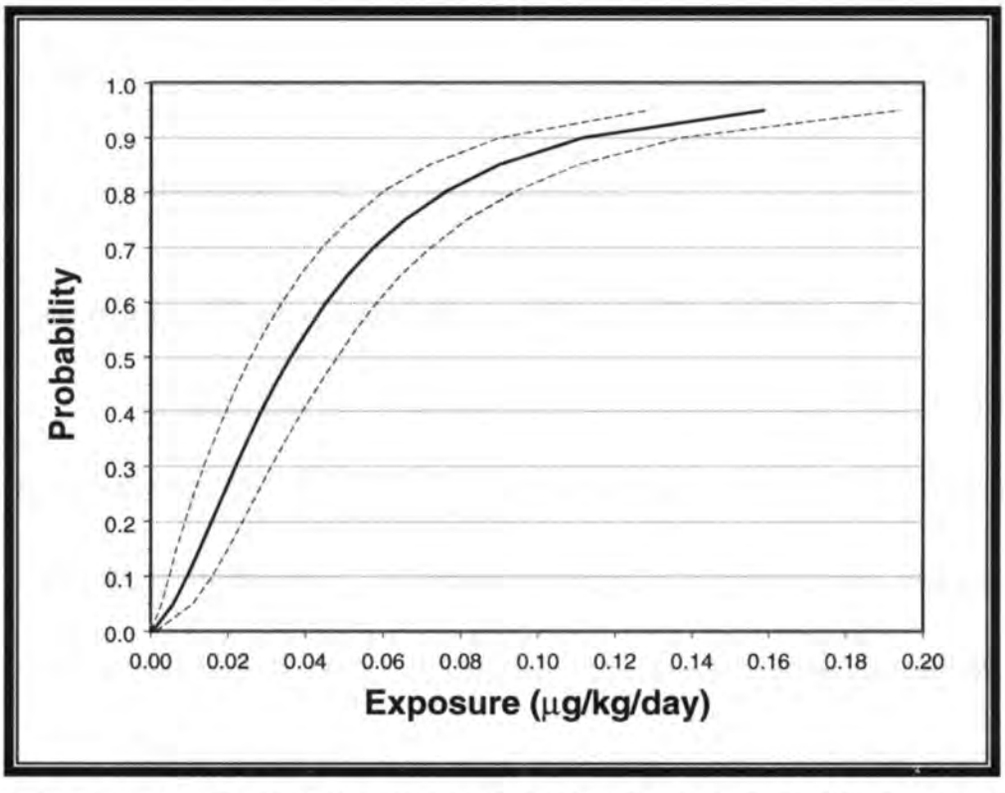

Figure 6–15. The Median Empirical Distribution (solid line) with 95th Percentiles (dashed lines) for the Two–Dimensional Monte Carlo Simulation Using Reduced Sample Sizes

The median curve in Figure 6–15 is nearly identical to the median curve in Figure 6–13. As expected, the prominent difference resulting from the reduced sample size simulation was the expansion of the 95th percentile boundaries.

The two–dimensional simulation using the reduced data sets resulted in 0.036, 0.161, 0.359, and 0.493 μg/kg/day for the 50th, 95th, 99th, and 99.5th percentiles respectively. These exposure percentiles are nearly identical to those obtained from the traditional and the two–dimensional simulation using the complete data sets. In addition to the percentiles, the distribution of exposures from this simulation was essentially identical to the distribution of exposures from the complete data two–dimensional simulation. The two–dimensional exposures from the reduced sample sizes were most accurately fit by a lognormal distribution (μ=0.0580, σ=0.0803).

Approximately 12.6% of the simulated results exceeded EPA's Reference Dose (0.1 μg/kg/day), and only 0.5% surpassed ATSDR's Minimal Risk Level (0.5 μg/kg/day).

Hierarchical Two–Dimensional Monte Carlo Simulations

As with the two–dimensional simulations, each hierarchical two–dimensional Monte Carlo simulation had 1,800 inner loop iterations and 800 outer loop iterations. A more complete explanation of how these sample sizes were obtained is given in the section *Two–Dimensional Monte Carlo Simulations.*

Once again, it was also assumed that uncertainty due to limited sample sizes was manifest in the location of the input distributions. Thus, the uncertainty associated with the median was estimated using the same parametric bootstrap technique previously described. For each dependent distribution (e.g., small lobsters or female adult consumption), one thousand

bootstraps of n values from the parent distribution were obtained, where n was the number of data points used to estimate the parent distribution. The 1,000 median estimates were combined to form a distribution of medians; the distribution of medians was used to characterize location uncertainty associated with limited sample sizes in the hierarchical two–dimensional simulation. The normal distribution accurately modeled the median values each time. The process is outlined in Figure 6–10.

The parent distributions, trials per sample, and the resulting distributions used to represent median uncertainty for mercury concentrations by lobster weight class are listed in Table 6–3 and the corresponding information for lobster consumption rate by gender and age class are listed in Table 6–4 (see Appendix B for additional distribution information). Both the parent and median uncertainty distributions were estimated with Crystal Ball.

	Parent Distribution	Trials per Sample	Median Uncertainty
Small Lobsters	Gamma (0.04, 0.16, 2.35)	167	Normal (0.359, 0.00816)
Regular Lobsters	Logistic (0.43, 0.13)	120	Normal (0.435, 0.00840)
Large Lobsters	Logistic (0.49, 0.14)	103	Normal (0.499, 0.00492)
Jumbo Lobsters	Logistic (0.70, 0.18)	117	Normal (0.711, 0.0115)

Table 6–3. Median Uncertainty Distributions Resulting from Bootstrapping Mercury Concentration Distributions by Lobster Weight Class

	Parent Distribution	Trials per Sample	Median Uncertainty
Infant Consumption	Logistic (103.76, 25.23)	42	Normal (103.744, 7.518)
Teen Consumption	Logistic (122.19, 41.45)	32	Normal (124.318, 13.112)
Female Adult Consumption	Logistic (155.07, 40.44)	316	Normal (156.527, 0.964)
Male Adult Consumption	Extreme Value (165.23, 78.03)	251	Normal (193.754, 2.824)

Table 6–4. Median Uncertainty Distributions Resulting from Bootstrapping Lobster Consumption Rate Distributions by Gender and Age Class

Each hierarchical two–dimensional Monte Carlo simulation resulted in 1,440,000 total iterations. Due to computational limitations, each simulation had to be performed in 16 batches with an outer loop sample size of 50 and the full inner loop sample size of 1,800. Every batch required approximately 30–45 minutes to run, extract, and save the results. Over 200 megabytes were necessary to store the data and simulation information from each hierarchical two–dimensional Monte Carlo simulation.

A diagram of the hierarchical two–dimensional process specific to this research is given in Figure 6–16.

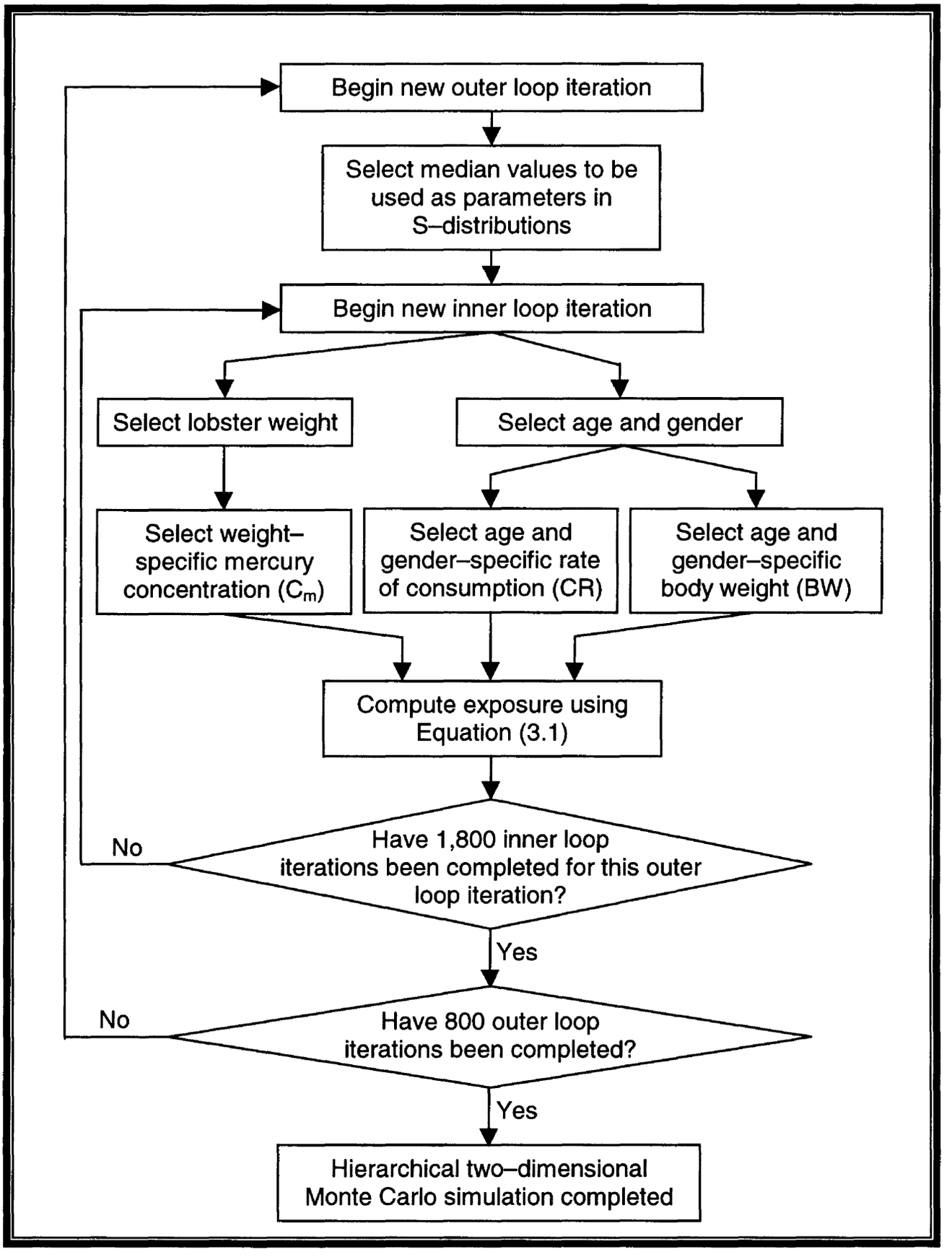

Figure 6–16. Hierarchical Two–Dimensional Monte Carlo Simulation Procedure Specific to This Research Problem

Figure 6–17 contains a sample of ten alternate realizations of exposure from this hierarchical two–dimensional simulation. The alternate realizations

differ due to the uncertainty from limited sample sizes. Once again, exposures at the icosatiles were stored for each inner loop. In Figure 6–18, the median exposure at each icosatile is given by a solid line, and ninety–five percent of the exposures at each icosatile lie between the dashed lines. Thus 95 percent of the realizations fall within the 95th percentile boundaries. Figure 6–18 may be interpreted in one of the following two ways: 95 percent of the alternate realizations had somewhere between 7 and 10% of the individuals exceeding an exposure of 0.10 μg/kg/day, or 95% of the alternate realizations resulted in a 90th percentile somewhere between 0.085 and 0.10 μg/kg/day. The maximum exposures (probability=1.00 in Figure 6–18) were not graphed as the values were too large. The median of the maximum exposures was 0.48 μg/kg/day, and the upper and lower 95th percentiles were 0.80 and 0.33 μg/kg/day respectively.

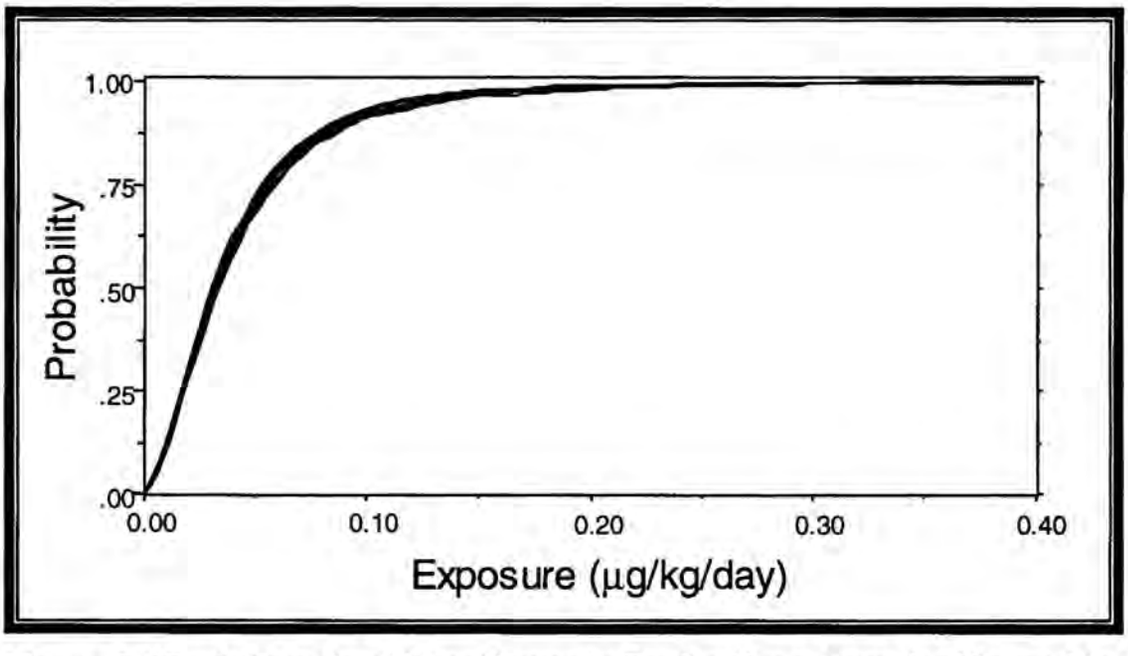

Figure 6–17. A Sample of Ten Alternate Realizations from the Hierarchical Two–Dimensional Monte Carlo Simulation

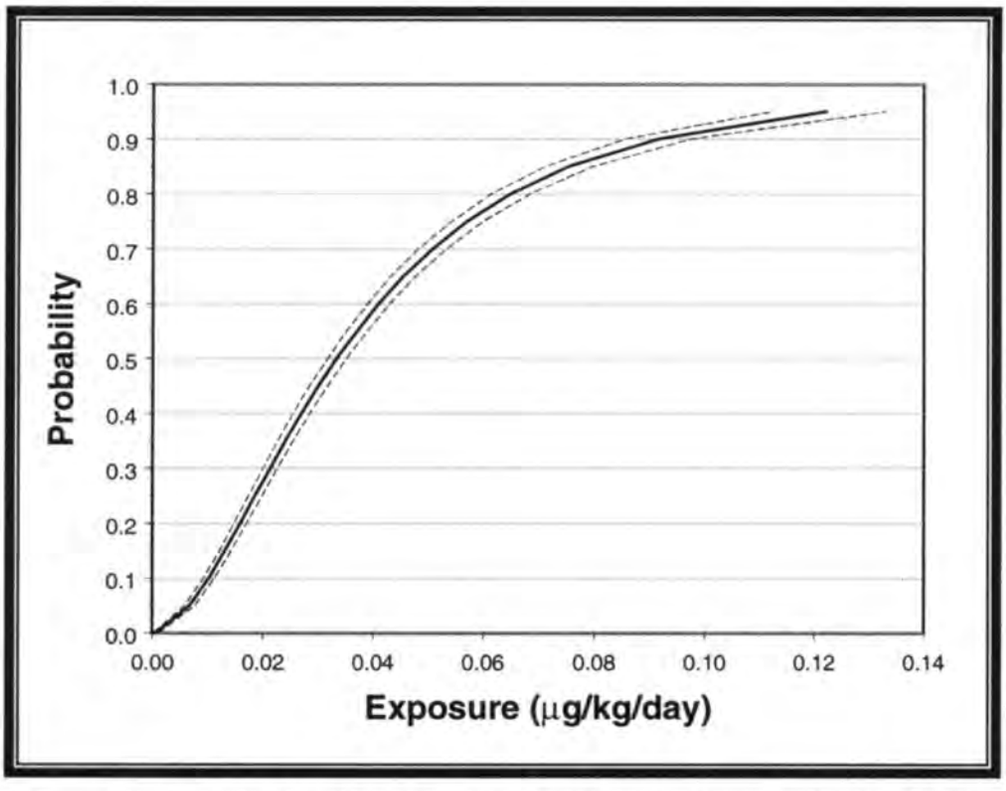

Figure 6–18. The Median Empirical Distribution (solid line) with 95th Percentiles (dashed lines) for the Hierarchical Two–Dimensional Monte Carlo Simulation

The median curve in Figure 6–18 is nearly identical to the empirical distribution for hierarchical simulation exposures in Figure 6–6.

The hierarchical two–dimensional simulation resulted in 0.033, 0.122, 0.216, and 0.265 μg/kg/day for the 50th, 95th, 99th, and 99.5th percentiles respectively. These exposure percentiles are nearly identical to those obtained from the hierarchical Monte Carlo simulation. In addition to the percentiles, the distribution of exposures from this simulation was essentially identical to the distribution of exposures from the hierarchical simulation, which is logical as the hierarchical aspect of these methods alters the exposure distributions in a similar manner. Using SAS, the hierarchical two–dimensional exposures were most accurately fit by a lognormal distribution (μ=0.0468, σ=0.0514).

Approximately 8.2% of the simulated results exceeded EPA's Reference Dose (0.1 μg/kg/day), and fewer than 0.1% surpassed ATSDR's Minimal Risk Level (0.5 μg/kg/day).

Discussion of Methods

Each of the methods in this chapter used to characterize exposure is appropriate under certain circumstances. As previously discussed, the ideal situation is to utilize as simple a method as possible without oversimplification of the problem.

The upper percentile point estimate exceeded all risk values as given in Chapter 2; consequently, a potential problem was identified and the use of probabilistic methods was justified.

The traditional Monte Carlo simulation did not characterize exposure as accurately as the hierarchical Monte Carlo simulation because of the strong dependencies among the input variables. Significant differences, particularly in the higher exposures, were noted in simulation results from these two methods as discussed earlier in this chapter in the *Hierarchical Monte Carlo Simulations* section. In brief, the hierarchical Monte Carlo method resulted in fewer exposures exceeding the risk values.

The two–dimensional Monte Carlo simulations did not contribute notable improvements as the uncertainty associated with limited sample sizes was negligible. In addition, the results were quite similar to the traditional Monte Carlo simulation results.

Likewise, the hierarchical two–dimensional Monte Carlo technique did not produce significantly different results from the hierarchical Monte Carlo method as result of negligible uncertainty.

Thus as a result of strong dependencies among input variables and a low uncertainty from limited sample sizes, the hierarchical Monte Carlo method was most appropriate for this research.

Uncertainty Analysis

The sensitivity analysis was discussed in the section *Point Estimates*. With the simulated data, it is now possible to carry out the remaining uncertainty analysis.

Table 6–5 through Table 6–10 display the different correlation coefficients for each of the simulation methods. A rank of importance for each input variable, with 1 being the most important, is given in parentheses following the correlation coefficients in the tables. Recall that the larger the absolute value of the correlation coefficient, the stronger the relationship between the input and output variable.

The correlation coefficients obtained with the traditional Monte Carlo simulation data are found in Table 6–5.

	Mercury Concentration	Consumption Rate	Body Weight
Pearson Correlation Coefficient	0.41 (2)	0.33 (3)	-0.42 (1)
Spearman Rank–Order Correlation Coefficient	0.62 (1)	0.56 (2)	-0.45 (3)
Partial Correlation Coefficient	0.48 (2)	0.39 (3)	-0.50 (1)
Partial Rank–Order Correlation Coefficient	0.88 (1)	0.85 (2)	-0.81 (3)

Table 6–5. Correlation Coefficients for Each Input Variable and Exposure Using Traditional Monte Carlo Simulation Data (Rank of Importance Given in Parentheses)

Both the Pearson correlation coefficients and the partial correlation coefficients resulted in the same ranks of importance for the input variables, yet these ranks differed from those obtained using the Spearman rank–order correlation coefficients and the partial rank–order correlation coefficients. As mentioned in the Methods Chapter, both the Pearson and partial correlation coefficients test for linear relationships, where the Spearman and partial rank–order correlation coefficients use ranks to test for monotonic relationships.

In order to determine which relationships were linear and which were not, each of the relationships was fit with linear and non–linear functions given in Table 6–6. Each of the non–linear functions in Table 6–6 can be converted to the form of the linear function, thus linear regression techniques may still be applied. The different fits were compared using the coefficient of determination (r^2), which gives the percent of the variation that can be explained by the fitted curve; consequently, better fits have higher r^2 values. In every instance, the power transformation provided the best fit among the non–linear functions.

Linear	$y = a + b \cdot x$
Exponential	$y = a \cdot e^{bx}$
Log base 10	$y = a + b \cdot \log(x)$
Log base e	$y = a + b \cdot \ln(x)$
Power	$y = a \cdot x^{b}$

Table 6–6. Linear and Non–Linear Functions

Exposure was assigned as the independent variable (y) and the input variable of interest as the dependent variable (x), although the relationship remains unchanged even if the independent and dependent variables were switched.

The coefficient of determination between exposure and mercury concentration was 0.17 for both the linear and power functions. For exposure and lobster consumption rate, r^2 was 0.11 for both the linear and power functions. These relationships can essentially be considered linear as no significant improvement was observed with the non–linear curves. Although the ranks of importance differed using the different correlation coefficients, the rank of importance for mercury concentration was always higher than that for consumption rate. Thus, all correlation coefficients maintained a consistent relationship between these two linear associations.

The coefficient of determination between exposure and body weight was 0.18 for the linear and 0.39 for the power function. The significant improvement in r^2 for the power function means that the non–linear curve characterized this

relationship more accurately than the linear model. Both the linear and non–linear curves can be seen in Figure 6–19.

These results were not surprising as an examination of Equation (3.1) reveals that exposure has a linear relationship with each of the input variables, except body weight. Exposure and body weight are inversely related, or in other words, they share a non–linear relationship that is characterized using a power function with an exponent of –1.

Recall that ranks from the Spearman and partial rank–order correlation coefficients are more accurate and reliable than those obtained using the Pearson and partial correlation coefficients for non–linear, monotonic relationships. Based on both the Spearman and partial rank–order correlation coefficients, the input variable of most importance was mercury concentration, followed by consumption rate, and finally body weight. The partial rank–order correlation coefficients showed that all three of the input variables contribute similar amounts to the overall uncertainty.

It should be noted that eight points ranging from 1.01 – 2.61 μg/kg/day were not plotted in Figure 6–19. All of these outlying points were from iterations using a body weight of approximately 7 kg, the minimum acceptable body weight.

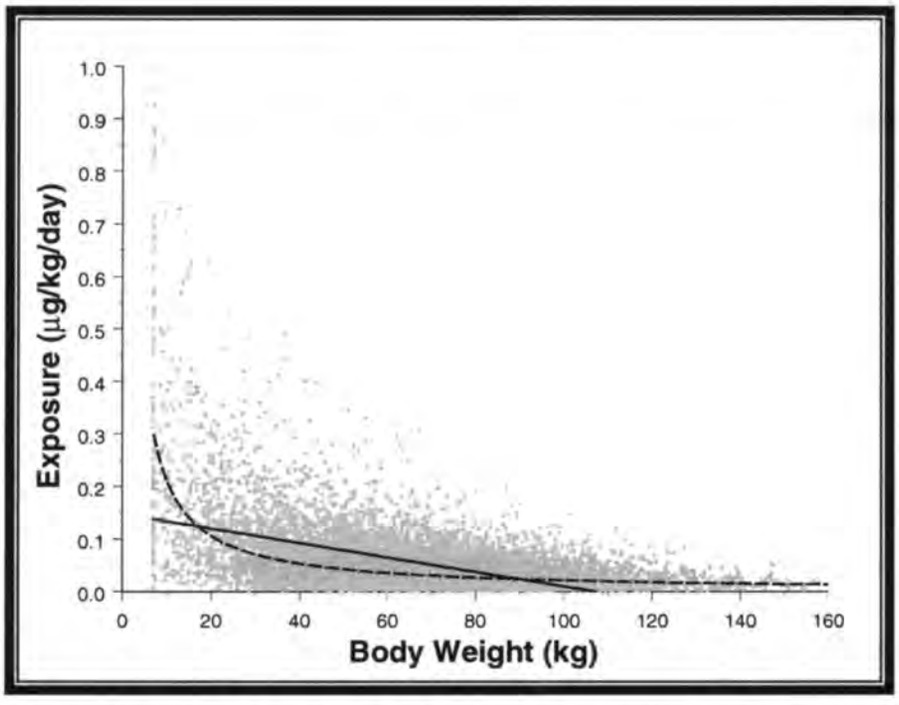

Figure 6–19. Association Between Exposure and Body Weight using Traditional Monte Carlo Simulation Data with the Linear Regression Line (solid line) and the Regression Line from the Power Function (dashed line) Superimposed

The correlation coefficients obtained with the hierarchical Monte Carlo simulation data are found in Table 6–7.

	Mercury Concentration	Consumption Rate	Body Weight
Pearson Correlation Coefficient	0.56 (1)	0.29 (3)	-0.39 (2)
Spearman Rank–Order Correlation Coefficient	0.67 (1)	0.41 (2)	-0.32 (3)
Partial Correlation Coefficient	0.69 (1)	0.59 (3)	-0.66 (2)
Partial Rank–Order Correlation Coefficient	0.86 (1)	0.81 (2)	-0.77 (3)

Table 6–7. Correlation Coefficients for Each Input Variable and Exposure Using Hierarchical Monte Carlo Simulation Data (Rank of Importance Given in Parentheses)

Both the Pearson correlation coefficients and the partial correlation coefficients resulted in the same ranks of importance for the input variables, yet these ranks differed from those obtained using the Spearman rank–order

correlation coefficients and the partial rank–order correlation coefficients. Thus, linear and non–linear functions were again fit to each of the relationships.

The coefficient of determination between exposure and mercury concentration was 0.31 for both the linear and power functions. For exposure and lobster consumption rate, r^2 was 0.08 for the linear function and 0.09 for the power function. Once again, these relationships can be considered linear as no significant improvement was observed with the non–linear functions. Although the ranks of importance differed using the different correlation coefficients, the rank of importance for mercury concentration was always higher than that for consumption rate. Thus, all correlation coefficients maintained a consistent relationship between these two linear associations.

The coefficient of determination between exposure and body weight was 0.15 for the linear and 0.24 for the power function. The significant improvement in r^2 for the power function means that the non–linear curve characterized this relationship more accurately than the linear model; thus ranks from the Spearman and partial rank–order correlation coefficients are more accurate and reliable than those obtained using the Pearson and partial correlation coefficients. Both the linear and non–linear curves can be seen in Figure 6–20. Based on both the Spearman and partial rank–order correlation coefficients, the input variable of most importance was mercury concentration, followed by consumption rate, and finally body weight. All three of the input variables contributed similar amounts to the overall uncertainty as evidenced by the partial

rank–order correlation coefficients. These results agree with those obtained from the traditional Monte Carlo simulation data.

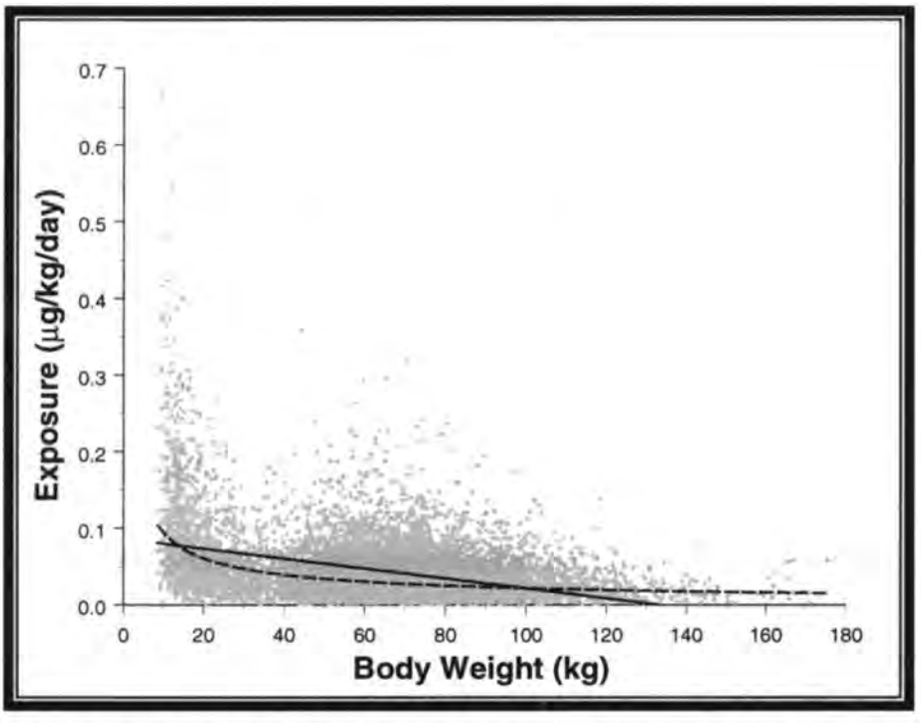

Figure 6–20. Association Between Exposure and Body Weight using Hierarchical Monte Carlo Simulation Data with the Linear Regression Line (solid line) and the Regression Line from the Power Function (dashed line) Superimposed

A slight depression in the general shape of the points is observed between approximately 20 and 50 kg in Figure 6–20. This is not observed in Figure 6–19; consequently, some new feature of the hierarchical simulation is most likely responsible. The age and gender–specific body weight distributions were first investigated. It is noted that males and females between the ages of six and eleven are most likely to have a body weight between 20 and 50 kg as seen in Figure 5–2 and Figure 5–3. The age and gender–specific consumption rates come from the same distribution for all children under twelve years of age. In Equation (3.1), higher body weights result in reduced exposure. Thus, the depression is most likely attributable to the fact that body weights for children ages 6–11 are two to three times greater than those for children ages 1–5, while

lobster consumption rates for children ages 1–11 come from the same distribution.

This is an indication of the advantages of hierarchical simulations. With smaller and smaller class sizes for age–specific body weights and age–specific consumption rates, the slight depression observed in Figure 6–20 would most likely disappear.

The correlation coefficients obtained using results from two–dimensional Monte Carlo simulations are found in Table 6–8 and Table 6–9.

	Mercury Concentration	Consumption Rate	Body Weight
Pearson Correlation Coefficient	0.41 (2)	0.34 (3)	-0.45 (1)
Spearman Rank–Order Correlation Coefficient	0.62 (1)	0.55 (2)	-0.45 (3)
Partial Correlation Coefficient	0.50 (2)	0.43 (3)	-0.53 (1)
Partial Rank–Order Correlation Coefficient	0.88 (1)	0.85 (2)	-0.80 (3)

Table 6–8. Correlation Coefficients for Each Input Variable and Exposure Using Two–Dimensional Monte Carlo Simulation Data from the Complete Data Set (Rank of Importance Given in Parentheses)

	Mercury Concentration	Consumption Rate	Body Weight
Pearson Correlation Coefficient	0.42 (2)	0.35 (3)	-0.45 (1)
Spearman Rank–Order Correlation Coefficient	0.63 (1)	0.54 (2)	-0.44 (3)
Partial Correlation Coefficient	0.50 (2)	0.44 (3)	-0.53 (1)
Partial Rank–Order Correlation Coefficient	0.88 (1)	0.85 (2)	-0.79 (3)

Table 6–9. Correlation Coefficients for Each Input Variable and Exposure Using Two–Dimensional Monte Carlo Simulation Data from the Reduced Data Set (Rank of Importance Given in Parentheses)

Both the Pearson correlation coefficients and the partial correlation coefficients resulted in the same ranks of importance for the input variables, yet once again these ranks differed from those obtained using the Spearman rank–order correlation coefficients and the partial rank–order correlation coefficients. The relationships among the variables were identical to those obtained using the traditional simulation data. Mercury concentration and lobster consumption rate had a linear association with exposure, while body weight had a non–linear, monotonic relationship with exposure. Thus ranks from the Spearman and partial rank–order correlation coefficients were used to evaluate uncertainty. Both the Spearman and partial rank–order correlation coefficients identified the input variable of most importance as mercury concentration, followed by consumption rate, and finally body weight. All three of the input variables contributed similar amounts to the overall uncertainty as evidenced by the partial rank–order correlation coefficients.

Once again, the similarity among the traditional Monte Carlo and the two–dimensional Monte Carlo was evident as all of these methods resulted in nearly identical correlation coefficients.

The correlation coefficients obtained using results from hierarchical two–dimensional Monte Carlo simulation are found in Table 6–10.

	Mercury Concentration	Consumption Rate	Body Weight
Pearson Correlation Coefficient	0.56 (1)	0.29 (3)	-0.41 (2)
Spearman Rank–Order Correlation Coefficient	0.66 (1)	0.41 (2)	-0.34 (3)
Partial Correlation Coefficient	0.69 (1)	0.60 (3)	-0.67 (2)
Partial Rank–Order Correlation Coefficient	0.86 (1)	0.81 (2)	-0.78 (3)

Table 6–10. Correlation Coefficients for Each Input Variable and Exposure Using Hierarchical Two–Dimensional Monte Carlo Simulation Data (Rank of Importance Given in Parentheses)

Both the Pearson correlation coefficients and the partial correlation coefficients resulted in the same ranks of importance for the input variables, yet these ranks differed from those obtained using the Spearman rank–order correlation coefficients and the partial rank–order correlation coefficients. The relationships among the variables were identical to those obtained using the hierarchical simulation data. Mercury concentration and lobster consumption rate had a linear association with exposure, while body weight had a non–linear, monotonic relationship with exposure. Thus ranks from the Spearman and partial rank–order correlation coefficients were again used to evaluate uncertainty. Both the Spearman and partial rank–order correlation coefficients identified the input variable of most importance as mercury concentration, followed by consumption rate, and finally body weight. All three of the input variables contributed similar amounts to the overall uncertainty as evidenced by the partial rank–order correlation coefficients.

The similarity between the hierarchical Monte Carlo and hierarchical two–dimensional Monte Carlo was evident as both methods resulted in nearly identical correlation coefficients.

Both the Spearman and partial rank–order correlation coefficients from each of the simulation techniques resulted in mercury concentration as the input variable of most importance followed by consumption rate then body weight. But within each simulation method, the partial rank–order correlation coefficients did not differ much for all three input variables.

Chapter 7

ADDITIONAL SCENARIOS OF INTEREST

Women of Childbearing Age

As discussed in Chapter 2, the subgroup most sensitive to methylmercury toxicity consists of the unborn child; consequently, methylmercury exposure for women of childbearing age is of particular interest. A hierarchical simulation comprising only women of childbearing age (i.e., 15–44) was used to explore this scenario (EPA, 1997b).

The histogram of exposures characterizing women of childbearing age is provided in Figure 7–1. The data were most accurately fit by a gamma distribution (L=0.0001, α=0.0206, β=1.7065). EPA's Reference Dose (0.1 μg/kg/day) was exceeded by 3.3% of the simulated exposures, yet none of the simulated exposures surpassed ATSDR's Minimal Risk Level (0.5 μg/kg/day). Recall that both the RfD and the MRL are intended to protect the most sensitive subgroups of the population.

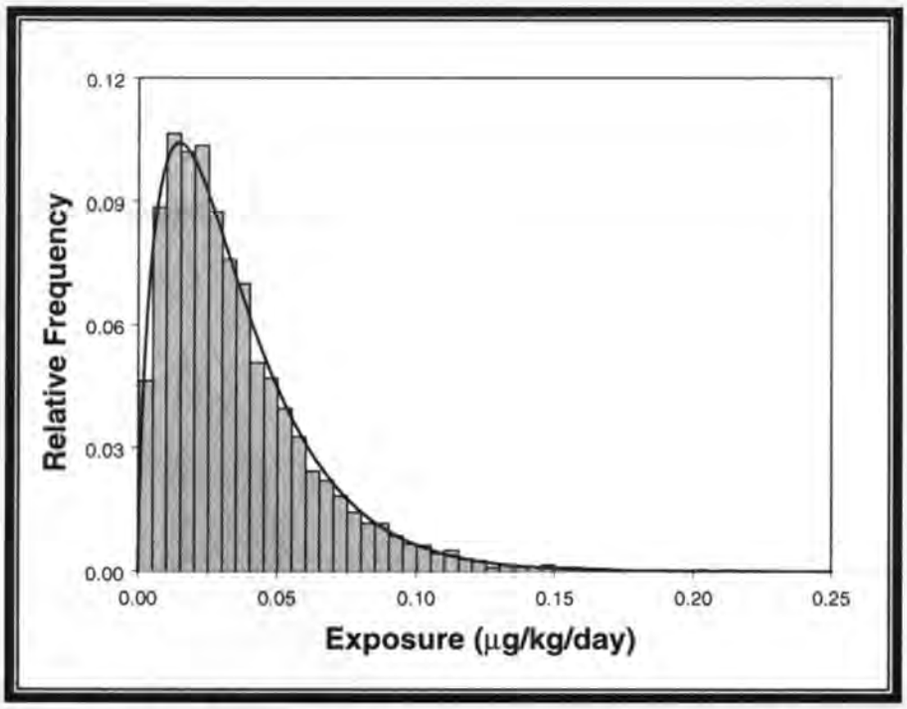

Figure 7–1. Exposures Characterizing Women of Childbearing Age with the Fitted Gamma Distribution Superimposed

Young Children

In addition to the fetus, children are particularly sensitive to methylmercury toxicity through age four; consequently, methylmercury exposure for young children is of special interest (EPA, 1997b). A hierarchical simulation comprising only children ages 1–4 was used to explore this scenario.

The histogram of exposures characterizing young children is provided in Figure 7–2. The data were most accurately fit by a lognormal distribution (μ=0.1053, σ=0.0998). EPA's Reference Dose (0.1 µg/kg/day) was exceeded by 38.2% of the simulated exposures, and 0.3% of the simulated exposures surpassed ATSDR's Minimal Risk Level (0.5 µg/kg/day). Recall that both of these risk values are intended to protect the most sensitive subgroups of the population. Although a surprisingly high proportion of iterations exceeded the

RfD, it should be noted that this simulation characterized children ages one through four who consumed Northern lobster during a given month.

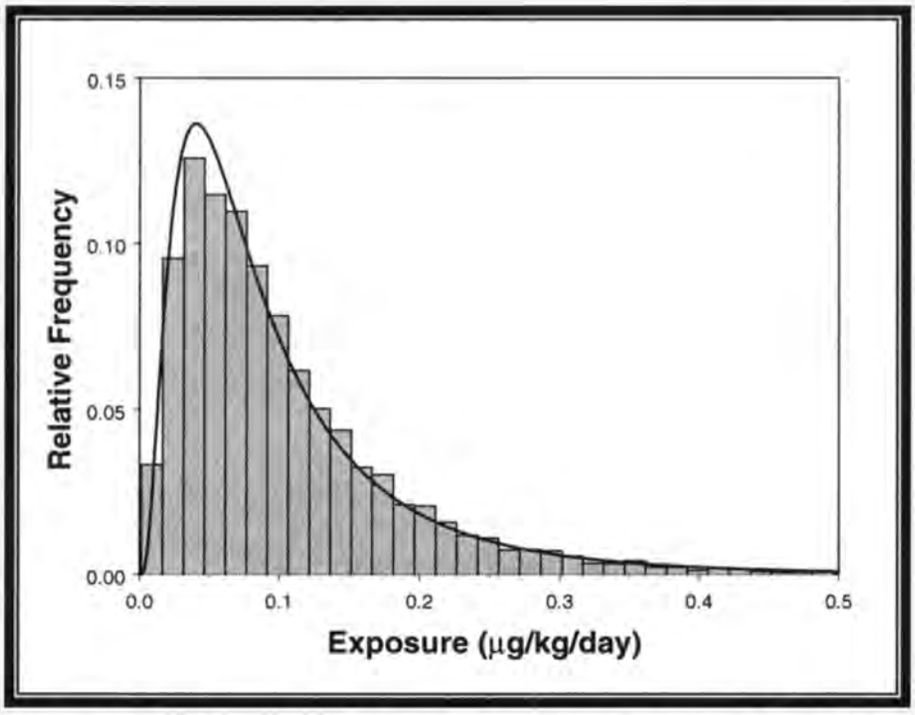

Figure 7–2. Exposures Characterizing Children Age 1–4 with the Fitted Lognormal Distribution Superimposed

Distinct Monthly Consumption Patterns

The exposures resulting from the consumption of one lobster per month, two lobsters per month, three lobsters per month, and four lobsters per month are also of interest. These scenarios were explored using four distinct hierarchical simulations. A diagram of the hierarchical simulation process used to estimate exposure from the consumption of n lobsters per month is given in Figure 7–3.

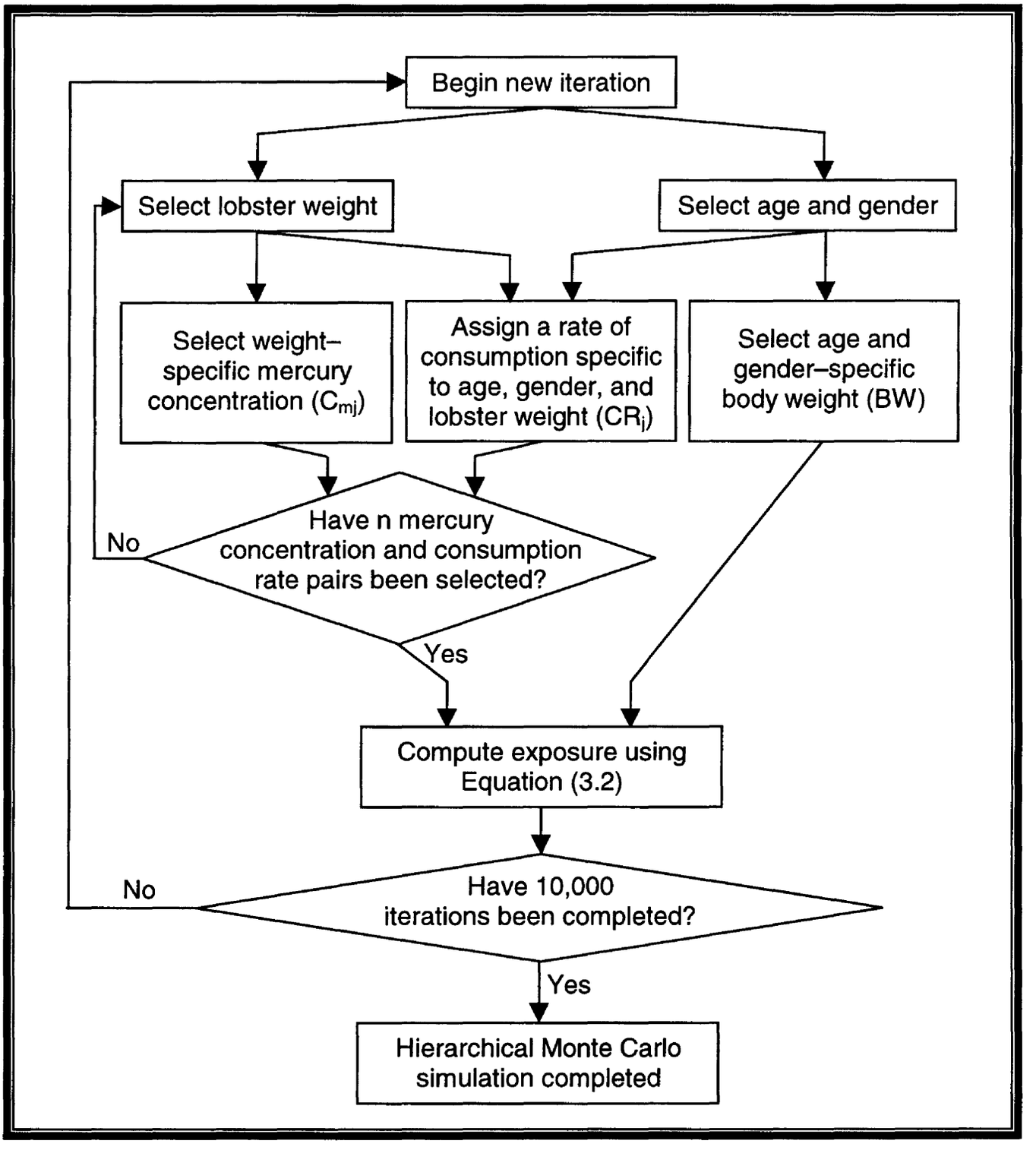

Figure 7–3. Hierarchical Monte Carlo Simulation Procedure Used to Estimate Exposure from the Consumption of n Lobsters per Month

For these simulations, the age and gender–specific lobster consumption distributions were replaced with point estimates of consumption specific to age, gender, and lobster weight as seen in Table 7–1. Below each consumption rate is the size of the lobster used to calculate the consumption rate; these

consumption rates were obtained by examination of the age and gender–specific consumption rates.

	Small Lobster	Regular Lobster	Large Lobster	Jumbo Lobster
Females & Males Age 1–11	3.314 g/day (1.00 lb.)	–	–	–
Females & Males Age 12–18	3.314 g/day (1.00 lb.)	4.142 g/day (1.25 lb.)	5.799 g/day (1.75 lb.)	8.285 g/day (2.50 lb.)
Females Age 19–98	3.728 g/day (1.125 lb.)	4.971 g/day (1.50 lb.)	6.628 g/day (2.00 lb.)	9.942 g/day (3.00 lb.)
Males Age 19–98	4.139 g/day (1.249 lb.)	5.795 g/day (1.749 lb.)	8.281 g/day (2.499 lb.)	13.252 g/day (3.999 lb.)

Table 7–1. Lobster Consumption Rates Specific to Age, Gender, and Lobster Weight

Equation (3.2) was used to calculate exposure for simulations involving the consumption of more than one lobster.

The histogram of exposures resulting from the consumption of one lobster per month is given in Figure 7–4. The data were most accurately fit by a lognormal distribution (μ=0.0414, σ=0.0383). EPA's Reference Dose (0.1 μg/kg/day) was exceeded by 5.9% of the simulated exposures, yet none of the simulated exposures surpassed ATSDR's Minimal Risk Level (0.5 μg/kg/day).

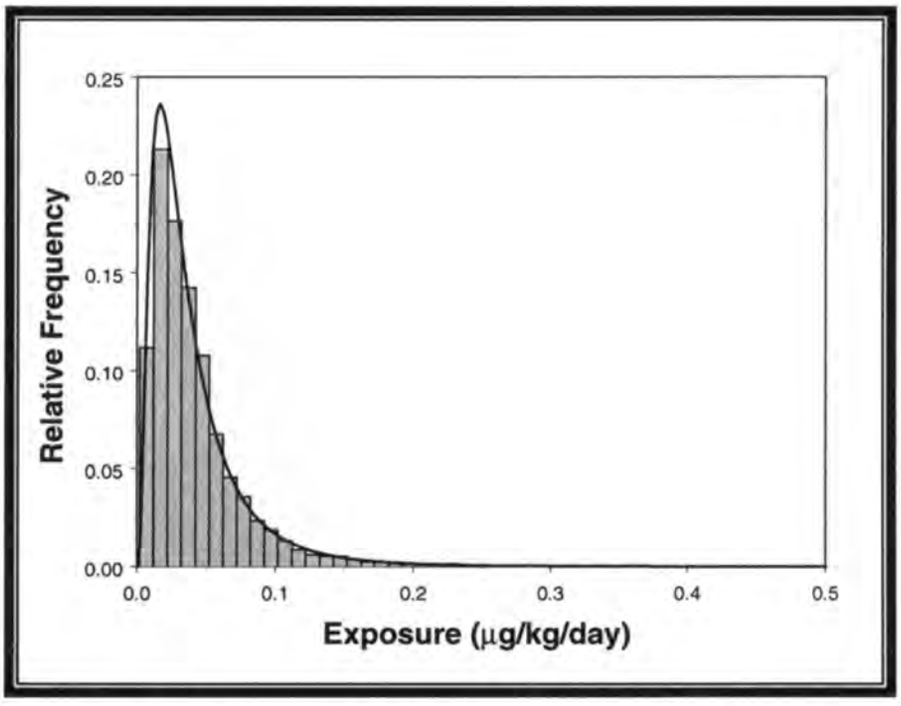

Figure 7–4. Exposures Resulting from the Consumption of One Lobster per Month with the Fitted Lognormal Distribution Superimposed

The histogram of exposures resulting from the consumption of two lobsters per month is given in Figure 7–5. The data were most accurately fit by a lognormal distribution (μ=0.0819, σ=0.0558). EPA's Reference Dose (0.1 µg/kg/day) was exceeded by 24.7% of the simulated exposures, while only 0.1% of the simulated exposures surpassed ATSDR's Minimal Risk Level (0.5 µg/kg/day).

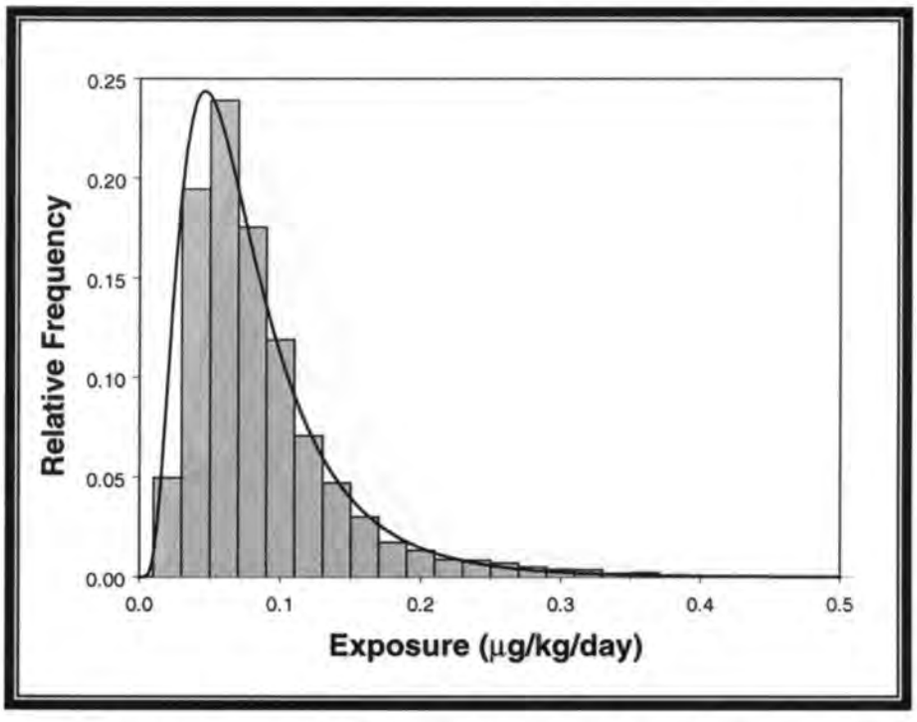

Figure 7–5. Exposures Resulting from the Consumption of Two Lobsters per Month with the Fitted Lognormal Distribution Superimposed

The histogram of exposures resulting from the consumption of three lobsters per month is given in Figure 7–6. The data were most accurately fit by a lognormal distribution (μ=0.1226, σ=0.0717). EPA's Reference Dose (0.1 µg/kg/day) was exceeded by 53.0% of the simulated exposures, while only 0.6% of the simulated exposures surpassed ATSDR's Minimal Risk Level (0.5 µg/kg/day).

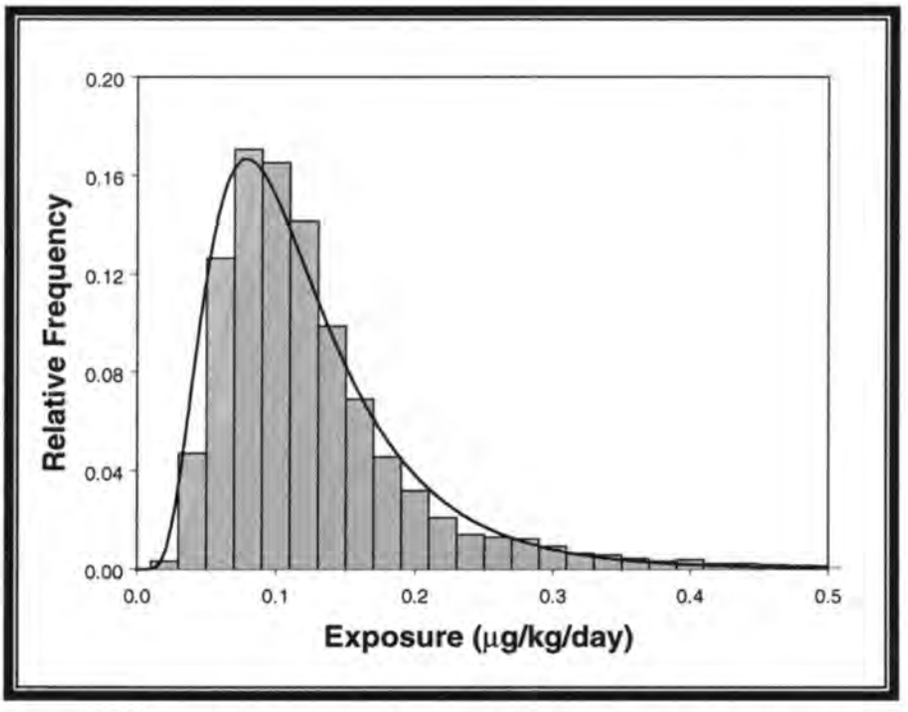

Figure 7–6. Exposures Resulting from the Consumption of Three Lobsters per Month with the Fitted Lognormal Distribution Superimposed

The histogram of exposures resulting from the consumption of four lobsters per month is given in Figure 7–7. The data were most accurately fit by a lognormal distribution (μ=0.1613, σ=0.0872). EPA's Reference Dose (0.1 µg/kg/day) was exceeded by 76.0% of the simulated exposures, while only 1.7% of the simulated exposures surpassed ATSDR's Minimal Risk Level (0.5 µg/kg/day).

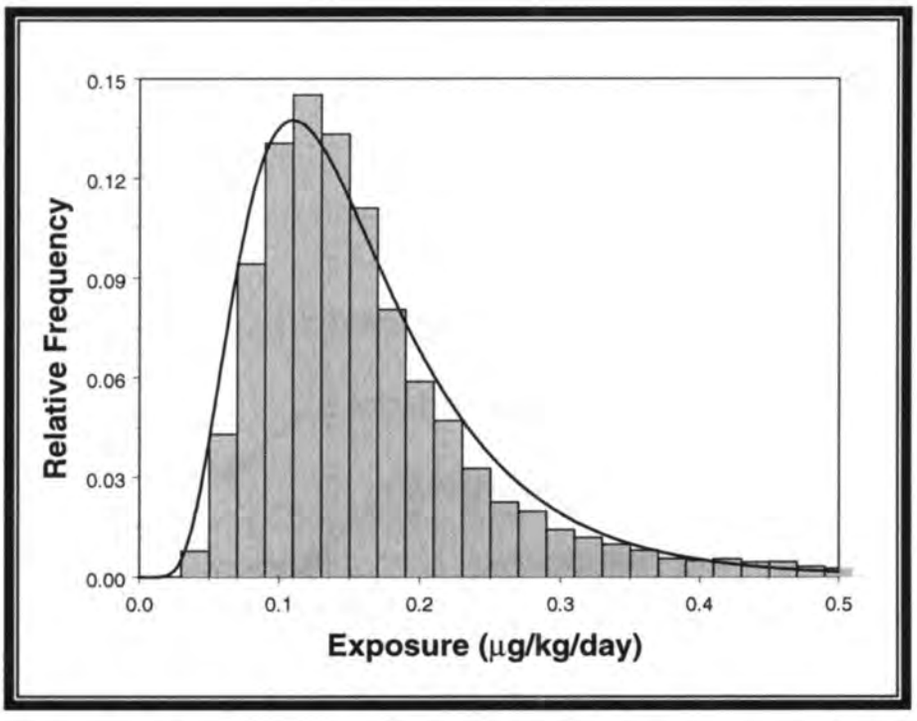

Figure 7–7. Exposures Resulting from the Consumption of Four Lobsters per Month with the Fitted Lognormal Distribution Superimposed

All four of the lognormal exposure distributions are overlaid in Figure 7–8 below.

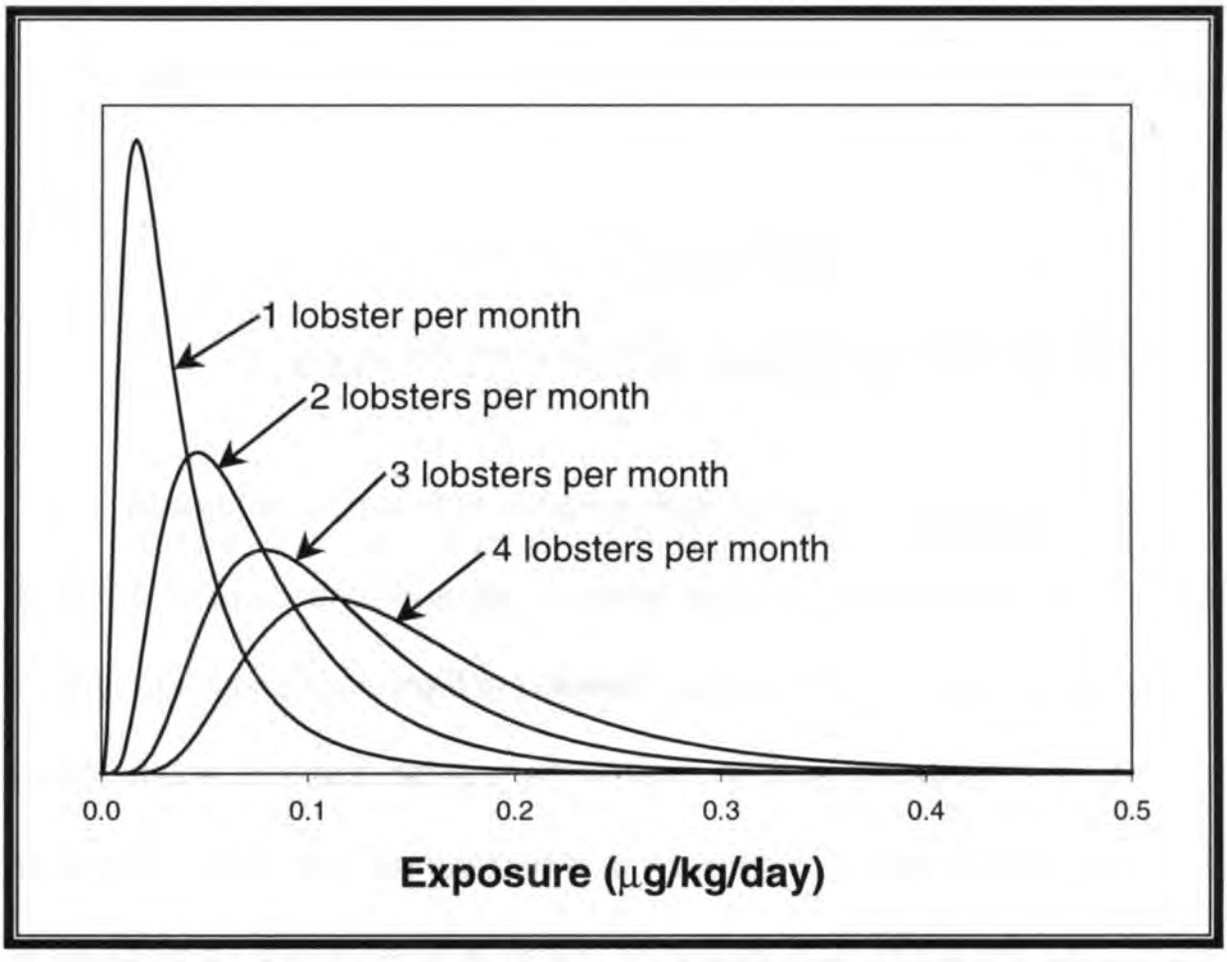

Figure 7–8. Lognormal Distributions of Exposure Resulting from the Consumption of One, Two, Three, and Four Lobsters per Month

The importance of the risk value is evident from these analyses. The simulation for more than one lobster per month resulted in a large proportion of exposures exceeding EPA's Reference Dose; however, even the simulation for four lobsters per month did not result in a high percentage of exposures exceeding ATSDR's Minimal Risk Level.

Chapter 8

EXPOSURE FROM MULTIPLE SPECIES

Almost all fish and shellfish contain at least trace amounts of methylmercury; consequently, in order to adequately characterize total methylmercury exposure it is necessary to consider multiple species. Distributions characterizing methylmercury concentrations are provided for the nine most frequently consumed marine species in the *Contaminant Data* section of Chapter 5. These nine species constitute approximately 75% of the total seafood consumption (Johnson and Doré, 1997).

Annual consumption of the most frequently consumed species was estimated using information provided by Johnson and Doré (1998) and Jacobs *et al.* (1998). The annual per capita consumption was 11.2 pounds per year for these nine species (Johnson and Doré, 1997). Annual consumption rates (see Table 8–1) for each age and gender class were calculated using U.S. population data and the annual per capita consumption for these species.

	Annual Consumption	Meals per Year
Infants Age 1–11	6 lbs/yr	24 4.0–oz meals/year
Females Age 12–18	9 lbs/yr	24 6.0–oz meals/year
Males Age 12–18	10 lbs/yr	24 6.7–oz meals/year
Females Age 19–98	11 lbs/yr	24 7.3–oz meals/year
Males Age 19–98	14 lbs/yr	24 9.3–oz meals/year

Table 8–1. Approximate Annual Consumption of the Most Frequently Consumed Marine Species

For this simulation it was assumed that each individual consumed two meals of the most frequently consumed species each month. Consequently, in order to characterize annual consumption each iteration in the simulation consisted of 24 meals. The probability of consuming a specific species for a meal was based on 1997 annual per capita consumption statistics for the U.S. population (Johnson and Doré, 1997). The percent of annual consumption among these nine species is provided in Table 8–2. A species is easily selected in Crystal Ball using a custom distribution with these percents (Sargent and Wainwright, 1996).

Species	Percent of Annual Consumption
Tuna	28.57%
Shrimp	22.32%
Pollock	14.29%
Salmon	12.50%
Cod	8.93%
Clams	4.46%
Flounder	3.57%
Crab	2.68%
Scallops	2.68%

Table 8–2. Percent of Annual Consumption Among the Nine Most Frequently Consumed Marine Species

A hierarchical simulation was used to characterize methylmercury exposure from the consumption of the most frequently consumed marine species. Exposure was calculated using Equation (3.2). A histogram of the simulated exposures resulting from consumption of the most frequently consumed marine species is given in Figure 8–1. The data were most accurately fit by a lognormal distribution (μ=0.0257, σ=0.0108). EPA's Reference Dose (0.1 μg/kg/day) was exceeded by only 0.1% of the simulated exposures, and none of the simulated exposures surpassed ATSDR's Minimal Risk Level (0.5 μg/kg/day). The iterations that exceeded the RfD shared some interesting characteristics. First, the average body weight was 22.5 lbs, with all weights less than 30 lbs. These iterations also had a high proportion of tuna meals, the species with the greatest potential for high concentrations among the nine most frequently consumed species. Tuna meals constituted 40% of the seafood meals for these iterations versus 29% for all of the iterations.

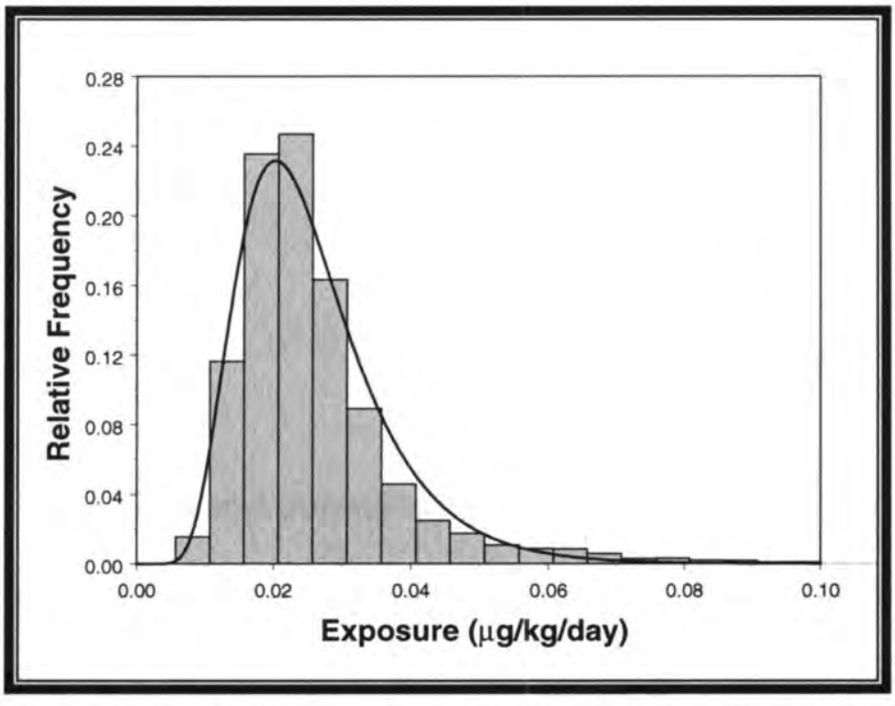

Figure 8–1. Exposures Resulting from the Consumption of the Most Frequently Consumed Marine Species with the Fitted Lognormal Distribution Superimposed

Chapter 9

CONCLUSIONS

Seafood consumption is associated with documented health benefits, yet high levels of methylmercury exposure from seafood consumption present potential health risks. In order to weigh seafood consumption benefits properly against possible risks, methylmercury exposure was evaluated using several methods.

As a part of this research a new simulation technique, the hierarchical two–dimensional Monte Carlo method, was developed. This method is most appropriate when dependencies among input variables are strong and the uncertainty from limited sample sizes is high.

Each of the techniques used to characterize exposure is appropriate under certain circumstances:

- Point estimates as a screening technique or if the cost of remediation is low,
- Traditional simulations with weak dependencies among input variables and low uncertainty from limited sample sizes,
- Hierarchical simulations with strong dependencies among input variables and low uncertainty from limited sample sizes,

- Two–dimensional simulations with weak dependencies among input variables and high uncertainty from limited sample sizes, and
- Hierarchical two–dimensional simulations with strong dependencies among input variables and high uncertainty from limited sample sizes.

A decision tree for these techniques is provided in Figure 9–1.

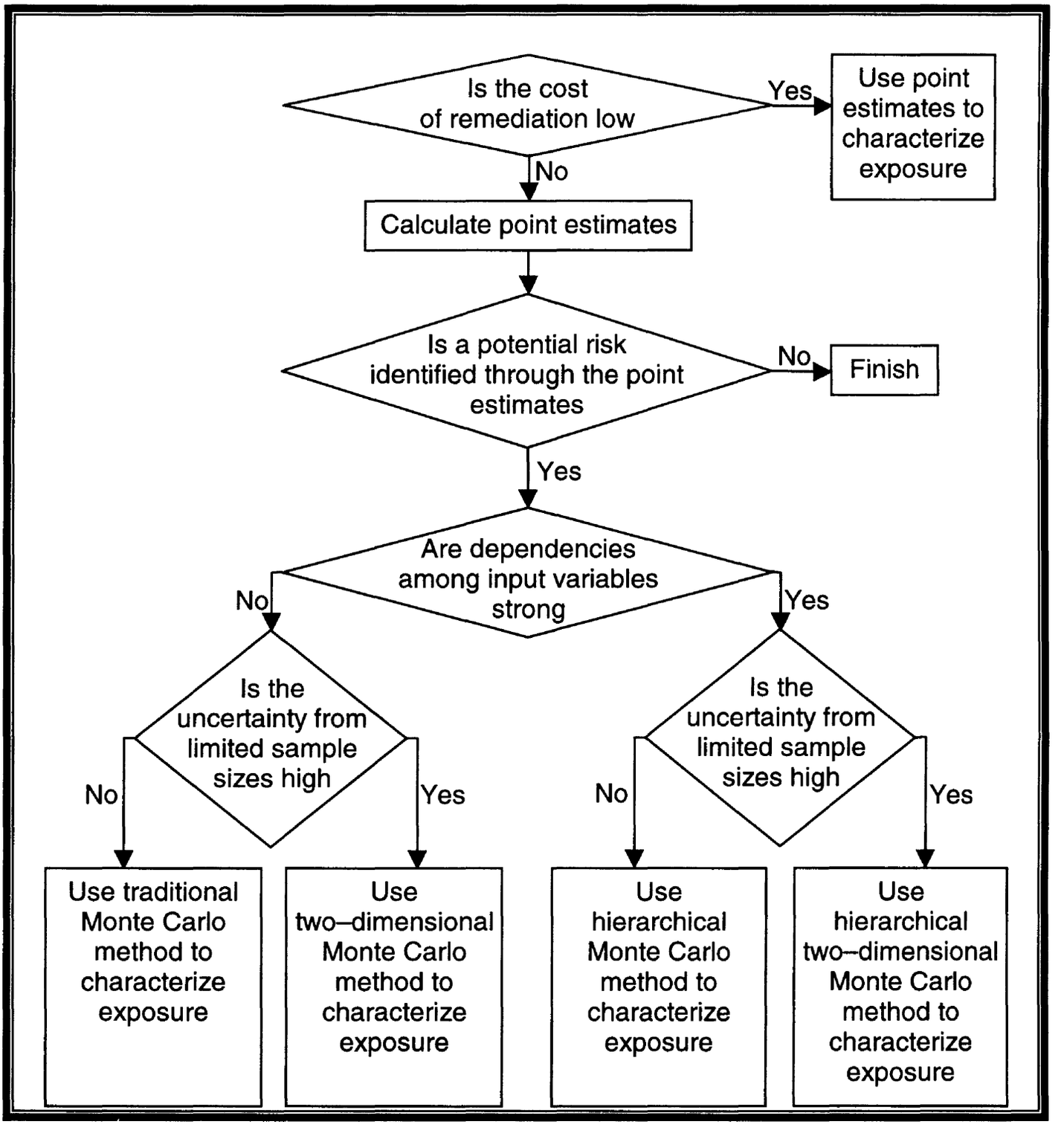

Figure 9–1. Decision Tree for Exposure Characteristic Methods

The different methods were all employed to execute a detailed analysis of methylmercury exposure from the consumption of Northern lobster.

Point estimates demonstrated that methylmercury exposure from Northern lobster consumption could potentially exceed current risk values; consequently, probabilistic methods were employed to further characterize exposure.

The most appropriate probabilistic method was the hierarchical simulation due to strong dependencies among input variables and negligible uncertainty given the large sample sizes. Seven and a half percent of the exposures from the hierarchical simulation exceeded EPA's Reference Dose (0.1 μg/kg/day) and fewer than 0.1% surpassed ATSDR's Minimal Risk Level (0.5 μg/kg/day).

A sensitivity analysis revealed that the most sensitive variable was lobster consumption rate, then mercury concentration, and finally body weight. Although the sensitivities were ranked, sensitivity indices from all three input variables were quite similar. Based on the Spearman and partial rank–order correlation coefficients, the greatest contribution to overall uncertainty was from uncertainty in mercury concentration, then lobster consumption, and finally body weight. But the partial rank–order correlation coefficients did not differ much for all three of the input variables.

Three additional scenarios were explored using the lobster data. First, methylmercury exposure in women of childbearing age was characterized using a hierarchical Monte Carlo simulation. EPA's Reference Dose (0.1 μg/kg/day) was exceeded by 3.3% of the simulated exposures, yet none of the simulated exposures surpassed ATSDR's Minimal Risk Level (0.5 μg/kg/day).

Next, methylmercury exposure was characterized for children between one and four years of age. EPA's Reference Dose was exceeded by 38.2% of the simulated exposures, and 0.3% of the simulated exposures surpassed ATSDR's Minimal Risk Level.

Finally, hierarchical simulations were used to explore the exposures resulting from the consumption of one, two, three, or four lobsters per month. EPA's Reference Dose was exceeded by 5.9% of the simulated exposures from the consumption of one lobster per month, 24.7% of the simulated exposures from the consumption of two lobsters per month, 53.0% of the simulated exposures from the consumption of three lobsters per month, and 76.0% of the simulated exposures from the consumption of four lobsters per month. However, none of the simulated exposures from the consumption of one lobster per month were greater than ATSDR's Minimal Risk Level, and the MRL was surpassed by only 0.1% of the simulated exposures from the consumption of two lobsters per month, 0.6% of the simulated exposures from the consumption of three lobsters per month, and 1.7% of the simulated exposures from the consumption of four lobsters per month.

Although an alarmingly high proportion of iterations exceeded the risk values in some of the scenarios, it should be remembered that these simulations characterized individuals who consumed Northern lobster during a given month. And this is a small proportion of the U.S. population, particularly when considering young children and teens.

Distributions of mercury concentration for the nine most frequently consumed marine species were used in a hierarchical Monte Carlo simulation to characterize mercury exposure from multiple species. EPA's Reference Dose was exceeded by only 0.1% of the simulated exposures, and none of the simulated exposures surpassed ATSDR's Minimal Risk Level. Again it should be

remembered that this simulation was performed for the population consuming two meals of these species each month.

Future Directions

The hierarchical, two–dimensional, and hierarchical two–dimensional Monte Carlo simulation techniques could benefit from a set of standard guidelines. Some guidelines are emerging for the traditional simulation, but the more advanced simulation techniques lack guidelines. As these advanced simulation techniques become more accepted it will be necessary to develop some "Rules of Thumb." For example, what constitutes "high" uncertainty from limited sample sizes and what is a "strong" dependency among input variables.

The immediate future could also be used to improve the multiple species simulation. Better estimates of seafood consumption patterns and additional species could greatly benefit this simulation.

Several federal agencies are currently collaborating to carry out the Fourth National Health and Nutrition Examination Survey (NHANES IV). As a part of this survey, the mercury concentration will be measured in hair and blood from several thousand individuals. Hair mercury concentrations provide a biological record of dietary exposure over a period of several months, while mercury concentrations in the blood account for more recent exposures. These biomarkers could be compared to exposures estimated using each participant's reported seafood consumption pattern.

These techniques could also be used to estimate exposure from additional species/contaminant combinations. Some examples might include the following: shark and mercury, swordfish and mercury, oysters and vibrio species, crabs and vibrio species, shrimp and salmonella, or clams and hepatitis.

These methods should be applied beyond the exposure assessment for problems such as the identification of sources of methylmercury exposure, pharmacokinetic differences in the way individuals distribute and eliminate methylmercury, and the detrimental effects caused by different methylmercury exposures.

Beyond these seafood safety applications, one can imagine countless potential research problems where these techniques would be beneficial.

Appendices

Appendix A

S–Distribution Approximation

Read a vector (v) containing values to be fit to the S-distribution with parameters g, h and α.

v := READPRN ("C:females.txt")

N := rows(v)

N = 699

i := 0..N - 1

Sort the values into increasing order.

v := sort(v)

Define function to return true (1) if x is an integer or false (0) otherwise.

$$\text{is\_int}(x) := \begin{cases} 1 & \text{if } \text{floor}(x) = x \\ 0 & \text{otherwise} \end{cases}$$

Function which returns quantiles for an array of samples (v) of size N.

$$\text{sample\_quantiles}(\text{num\_samples}, \text{sample\_array}) := \left| \begin{array}{l} qq_0 \leftarrow 0 \\ \text{for } ii \in 1..\text{num\_samples} - 1 \\ \quad \left| \begin{array}{l} k \leftarrow ii \cdot \dfrac{\dfrac{100}{\text{num\_samples}}}{100} \cdot \text{num\_samples} \\ qq_{ii} \leftarrow \dfrac{\text{sample\_array}_{k-1} + \text{sample\_array}_k}{2} \quad \text{if } \text{is\_int}(k) \\ qq_{ii} \leftarrow \text{sample\_array}_{\text{floor}(k)} \quad \text{otherwise} \end{array} \right. \\ qq \end{array} \right.$$

Read in coefficient tables from files.

c0 := READPRN("c0_tab.prn")
d0 := READPRN("d0_tab.prn")
c1 := READPRN("c1_tab.prn")
d1 := READPRN("d1_tab.prn")
c2 := READPRN("c2_tab.prn")
d2 := READPRN("d2_tab.prn")
μstand := READPRN("means.prn")
σstand := READPRN("vars.prn")

The tolerance level must be set low, but not too low, to use the Minerr function (play with this if Minerr is not working).

TOL := 0.0000001

findparams(μ, σ, q) :=

best_so_far ← 999999.0

$$save \leftarrow \begin{bmatrix} 0 \\ 0 \end{bmatrix}$$

for $j \in 1 .. rows(c0) - 1$

for $k \in 1 .. cols(c0) - 1$

if $c0_{j,k} \neq 0$

$$\alpha \leftarrow \sqrt{\frac{\sigma stand_{j,k}}{\sigma}}$$

$$median \leftarrow \mu - \frac{\mu stand_{j,k}}{\alpha}$$

$SSE \leftarrow 0$

for $p \in 1 .. rows(q) - 1$

$$t \leftarrow \sqrt{\ln\left[\frac{1}{\left[\frac{\left(p \cdot \frac{100}{rows(q)}\right)}{100}\right]^2}\right]}$$

$$SSE \leftarrow SSE + \left[q_p - \left[median + \frac{t - \frac{c0_{j,k} + c1_{j,k} \cdot t + c2_{j,k} \cdot t^2}{1 + d0_{j,k} \cdot t + d1_{j,k} \cdot t^2 + d2_{j,k} \cdot t^3}}{\alpha}\right]\right]^2$$

if $SSE < best\_so\_far$

best_so_far ← SSE

$$save \leftarrow \begin{bmatrix} \alpha \\ c0_{0,k} \\ c0_{j,0} \\ median \\ var(v) \\ SSE \end{bmatrix}$$

save

mean(v) = 60.599370529

var(v) = 160.39027886

inds := findparams(mean(v), var(v), sample_quantiles(N, v))

These values are the α, g, h, median, variance, and SSE respectively.

$$\text{inds} = \begin{bmatrix} 0.105358547 \\ 0.8 \\ 2 \\ 59.837211194 \\ 160.39027886 \\ 145.682017351 \end{bmatrix}$$

The following files are used in the program above:

c0_tab.prn

0	0	0.1	0.2	0.3	0.4	0.5	0.6	0.7	0.8	0.9	1	1.1	1.2	1.3	1.4
0.5	-16.0782	-19.3456	-43.9177	-67.5421	-120.7135	0	0	0	0	0	0	0	0	0	0
0.6	-14.1874	-16.1664	-29.5752	-50.0000	-64.8229	-89.4550	0	0	0	0	0	0	0	0	0
0.7	-13.2792	-13.9004	-25.1160	-49.4289	-60.2234	-47.8074	-82.5436	0	0	0	0	0	0	0	0
0.8	-12.4774	-12.4042	-22.1274	-39.8493	-26.9283	-30.1601	-41.7719	-80.0119	0	0	0	0	0	0	0
0.9	-11.8214	-11.4243	-20.6917	-17.4161	-18.2573	-21.2805	-27.2799	-40.0255	-79.1746	0	0	0	0	0	0
1.0	-22.5524	-24.6408	-12.6391	-12.9219	-14.1493	-16.3527	-20.0003	-26.3769	-39.4612	-79.2615	0	0	0	0	0
1.1	-11.0149	-10.0768	-10.0791	-10.6350	-11.6767	-13.2922	-15.7286	-19.5511	-26.1032	-39.4504	-79.9157	0	0	0	0
1.2	-8.6097	-8.4160	-8.6278	-9.1553	-9.9962	-11.2142	-12.9534	-15.4983	-19.4361	-26.1471	-39.7619	-80.7941	0	0	0
1.3	-7.4102	-7.3959	-7.6338	-8.0893	-8.7687	-9.7147	-11.0151	-12.8308	-15.4614	-19.5123	-26.3855	-40.2157	-81.3899	0	0
1.4	-6.6312	-6.6703	-6.8896	-7.2737	-7.8280	-8.5807	-9.5880	-10.9481	-12.8313	-15.5486	-19.7132	-26.7099	-40.5533	-81.1595	0
1.5	-6.3959	-6.1134	-6.3031	-6.6251	-7.0822	-7.6929	-8.4947	-9.5507	-10.9660	-12.9180	-15.7203	-19.9659	-26.9495	-40.4751	-80.0115
1.6	-5.6334	-5.6668	-5.8254	-6.0950	-6.4755	-6.9790	-7.6309	-8.4738	-9.5760	-11.0471	-13.0645	-15.9219	-20.1431	-26.8979	-39.9045
1.7	-5.2800	-5.2981	-5.4272	-5.6527	-5.9720	-6.3926	-6.9318	-7.6193	-8.5014	-9.6496	-11.1715	-13.2263	-16.0526	-20.0920	-26.5059
1.8	-4.9878	-4.9876	-5.0898	-5.2779	-5.5475	-5.9025	-6.3548	-6.9253	-7.6467	-8.5671	-9.7550	-11.3014	-13.3209	-15.9963	-19.7873
1.9	-4.7419	-4.7225	-4.7999	-4.9562	-5.1848	-5.4870	-5.8708	-6.3512	-6.9513	-7.7048	-8.6565	-9.8593	-11.3683	-13.2604	-15.7471
2.0	-4.5328	-4.4935	-4.5483	-4.6771	-4.8714	-5.1305	-5.4594	-5.8687	-6.3753	-7.0027	-7.7808	-8.7404	-9.9054	-11.3063	-13.0527
2.1	-4.3539	-4.2942	-4.3282	-4.4330	-4.5983	-4.8216	-5.1056	-5.4580	-5.8907	-6.4207	-7.0677	-7.8487	-8.7713	-9.8446	-11.1322
2.2	-4.2004	-4.1197	-4.1342	-4.2177	-4.3582	-4.5515	-4.7986	-5.1045	-5.4780	-5.9312	-6.4766	-7.1230	-7.8688	-8.7136	-9.6986
2.3	-4.0689	-3.9663	-3.9623	-4.0268	-4.1457	-4.3136	-4.5297	-4.7973	-5.1227	-5.5142	-5.9797	-6.5223	-7.1357	-7.8154	-8.5913
2.4	-3.9571	-3.8298	-3.8094	-3.8566	-3.9567	-4.1026	-4.2925	-4.5282	-4.8139	-5.1553	-5.5568	-6.0179	-6.5300	-7.0873	-7.7134
2.5	-3.8630	-3.7123	-3.6729	-3.7041	-3.7875	-3.9144	-4.0820	-4.2908	-4.5434	-4.8435	-5.1931	-5.5893	-6.0224	-6.4866	-7.0014
2.6	-3.7855	-3.6077	-3.5507	-3.5670	-3.6353	-3.7457	-3.8940	-4.0799	-4.3046	-4.5704	-4.8775	-5.2213	-5.5919	-5.9841	-6.4147
2.7	-3.7240	-3.5160	-3.4412	-3.4434	-3.4981	-3.5937	-3.7253	-3.8938	-4.0926	-4.3296	-4.6013	-4.9023	-5.2227	-5.5582	-5.9236
2.8	-3.6787	-3.4363	-3.3430	-3.3316	-3.3737	-3.4562	-3.5732	-3.7224	-3.9033	-4.1158	-4.3580	-4.6237	-4.9032	-5.1933	-5.5072
2.9	-3.6495	-3.3679	-3.2551	-3.2302	-3.2607	-3.3315	-3.3723	-3.5698	-3.7332	-3.9249	-4.1422	-4.3784	-4.6245	-4.8775	-5.1502
3.0	-3.6381	-3.2893	-3.1763	-3.1383	-3.1578	-3.2178	-3.3103	-3.4333	-3.5799	-3.7537	-3.9497	-4.1611	-4.3793	-4.6021	-4.8412

c1_tab.prn

0	0	0.1	0.2	0.3	0.4	0.5	0.6	0.7	0.8	0.9	1	1.1	1.2	1.3	1.4
0.5	-128.9238	-108.3040	-730.0920	-949.0040	-1162.335	0	0	0	0	0	0	0	0	0	0
0.6	-113.8897	-93.8430	-393.8961	-966.7443	-748.4182	-407.6449	0	0	0	0	0	0	0	0	0
0.7	-114.3825	-77.3803	-318.4160	-845.7238	-895.9203	-282.2945	-236.5673	0	0	0	0	0	0	0	0
0.8	-108.7077	-69.3206	-265.2759	-616.6134	-213.2339	-143.5262	-129.3513	-169.5211	0	0	0	0	0	0	0
0.9	-102.6505	-66.1493	-242.8841	-125.0218	-87.4687	-72.4890	-70.0455	-82.6352	-141.8257	0	0	0	0	0	0
1.0	-346.9992	-197.4961	-80.6665	-57.3893	-45.6158	-40.0958	-39.5374	-45.3084	-64.4267	-134.8628	0	0	0	0	0
1.1	-96.6167	-61.3251	-43.4412	-33.2251	-27.2451	-24.1985	-23.7331	-26.6600	-35.5513	-58.9826	-140.0213	0	0	0	0
1.2	-53.7587	-37.7009	-27.9248	-21.6982	-17.7605	-15.5697	-15.0473	-16.6052	-21.4985	-32.9696	-60.6065	-149.1029	0	0	0
1.3	-36.6526	-26.5021	-19.8117	-15.3025	-12.3121	-10.5379	-9.9444	-10.7860	-13.7740	-20.5073	-34.5656	-65.0684	-150.3056	0	0
1.4	-27.6862	-20.2021	-15.0154	-11.4052	-8.9367	-7.3996	-6.7660	-7.2003	-9.1514	-13.5456	-22.1170	-37.8921	-66.5511	-131.7519	0
1.5	-27.8563	-16.2829	-11.9473	-8.8727	-6.7261	-5.3418	-4.6871	-4.8720	-6.1988	-9.2582	-15.0287	-24.7563	-39.2439	-58.6304	-93.1573
1.6	-19.0735	-13.6909	-9.8795	-7.1493	-5.2176	-3.9382	-3.2740	-3.2954	-4.2140	-6.4296	-10.5401	-17.1009	-25.7665	-34.3072	-40.3498
1.7	-16.7906	-11.9042	-8.4337	-5.9370	-4.1554	-2.9525	-2.2836	-2.1926	-2.8277	-4.4675	-7.4903	-12.1253	-17.7223	-22.0294	-22.4327
1.8	-15.2198	-10.6404	-7.3987	-5.0641	-3.3909	-2.2448	-1.5744	-1.4020	-1.8316	-3.0569	-5.3173	-8.6651	-12.3903	-14.5817	-13.2748
1.9	-14.1293	-9.7368	-6.6455	-4.4254	-2.8314	-1.7286	-1.0578	-0.8251	-1.1005	-2.0174	-3.7195	-6.1562	-8.6393	-9.6194	-7.7286
2.0	-13.3855	-9.0903	-6.0953	-3.9553	-2.4189	-1.3488	-0.6784	-0.3997	-0.5571	-1.2387	-2.5215	-4.2916	-5.9123	-6.1513	-4.0932
2.1	-12.9036	-8.6367	-5.6953	-3.6088	-2.1145	-1.0689	-0.3988	-0.0843	-0.1501	-0.6496	-1.6116	-2.8860	-3.8964	-3.6710	-1.6238
2.2	-12.6296	-8.3308	-5.4105	-3.3558	-1.8913	-0.8638	-0.1938	0.1485	0.1551	-0.2021	-0.9168	-1.8189	-2.3938	-1.8798	0.0759
2.3	-12.5276	-8.1448	-5.2162	-3.1767	-1.7303	-0.7160	-0.0454	0.3193	0.3830	0.1380	-0.3853	-1.0065	-1.2709	-0.5833	1.2458
2.4	-12.5792	-8.0388	-5.0950	-3.0553	-1.6191	-0.6126	0.0592	0.4419	0.5511	0.3948	0.0208	-0.3885	-0.4322	0.3531	2.0415
2.5	-12.7707	-8.0591	-5.0350	-2.9815	-1.5472	-0.5443	0.1291	0.5267	0.6725	0.5867	0.3292	0.0802	0.1923	1.0272	2.5842
2.6	-13.0964	-8.1378	-5.0273	-2.9471	-1.5074	-0.5047	0.1716	0.5814	0.7569	0.7272	0.5609	0.4334	0.6545	1.5051	2.9373
2.7	-13.5612	-8.2869	-5.0658	-2.9465	-1.4947	-0.4883	0.1917	0.5885	0.8119	0.8271	0.7324	0.6968	0.9937	1.8412	3.1591
2.8	-14.1769	-8.5064	-5.1465	-2.9751	-1.5042	-0.4914	0.1937	0.6236	0.8430	0.8944	0.8561	0.8902	1.2395	2.0719	3.2874
2.9	-14.9514	-8.7970	-5.2667	-3.0297	-1.5339	-0.5108	0.7995	0.6190	0.8549	0.9355	0.9418	1.0289	1.4124	2.2243	3.3499
3.0	-15.9216	-8.8868	-5.4232	-3.1089	-1.5806	-0.5442	0.1544	0.5850	0.8509	0.9553	0.9968	1.1242	1.5308	2.3186	3.3654

c2_tab.prn

0	0	0.1	0.2	0.3	0.4	0.5	0.6	0.7	0.8	0.9	1	1.1	1.2	1.3	1.4
0.5	172.2301	143.4900	811.0143	997.5759	1168.7229	0	0	0	0	0	0	0	0	0	0
0.6	158.6212	129.7058	466.8316	1057.2712	792.2605	447.3281	0	0	0	0	0	0	0	0	0
0.7	163.7989	112.3872	395.6855	974.9946	984.0244	318.5643	283.6795	0	0	0	0	0	0	0	0
0.8	160.6653	104.4986	344.1948	745.8210	259.8198	177.3937	163.2180	219.3787	0	0	0	0	0	0	0
0.9	156.3971	102.5124	326.7606	169.5908	120.1693	100.9847	98.4704	115.5945	192.5710	0	0	0	0	0	0
1.0	511.3211	299.5162	121.0186	87.7758	71.3882	64.0490	63.6703	71.7390	96.8051	185.4251	0	0	0	0	0
1.1	154.9734	99.9256	72.5960	57.4099	48.8656	44.8110	44.5525	48.9383	60.9806	90.8408	189.7074	0	0	0	0
1.2	93.2771	67.2241	51.7958	42.3153	36.6158	33.7183	33.3555	35.9206	42.8279	57.7968	91.9021	197.6921	0	0	0
1.3	68.2970	51.3671	40.5625	33.5735	29.1949	26.8374	26.3291	27.8906	32.2922	41.3101	58.9527	95.7532	198.4169	0	0
1.4	54.9976	42.2340	33.6965	28.0083	24.3424	22.2690	21.6475	22.6019	25.5990	31.6374	42.5954	61.8686	96.7166	180.9534	0
1.5	55.9173	36.4169	29.1541	24.2281	20.9859	19.0772	18.3683	18.9259	21.0508	25.3623	32.8861	44.9543	62.7739	88.6407	145.1284
1.6	41.9856	32.4812	25.9882	21.5380	18.5647	16.7551	15.9783	16.2583	17.7952	20.9970	26.4694	34.7578	45.5830	57.3918	70.7196
1.7	38.4751	29.7095	23.6996	19.5578	16.7602	15.0126	14.1792	14.2556	15.3715	17.8027	21.9168	27.8959	35.0346	41.2967	45.1930
1.8	36.0485	27.7103	22.0060	18.0646	15.3831	13.6729	12.7916	12.7112	13.5124	15.3779	18.5268	22.9478	27.8283	31.2949	31.9333
1.9	34.3690	26.2564	20.7321	16.9186	14.3120	12.6228	11.6993	11.4951	12.0525	13.4880	15.9177	19.2198	22.5857	24.4307	23.7018
2.0	33.2427	25.2023	19.7694	16.0312	13.4688	11.7881	10.8271	10.5224	10.8865	11.9861	13.8646	16.3325	18.6286	19.4577	18.1112
2.1	32.5471	24.4567	19.0445	15.3401	12.8002	11.1182	10.1226	9.7345	9.9433	10.7758	12.2228	14.0563	15.5775	15.7457	14.1288
2.2	32.2046	23.9549	18.5075	14.8028	12.2678	10.5773	9.5493	9.0916	9.1728	9.7908	10.8967	12.2416	13.1937	12.9272	11.2157
2.3	32.1647	23.6575	18.1236	14.3914	11.8441	10.1397	9.0804	8.5626	8.5391	8.9826	9.8173	10.7831	11.3157	10.7643	9.0518
2.4	32.4051	23.4996	17.8672	14.0822	11.5110	9.7856	8.6960	8.1265	8.0154	8.3166	8.9336	9.6047	9.8271	9.0921	7.4309
2.5	32.9099	23.5730	17.7215	13.8599	11.2521	9.5006	8.3816	7.7663	7.5815	7.7656	8.2073	8.6482	8.6411	7.7893	6.1936
2.6	33.6768	23.7574	17.6734	13.7125	11.0565	9.2743	8.1251	7.4694	7.2218	7.3091	7.6091	7.8692	7.6926	6.7727	5.2533
2.7	34.7226	24.0791	17.7145	13.6313	10.9158	9.0976	7.9181	7.2638	6.9238	6.9305	7.1153	7.2332	6.9306	5.9721	4.5306
2.8	36.0777	24.5413	17.8390	13.6089	10.8223	8.9642	7.7529	7.0261	6.6781	6.6170	6.7077	6.7130	6.3160	5.3394	3.9724
2.9	37.7652	25.1489	18.0438	13.6410	10.7726	8.8684	6.5528	6.8653	6.4764	6.3582	6.3712	6.2869	5.8211	4.8375	3.5384
3.0	39.8660	25.3717	18.3244	13.7250	10.7610	8.8060	7.5281	6.7656	6.3128	6.1457	6.0948	5.9386	5.4201	4.4380	3.2001

d0_tab.prn

0	0	0.1	0.2	0.3	0.4	0.5	0.6	0.7	0.8	0.9	1	1.1	1.2	1.3	1.4
0.5	18.2137	14.0624	53.5421	49.4545	34.6011	0	0	0	0	0	0	0	0	0	0
0.6	19.8140	15.3204	40.7767	68.5313	41.5286	15.6668	0	0	0	0	0	0	0	0	0
0.7	23.3263	15.7318	42.4980	85.9595	70.9000	19.3007	11.2758	0	0	0	0	0	0	0	0
0.8	25.8385	16.7307	43.9122	81.2734	26.4411	16.0102	11.7288	9.4763	0	0	0	0	0	0	0
0.9	28.0299	18.3261	48.0667	24.2365	16.3486	12.5946	10.5264	9.3270	8.6550	0	0	0	0	0	0
1.0	94.1145	56.2058	21.9572	15.6826	12.3501	10.4102	9.2517	8.5973	8.3157	8.3454	0	0	0	0	0
1.1	33.1810	21.4641	15.6375	12.3243	10.3050	9.0475	8.2759	7.8716	7.7647	7.9266	8.3315	0	0	0	0
1.2	22.6014	16.4789	12.8491	10.5692	9.0941	8.1432	7.5652	7.2799	7.2494	7.4573	7.8790	8.4142	0	0	0
1.3	18.3306	14.0467	11.3117	9.5092	8.3066	7.5181	7.0392	6.8136	6.8158	7.0361	7.4522	7.9656	8.3162	0	0
1.4	16.0806	12.6522	10.3617	8.8123	7.7602	7.0629	6.6384	6.4421	6.4554	6.6723	7.0736	7.5674	7.9096	7.7626	0
1.5	17.1077	11.7803	9.7337	8.3286	7.3636	6.7188	6.3233	6.1397	6.1520	6.3560	6.7349	7.2040	7.5358	7.4114	6.7456
1.6	14.0142	11.2139	9.3035	7.9812	7.0667	6.4508	6.0696	5.8881	5.8917	6.0763	6.4257	6.8608	7.1698	7.0543	6.4283
1.7	13.5291	10.8432	9.0045	7.7272	6.8395	6.2380	5.8611	5.6752	5.6650	5.8256	6.1394	6.5306	6.8019	6.6784	6.0817
1.8	13.2565	10.6084	8.7991	7.5407	6.6641	6.0667	5.6877	5.4928	5.4658	5.5990	5.8728	6.2123	6.4330	6.2869	5.7109
1.9	13.1387	10.4751	8.6633	7.4053	6.5281	5.9278	5.5419	5.3353	5.2895	5.3938	5.6250	5.9080	6.0701	5.8918	5.3303
2.0	13.1445	10.4213	8.5825	7.3108	6.4239	5.8151	5.4192	5.1989	5.1333	5.2081	5.3962	5.6213	5.7216	5.5071	4.9567
2.1	13.2553	10.4338	8.5470	7.2494	6.3461	5.7243	5.3159	5.0806	4.9950	5.0407	5.1866	5.3552	5.3953	5.1448	4.6039
2.2	13.4607	10.5032	8.5504	7.2161	6.2906	5.6524	5.2296	4.9787	4.8729	4.8908	4.9965	5.1118	5.0958	4.8126	4.2811
2.3	13.7557	10.6254	8.5883	7.2082	6.2544	5.5971	5.1583	4.8911	4.7659	4.7571	4.8256	4.8920	4.8258	4.5145	3.9928
2.4	14.1428	10.7837	8.6577	7.2224	6.2360	5.5565	5.1002	4.8167	4.6726	4.6390	4.6733	4.6959	4.5858	4.2513	3.7409
2.5	14.6249	11.0195	8.7573	7.2575	6.2334	5.5292	5.0546	4.7543	4.5921	4.5354	4.5387	4.5224	4.3747	4.0212	3.5199
2.6	15.2092	11.2921	8.8860	7.3121	6.2457	5.5143	5.0201	4.7032	4.5234	4.4455	4.4209	4.3704	4.1906	3.8229	3.3310
2.7	15.9099	11.6162	9.0440	7.3859	6.2720	5.5111	4.9962	4.6777	4.4658	4.3682	4.3186	4.2383	4.0313	3.6521	3.1692
2.8	16.7469	11.9970	9.2320	7.4782	6.3115	5.5188	4.9820	4.6312	4.4186	4.3027	4.2307	4.1243	3.8940	3.5059	3.0316
2.9	17.7374	12.4407	9.4510	7.5891	6.3644	5.5368	4.5091	4.6090	4.3808	4.2482	4.1561	4.0268	3.7772	3.3814	2.9144
3.0	18.9238	12.7181	9.7015	7.7194	6.4299	5.5650	4.9812	4.6078	4.3522	4.2039	4.0938	3.9444	3.6778	3.2757	2.8151

d1_tab.prn

0	0	0.1	0.2	0.3	0.4	0.5	0.6	0.7	0.8	0.9	1	1.1	1.2	1.3	1.4
0.5	29.2034	19.9516	88.3916	72.9399	41.2941	0	0	0	0	0	0	0	0	0	0
0.6	28.5472	19.9058	60.4030	110.3760	53.1470	14.2160	0	0	0	0	0	0	0	0	0
0.7	30.5096	18.2183	56.6642	115.8462	89.8645	19.0595	8.0390	0	0	0	0	0	0	0	0
0.8	30.4138	17.4725	52.3078	97.9678	27.4073	13.9735	8.4537	5.5452	0	0	0	0	0	0	0
0.9	29.7080	17.3842	51.3232	22.8935	13.4887	9.0204	6.5682	5.1601	4.3961	0	0	0	0	0	0
1.0	98.6481	51.7511	18.6970	11.7635	8.0931	5.9682	4.7133	4.0262	3.7728	3.9052	0	0	0	0	0
1.1	28.9456	16.8437	10.8458	7.4511	5.3950	4.1252	3.3607	2.9808	2.9253	3.1835	3.7540	0	0	0	0
1.2	16.7728	10.8684	7.3897	5.2210	3.8305	2.9447	2.4177	2.1754	2.1904	2.4627	2.9883	3.6773	0	0	0
1.3	11.7788	7.9174	5.4745	3.8811	2.8306	2.1518	1.7491	1.5740	1.6108	1.8636	2.3283	2.9209	3.3663	0	0
1.4	9.0733	6.1797	4.2714	2.9977	2.1456	1.5902	1.2607	1.1207	1.1597	1.3834	1.7890	2.3036	2.6898	2.5868	0
1.5	8.9750	5.0429	3.4514	2.3765	1.6513	1.1761	0.8929	0.7720	0.8051	0.9974	1.3475	1.7931	2.1305	2.0480	1.4414
1.6	6.3179	4.2479	2.8602	1.9182	1.2802	0.8603	0.6084	0.4982	0.5219	0.6837	0.9815	1.3618	1.6500	1.5775	1.0518
1.7	5.5251	3.6642	2.4158	1.5677	0.9925	0.6130	0.3834	0.2793	0.2927	0.4256	0.6749	0.9928	1.2289	1.1554	0.6953
1.8	4.9406	3.2201	2.0709	1.2918	0.7639	0.4150	0.2021	0.1017	0.1050	0.2117	0.4166	0.6759	0.8595	0.7772	0.3710
1.9	4.4972	2.8733	1.7962	1.0694	0.5781	0.2534	0.0536	-0.0443	-0.0502	0.0333	0.1988	0.4048	0.5387	0.4445	0.0838
2.0	4.1552	2.5967	1.5730	0.8867	0.4247	0.1195	-0.0696	-0.1655	-0.1794	-0.1159	0.0153	0.1747	0.2646	0.1591	-0.1619
2.1	3.8891	2.3726	1.3883	0.7341	0.2959	0.0069	-0.1730	-0.2672	-0.2876	-0.2410	-0.1389	-0.0189	0.0341	-0.0796	-0.3651
2.2	3.6816	2.1884	1.2333	0.6046	0.1863	-0.0888	-0.2607	-0.3530	-0.3788	-0.3462	-0.2682	-0.1806	-0.1569	-0.2749	-0.5282
2.3	3.5210	2.0359	1.1017	0.4934	0.0918	-0.1711	-0.3358	-0.4262	-0.4561	-0.4348	-0.3765	-0.3149	-0.3133	-0.4318	-0.6559
2.4	3.4000	1.9047	0.9885	0.3968	0.0096	-0.2427	-0.4009	-0.4891	-0.5219	-0.5097	-0.4671	-0.4258	-0.4402	-0.5562	-0.7536
2.5	3.3127	1.8028	0.8902	0.3118	-0.0630	-0.3057	-0.4577	-0.5436	-0.5784	-0.5732	-0.5430	-0.5173	-0.5428	-0.6539	-0.8278
2.6	3.2553	1.7143	0.8041	0.2363	-0.1277	-0.3616	-0.5078	-0.5912	-0.6272	-0.6274	-0.6069	-0.5928	-0.6254	-0.7301	-0.8829
2.7	3.2263	1.6402	0.7280	0.1685	-0.1859	-0.4118	-0.5524	-0.6319	-0.6697	-0.6740	-0.6608	-0.6553	-0.6920	-0.7896	-0.9237
2.8	3.2254	1.5792	0.6601	0.1069	-0.2389	-0.4574	-0.5926	-0.6705	-0.7071	-0.7143	-0.7066	-0.7072	-0.7459	-0.8359	-0.9536
2.9	3.2514	1.5297	0.5992	0.0504	-0.2877	-0.4991	-0.6516	-0.7042	-0.7402	-0.7494	-0.7458	-0.7507	-0.7896	-0.8720	-0.9753
3.0	3.3085	1.4457	0.5437	-0.0019	-0.3331	-0.5378	-0.6628	-0.7346	-0.7699	-0.7804	-0.7797	-0.7873	-0.8254	-0.9005	-0.9911

d2_tab.prn

0	0	0.1	0.2	0.3	0.4	0.5	0.6	0.7	0.8	0.9	1	1.1	1.2	1.3	1.4
0.5	-1.2160	-0.2358	2.1134	6.0892	7.7824	0	0	0	0	0	0	0	0	0	0
0.6	-1.5808	-0.6615	-0.6338	1.1119	3.8782	2.3948	0	0	0	0	0	0	0	0	0
0.7	-1.9638	-0.8476	-1.7714	-1.1306	1.6261	1.2438	1.1394	0	0	0	0	0	0	0	0
0.8	-2.1419	-0.9709	-2.3318	-2.9170	-0.1982	0.2945	0.4830	0.5744	0	0	0	0	0	0	0
0.9	-2.2122	-1.0709	-2.7426	-0.8735	-0.2777	-0.0089	0.1280	0.1973	0.2230	0	0	0	0	0	0
1.0	-7.7756	-3.4823	-1.0441	-0.4939	-0.2179	-0.0705	0.0041	0.0286	0.0094	-0.0591	0	0	0	0	0
1.1	-2.2795	-1.1474	-0.6075	-0.3171	-0.1536	-0.0644	-0.0249	-0.0265	-0.0698	-0.1646	-0.3267	0	0	0	0
1.2	-1.3054	-0.7272	-0.4021	-0.2117	-0.1005	-0.0411	-0.0205	-0.0348	-0.0875	-0.1892	-0.3533	-0.5808	0	0	0
1.3	-0.8977	-0.5122	-0.2809	-0.1406	-0.0581	-0.0158	-0.0055	-0.0255	-0.0806	-0.1807	-0.3380	-0.5499	-0.7647	0	0
1.4	-0.6716	-0.3808	-0.2002	-0.0892	-0.0241	0.0077	0.0122	-0.0103	-0.0644	-0.1597	-0.3071	-0.5034	-0.6995	-0.7911	0
1.5	-0.6548	-0.2914	-0.1420	-0.0498	0.0036	0.0285	0.0295	0.0064	-0.0453	-0.1345	-0.2710	-0.4515	-0.6311	-0.7145	-0.6383
1.6	-0.4314	-0.2261	-0.0976	-0.0186	0.0266	0.0467	0.0454	0.0226	-0.0260	-0.1085	-0.2335	-0.3978	-0.5604	-0.6352	-0.5646
1.7	-0.3582	-0.1760	-0.0624	0.0070	0.0461	0.0626	0.0599	0.0377	-0.0077	-0.0834	-0.1969	-0.3444	-0.4887	-0.5530	-0.4866
1.8	-0.3016	-0.1359	-0.0334	0.0285	0.0628	0.0765	0.0728	0.0515	0.0093	-0.0599	-0.1621	-0.2929	-0.4182	-0.4702	-0.4066
1.9	-0.2562	-0.1027	-0.0089	0.0470	0.0774	0.0888	0.0844	0.0640	0.0248	-0.0382	-0.1298	-0.2446	-0.3509	-0.3901	-0.3284
2.0	-0.2186	-0.0746	0.0122	0.0632	0.0903	0.0998	0.0947	0.0751	0.0387	-0.0187	-0.1004	-0.2002	-0.2889	-0.3159	-0.2558
2.1	-0.1867	-0.0500	0.0310	0.0777	0.1018	0.1096	0.1040	0.0851	0.0512	-0.0012	-0.0740	-0.1604	-0.2332	-0.2495	-0.1912
2.2	-0.1590	-0.0281	0.0479	0.0908	0.1123	0.1186	0.1123	0.0941	0.0623	0.0144	-0.0507	-0.1253	-0.1843	-0.1917	-0.1357
2.3	-0.1344	-0.0082	0.0634	0.1029	0.1220	0.1267	0.1199	0.1021	0.0722	0.0281	-0.0302	-0.0946	-0.1422	-0.1427	-0.0892
2.4	-0.1121	0.0104	0.0778	0.1142	0.1310	0.1343	0.1269	0.1094	0.0810	0.0402	-0.0123	-0.0682	-0.1065	-0.1017	-0.0512
2.5	-0.0914	0.0276	0.0916	0.1249	0.1395	0.1413	0.1333	0.1160	0.0888	0.0509	0.0033	-0.0456	-0.0763	-0.0678	-0.0202
2.6	-0.0718	0.0444	0.1048	0.1352	0.1476	0.1480	0.1392	0.1220	0.0959	0.0603	0.0168	-0.0262	-0.0510	-0.0400	0.0047
2.7	-0.0528	0.0608	0.1177	0.1451	0.1554	0.1543	0.1448	0.1274	0.1022	0.0685	0.0285	-0.0098	-0.0299	-0.0173	0.0246
2.8	-0.0340	0.0772	0.1305	0.1549	0.1630	0.1605	0.1501	0.1326	0.1079	0.0759	0.0386	0.0043	-0.0123	0.0013	0.0405
2.9	-0.0149	0.0937	0.1433	0.1647	0.1704	0.1664	0.1517	0.1374	0.1132	0.0824	0.0475	0.0163	0.0025	0.0166	0.0532
3.0	0.0050	0.1109	0.1563	0.1744	0.1779	0.1722	0.1600	0.1420	0.1180	0.0882	0.0552	0.0265	0.0148	0.0291	0.0634

means.prn

0	0	0.1	0.2	0.3	0.4	0.5	0.6	0.7	0.8	0.9	1	1.1	1.2	1.3	1.4
0.5	0.6247	0.7754	1.0255	1.5236	3.0129	0	0	0	0	0	0	0	0	0	0
0.6	0.5184	0.6178	0.7643	1.0068	1.4894	2.932	0	0	0	0	0	0	0	0	0
0.7	0.4429	0.512	0.6069	0.7478	0.9804	1.4426	2.823	0	0	0	0	0	0	0	0
0.8	0.3864	0.4365	0.5017	0.5918	0.7251	0.9448	1.3804	2.6796	0	0	0	0	0	0	0
0.9	0.3422	0.3795	0.4263	0.4874	0.5712	0.6949	0.8979	1.2992	2.4935	0	0	0	0	0	0
1.0	0.3063	0.335	0.3695	0.4126	0.4682	0.5441	0.6553	0.837	1.1943	2.2541	0	0	0	0	0
1.1	0.277	0.2994	0.3251	0.356	0.3941	0.443	0.5089	0.6044	0.7587	1.0598	1.9473	0	0	0	0
1.2	0.2529	0.27	0.2894	0.3118	0.3382	0.3702	0.4105	0.4636	0.539	0.6584	0.8875	1.5539	0	0	0
1.3	0.2319	0.2453	0.26	0.2762	0.2944	0.3152	0.3395	0.3688	0.4057	0.4554	0.5301	0.6664	1.0474	0	0
1.4	0.214	0.2246	0.2354	0.2469	0.2591	0.2721	0.2858	0.3004	0.3157	0.3318	0.3485	0.3653	0.381	0.3893	0
1.5	0.1982	0.2066	0.2145	0.2223	0.23	0.2373	0.2436	0.2484	0.2505	0.248	0.2373	0.211	0.1519	0.0083	-0.4785
1.6	0.185	0.1909	0.1964	0.2014	0.2056	0.2085	0.2094	0.2074	0.2008	0.1869	0.1613	0.1155	0.0325	-0.1279	-0.4868
1.7	0.1725	0.177	0.1807	0.1834	0.1848	0.1843	0.1812	0.1742	0.1615	0.1402	0.1056	0.0496	-0.0429	-0.2026	-0.5025
1.8	0.1621	0.1649	0.1668	0.1676	0.1668	0.1636	0.1574	0.1466	0.1295	0.1031	0.0627	0.0007	-0.096	-0.2524	-0.5193
1.9	0.1523	0.1541	0.1546	0.1538	0.151	0.1457	0.137	0.1233	0.1029	0.0727	0.0283	-0.0374	-0.1363	-0.2892	-0.536
2.0	0.1435	0.1444	0.1436	0.1414	0.1372	0.1301	0.1193	0.1033	0.0803	0.0473	0	-0.0683	-0.1683	-0.3185	-0.5521
2.1	0.1353	0.1353	0.1338	0.1304	0.1248	0.1163	0.1038	0.0859	0.0608	0.0256	-0.0238	-0.0939	-0.1947	-0.3429	-0.5675
2.2	0.1282	0.1273	0.1248	0.1205	0.1138	0.104	0.0901	0.0707	0.0439	0.0069	-0.0443	-0.1158	-0.2171	-0.3637	-0.582
2.3	0.1215	0.1201	0.1168	0.1115	0.1038	0.0929	0.0778	0.0571	0.0289	-0.0095	-0.0621	-0.1347	-0.2364	-0.3819	-0.5958
2.4	0.1156	0.1133	0.1094	0.1034	0.0948	0.083	0.0668	0.045	0.0156	-0.024	-0.0778	-0.1513	-0.2534	-0.398	-0.6087
2.5	0.1099	0.1072	0.1026	0.0959	0.0866	0.0739	0.0569	0.0341	0.0037	-0.037	-0.0917	-0.166	-0.2685	-0.4126	-0.6209
2.6	0.1048	0.1015	0.0963	0.0891	0.0791	0.0657	0.0479	0.0242	-0.0071	-0.0487	-0.1042	-0.1792	-0.282	-0.4258	-0.6324
2.7	0.0997	0.0962	0.0906	0.0828	0.0722	0.0582	0.0396	0.0152	-0.0169	-0.0592	-0.1155	-0.1912	-0.2943	-0.4378	-0.6432
2.8	0.0956	0.0914	0.0853	0.077	0.0659	0.0512	0.0321	0.007	-0.0258	-0.0688	-0.1258	-0.202	-0.3055	-0.4489	-0.6534
2.9	0.0915	0.0868	0.0804	0.0716	0.06	0.0448	0.0251	-0.0006	-0.034	-0.0776	-0.1352	-0.2119	-0.3157	-0.4591	-0.663
3.0	0.0872	0.0825	0.0759	0.0666	0.0545	0.0389	0.0187	-0.0075	-0.0415	-0.0857	-0.1438	-0.221	-0.3252	-0.4686	-0.6721

vars.prn

0	0	0.1	0.2	0.3	0.4	0.5	0.6	0.7	0.8	0.9	1	1.1	1.2	1.3	1.4
0.5	3.8354	6.1674	11.2917	26.1852	108.0407	0	0	0	0	0	0	0	0	0	0
0.6	2.7338	4.0546	6.5326	11.9863	27.8603	115.2357	0	0	0	0	0	0	0	0	0
0.7	2.0616	2.8938	4.3023	6.9479	12.7807	29.7898	123.5903	0	0	0	0	0	0	0	0
0.8	1.6205	2.1856	3.0757	4.5848	7.4255	13.7021	32.0474	133.458	0	0	0	0	0	0	0
0.9	1.315	1.721	2.3274	3.2846	4.9118	7.983	14.7884	34.7378	145.354	0	0	0	0	0	0
1.0	1.0946	1.399	1.8359	2.4905	3.5277	5.296	8.6456	16.0951	38.0166	160.0575	0	0	0	0	0
1.1	0.9297	1.1661	1.4953	1.9693	2.6821	3.8153	5.7563	9.4499	17.7051	42.1229	178.8015	0	0	0	0
1.2	0.8028	0.9921	1.2489	1.6076	2.1263	2.9099	4.1625	6.3203	10.452	19.7485	47.444	203.6587	0	0	0
1.3	0.7034	0.8585	1.0647	1.3459	1.7405	2.3145	3.1872	4.5918	7.0306	11.7409	22.4405	54.6512	38.4263	0	0
1.4	0.6238	0.7534	0.9232	1.1501	1.4613	1.9009	2.5451	3.533	5.1384	7.9562	13.467	26.1654	65.0299	291.0825	0
1.5	0.5591	0.6693	0.8119	0.9997	1.2524	1.6015	2.099	2.8354	3.9779	5.8596	9.2157	15.906	31.6907	81.4843	383.1573
1.6	0.5053	0.6008	0.7228	0.8814	1.0917	1.3773	1.7757	2.3503	3.2125	4.572	6.856	11.0316	19.6294	40.8653	112.9058
1.7	0.4608	0.5443	0.6502	0.7866	0.9654	1.2048	1.5336	1.9986	2.6798	3.7218	5.4045	8.3198	13.8795	26.0902	59.9632
1.8	0.4228	0.497	0.5903	0.7094	0.8641	1.0692	1.3473	1.735	2.2933	3.1295	4.4449	6.6489	10.673	19.0219	40.6055
1.9	0.3906	0.457	0.5402	0.6456	0.7816	0.9604	1.2007	1.5321	2.0036	2.6996	3.7759	5.543	8.694	15.0724	31.3312
2.0	0.3629	0.4229	0.4979	0.5923	0.7135	0.8718	1.0832	1.3725	1.7804	2.3771	3.2899	4.7712	7.383	12.6328	26.153
2.1	0.339	0.3937	0.4618	0.5473	0.6566	0.7987	0.9874	1.2444	1.6048	2.1286	2.9252	4.2104	6.4677	11.0166	22.9615
2.2	0.3179	0.3683	0.4307	0.5089	0.6084	0.7375	0.9083	1.1401	1.4639	1.933	2.6442	3.7895	5.8026	9.8891	20.8534
2.3	0.2995	0.3461	0.4037	0.4758	0.5674	0.6858	0.8421	1.0539	1.3491	1.7762	2.423	3.4653	5.3036	9.0708	19.3879
2.4	0.2831	0.3266	0.3802	0.4471	0.532	0.6416	0.7862	0.9818	1.2543	1.6484	2.2456	3.2101	4.9196	8.4578	18.328
2.5	0.2687	0.3094	0.3595	0.4221	0.5014	0.6037	0.7386	0.9209	1.1751	1.5429	2.1012	3.0057	4.6176	7.9868	17.5371
2.6	0.2557	0.2941	0.3413	0.4001	0.4747	0.5708	0.6975	0.869	1.1081	1.4547	1.982	2.8393	4.3759	7.6173	16.9318
2.7	0.2443	0.2805	0.3251	0.3807	0.4512	0.5421	0.662	0.8243	1.0511	1.3802	1.8824	2.702	4.1795	7.3221	16.4586
2.8	0.2336	0.2682	0.3106	0.3635	0.4304	0.5169	0.631	0.7857	1.002	1.3168	1.7985	2.5876	4.0178	7.0827	16.082
2.9	0.2242	0.2572	0.2976	0.3481	0.412	0.4946	0.6038	0.7519	0.9595	1.2623	1.727	2.4911	3.883	6.886	15.7778
3.0	0.2159	0.2472	0.2858	0.3343	0.3956	0.4749	0.5798	0.7223	0.9225	1.2152	1.6656	2.4091	3.7697	6.7226	15.5288

Appendix B

Classic Statistical Distributions

Exponential Distribution

Parameters: rate (λ)

PDF:
$$f(x) = \begin{cases} \lambda e^{-\lambda x} & \text{if } x \geq 0 \\ 0 & \text{if } x < 0 \end{cases}$$

Guidelines: $\lambda > 0$

Extreme Value Distribution

Parameters: mode (m), scale (α)

PDF:
$$f(x) = \frac{1}{\alpha} \cdot z \cdot e^{-z} \quad \text{for } -\infty < x < \infty$$

where $z = e^{-\left(\frac{x-m}{\alpha}\right)}$

Left–Truncated PDF:
$$f(x) = \begin{cases} \dfrac{\frac{1}{\alpha} \cdot z \cdot e^{-z}}{1 - F(\min)} & \text{if } \min < x \\ 0 & \text{if } \min \geq x \end{cases}$$

where F(min) is the CDF evaluated at the truncated value (min)

Guidelines: $\alpha > 0$

Note that the Extreme Value Distribution is also known as the Gumbel Distribution

Gamma Distribution

Parameters: location (L), scale (α), shape (β)

PDF:
$$f(x) = \begin{cases} \dfrac{(x-L)^{\beta-1} \cdot e^{-\left(\frac{x-L}{\alpha}\right)}}{\Gamma(\beta) \cdot \alpha^{\beta}} & \text{if } x > L \\ 0 & \text{if } x \leq L \end{cases}$$

Left–Truncated PDF:

$$f(x) = \begin{cases} \dfrac{\left(\dfrac{(x-L)^{\beta-1} \cdot e^{-\left(\frac{x-L}{\alpha}\right)}}{\Gamma(\beta) \cdot \alpha^{\beta}}\right)}{1 - F(\min)} & \text{if } x > \min \geq L \\ 0 & \text{if } x \leq \min \end{cases}$$

where F(min) is the CDF evaluated at the truncated value (min)

Guidelines: $\beta > 0$, $\alpha > 0$

Logistic Distribution

Parameters: mean (μ), scale (α)

PDF: $$f(x) = \frac{z}{a \cdot (1+z)^2} \qquad \text{for } -\infty < x < \infty$$

where $z = e^{-\left(\frac{x-\mu}{\alpha}\right)}$

Left–Truncated PDF:

$$f(x) = \begin{cases} \dfrac{\left(\dfrac{z}{a \cdot (1+z)^2}\right)}{1 - F(\min)} & \text{if } \min < x \\ 0 & \text{if } \min \geq x \end{cases}$$

where F(min) is the CDF evaluated at the truncated value (min)

Guidelines: $\alpha > 0$

Lognormal Distribution

Parameters: mean (μ), standard deviation (σ)

PDF:

$$f(x) = \begin{cases} \dfrac{1}{\sqrt{2\pi} \cdot \sigma_{LN} \cdot x} \cdot e^{\frac{-(\ln(x)-\mu_{LN})^2}{2\sigma_{LN}^2}} & \text{if } x > 0 \\ 0 & \text{if } x \leq 0 \end{cases}$$

where $\mu_{LN} = \ln\left(\dfrac{\mu^2}{\sqrt{\sigma^2 + \mu^2}}\right)$ and $\sigma_{LN} = \sqrt{\ln\left(\dfrac{\sigma^2 + \mu^2}{\mu^2}\right)}$

Guidelines: $\sigma > 0$

Normal Distribution

Parameters: mean (μ), standard deviation (σ)

PDF:
$$f(x) = \frac{1}{\sqrt{2\pi}\cdot\sigma}\cdot e^{\frac{-(x-\mu)^2}{2\sigma^2}} \qquad \text{for } -\infty < x < \infty$$

Left–Truncated PDF:
$$f(x) = \begin{cases} \dfrac{\left(\dfrac{1}{\sqrt{2\pi}\cdot\sigma}\cdot e^{\frac{-(x-\mu)^2}{2\sigma^2}}\right)}{1-F(\min)} & \text{if } \min < x \\ 0 & \text{if } \min \geq x \end{cases}$$

where F(min) is the CDF evaluated at the truncated value (min)

Guidelines: $\sigma > 0$

Weibull Distribution

Parameters: location (L), scale (α), shape (β)

PDF:
$$f(x) = \begin{cases} \left(\dfrac{\beta}{\alpha}\right)\cdot\left(\dfrac{x-L}{\alpha}\right)^{\beta-1}\cdot e^{-\left(\frac{x-L}{\alpha}\right)^{\beta}} & \text{if } x > L \\ 0 & \text{if } x \leq L \end{cases}$$

Left–Truncated PDF:
$$f(x) = \begin{cases} \dfrac{\left(\left(\dfrac{\beta}{\alpha}\right)\cdot\left(\dfrac{x-L}{\alpha}\right)^{\beta-1}\cdot e^{-\left(\frac{x-L}{\alpha}\right)^{\beta}}\right)}{1-F(\min)} & \text{if } x > \min \geq L \\ 0 & \text{if } x \leq \min \end{cases}$$

where F(min) is the CDF evaluated at the truncated value (min)

Guidelines: $\alpha > 0$, $\beta > 0$

Appendix C

Data Characterizing Consumption of Northern Lobster

Infant Consumption

Gender	*Age*	*Consumption (g/month)*
F	2	79
F	3	48
F	3	79
F	3	79
F	4	79
F	5	79
F	6	114
F	7	114
F	7	114
F	7	114
F	8	114
F	9	82
F	9	114
F	10	217
M	1	46
M	2	8
M	2	79
M	2	79
M	2	158
M	4	79
M	4	79
M	4	79
M	4	79
M	4	158
M	5	79
M	5	204
M	6	11
M	6	228
M	7	114
M	8	80
M	8	180
M	9	114
M	10	67
M	10	114
M	10	114
M	11	114
M	11	114
M	11	143
M	11	164
U	3	79
U	7	114
U	10	114

Teen Consumption

Gender	*Age*	*Consumption (g/month)*
F	12	38
F	12	120
F	12	120
F	12	240
F	13	9
F	13	120
F	13	213
F	14	9
F	14	22
F	14	70
F	14	120
F	14	151
F	14	240
F	15	64
F	15	70
F	15	120
F	16	120
F	16	240
F	16	360
F	17	38
F	17	120
M	12	157
M	13	58
M	13	92
M	13	157
M	14	92
M	14	157
M	17	92
M	17	157
M	17	157
M	17	157
M	17	157

Adult Female Consumption

Age	Consumption (g/month)
19	150
19	150
19	150
19	150
20	88
20	150
20	150
21	47
21	150
22	88
22	88
22	150
22	150
23	9
23	88
23	150
23	150
23	150
23	150
23	150
23	150
23	150
23	184
23	300
23	300
24	150
24	150
24	150
24	150
24	150
24	150
24	150
24	150
24	150
24	150
24	150
24	540
25	150
25	150
25	150
25	150
25	150
25	150
25	150

Age	Consumption (g/month)
25	150
25	150
26	88
26	150
26	150
26	150
26	150
26	238
26	300
27	58
27	88
27	88
27	150
27	150
27	150
27	150
27	150
27	150
27	150
27	150
27	150
28	88
28	150
28	150
28	150
28	150
28	150
28	150
28	150
28	150
28	150
28	165
28	300
28	412
28	450
29	60
29	88
29	150
29	150
29	150
29	150
29	150
29	150

Age	Consumption (g/month)
29	172
30	30
30	106
30	150
30	150
30	150
30	150
30	150
30	150
30	150
30	150
30	150
30	150
30	150
30	300
31	14
31	23
31	40
31	150
31	150
31	150
31	150
31	150
31	150
31	150
31	212
31	300
31	450
32	88
32	150
32	150
32	150
32	150
32	150
32	150
32	150
32	192
32	249
32	300
33	150
33	150
33	150
33	150
33	150
33	150
33	150
33	150

Age	Consumption (g/month)
34	88
34	150
35	150
35	150
35	150
35	150
35	150
35	150
35	180
36	9
36	83
36	150
36	150
36	150
36	150
36	150
36	188
36	300
37	88
37	150
37	150
37	150
37	150
37	176
37	300
38	88
38	150
38	150
38	150
38	150
38	387
38	426
39	88
39	150
39	150
39	238
39	450
40	88
40	150
40	150
40	150
40	150
40	150
40	238
40	387
41	88
41	88

Adult Female Consumption (cont.)

Age	Consumption (g/month)
41	150
41	150
41	150
42	88
42	150
42	150
42	150
42	150
42	150
43	55
43	150
43	150
43	150
43	150
43	150
43	250
44	150
44	150
44	150
44	150
45	150
45	264
45	286
46	39
46	88
46	150
47	216
47	387
48	96
48	150
48	150
48	150
48	150
48	150
48	300
48	450
49	150
49	150
49	150
50	17
50	88
50	88
50	150
50	150
50	150
50	150

Age	Consumption (g/month)
50	300
51	47
51	88
51	88
51	150
51	150
51	150
51	150
51	150
51	150
51	300
52	88
52	150
52	150
52	150
52	300
52	321
53	78
53	150
53	150
53	150
53	150
53	150
53	150
53	387
53	434
54	80
54	88
54	88
54	90
54	150
54	150
54	150
55	91
55	156
55	624
56	91
56	99
56	156
56	156
56	156
56	156
56	312
56	462
57	91

Age	Consumption (g/month)
57	156
57	156
57	156
57	226
58	156
58	156
58	156
58	156
58	156
58	156
58	156
59	156
59	156
59	156
59	156
59	156
59	156
59	156
59	156
59	312
60	96
60	156
60	312
61	156
61	156
62	40
62	55
62	156
63	91
63	156
63	156
63	405
64	156
65	156
65	156
65	312
66	156
67	37
67	312
68	156
68	156
69	91
69	468
70	156
74	91
76	167

Age	Consumption (g/month)
78	167

Adult Male Consumption

Age	Consumption (g/month)	Age	Consumption (g/month)	Age	Consumption (g/month)	Age	Consumption (g/month)
19	190	28	190	32	190	42	111
19	1253	28	190	32	190	42	190
20	111	28	190	32	190	42	190
20	190	28	190	32	190	42	190
20	190	28	288	32	190	42	570
20	380	28	380	32	380	43	104
21	68	29	190	33	111	43	190
21	190	29	190	33	190	43	190
22	190	29	190	33	190	43	190
22	190	29	190	33	190	43	190
23	190	29	190	33	222	44	111
23	190	29	190	34	190	44	190
23	190	29	190	34	190	44	317
24	190	29	190	34	190	45	111
24	190	30	111	34	190	45	190
24	190	30	146	35	111	45	190
24	190	30	190	35	190	45	190
25	22	30	190	35	190	45	680
25	190	30	190	35	190	46	190
25	190	30	190	35	190	46	190
25	190	30	190	35	190	46	190
25	190	30	190	36	111	46	190
25	190	30	190	36	190	46	222
26	111	30	222	36	190	47	570
26	190	30	492	36	190	47	722
26	190	31	51	36	190	48	21
26	190	31	111	36	190	48	190
26	190	31	190	37	186	48	760
26	190	31	190	37	380	49	190
26	380	31	190	38	111	49	190
27	190	31	190	38	132	49	190
27	190	31	190	38	190	49	190
27	190	31	190	39	11	49	380
27	190	31	190	39	190	50	111
27	190	31	190	39	190	50	190
27	190	31	190	39	190	50	380
27	190	31	222	39	190	51	111
27	190	31	268	40	111	51	492
27	380	31	312	40	190	52	190
28	76	31	380	40	405	52	190
28	111	32	18	41	190	52	380
28	190	32	38	41	190	52	492
28	190	32	111	41	190	53	111
28	190	32	190	41	190	53	111
28	190	32	190	41	190	53	190

Adult Male Consumption (cont.)

Age	Consumption (g/month)
53	190
53	190
53	190
53	190
53	300
53	380
54	114
54	190
54	190
54	190
54	190
55	52
55	118
55	203
56	15
56	106
56	203
56	203
56	282
57	110
57	118
57	118
57	203
57	203
57	203
57	203
57	406
57	406
57	406
58	118
58	118
58	128
58	230
59	62
59	118
59	203
59	203
59	203
59	203
59	203
59	203
59	203
59	203
59	406
59	406

Age	Consumption (g/month)
59	587
60	203
60	203
60	203
60	203
61	203
61	203
61	294
62	48
63	52
64	62
64	203
64	203
64	203
66	72
66	203
66	203
67	203
69	203
70	118
70	203
70	632
73	118
74	118
77	216
77	216

Appendix D

Data Characterizing Northern Lobster Mercury Concentrations

Weight (kg)	*Mercury Concentration (ppm)*
0.339	0.610
0.339	0.743
0.347	0.637
0.364	0.597
0.366	1.155
0.367	0.490
0.370	0.688
0.370	0.688
0.373	0.195
0.375	0.537
0.378	0.950
0.380	0.135
0.380	0.655
0.383	0.713
0.385	0.320
0.389	0.625
0.390	0.215
0.390	0.547
0.390	0.680
0.394	0.690
0.395	0.385
0.395	0.780
0.395	0.790
0.397	0.180
0.400	0.185
0.401	0.500
0.402	0.170
0.404	0.193
0.405	0.460
0.406	0.410
0.407	0.405
0.408	0.490
0.410	0.180
0.410	0.185
0.411	0.207
0.411	0.320
0.411	0.615
0.412	0.130
0.413	0.190
0.414	0.413
0.415	0.435

Weight (kg)	*Mercury Concentration (ppm)*
0.417	0.700
0.418	0.325
0.420	0.310
0.420	0.723
0.422	0.570
0.422	0.663
0.425	0.325
0.425	0.843
0.426	0.180
0.428	0.075
0.429	0.680
0.429	0.685
0.430	0.100
0.430	0.300
0.432	0.100
0.433	0.150
0.434	0.195
0.435	0.370
0.435	0.503
0.436	0.395
0.436	0.527
0.436	0.860
0.438	0.795
0.438	0.950
0.439	0.200
0.439	0.530
0.439	0.933
0.440	0.340
0.440	0.370
0.440	0.500
0.442	0.228
0.444	0.513
0.445	0.840
0.446	0.337
0.446	0.753
0.448	0.183
0.448	0.700
0.449	0.210
0.449	0.487
0.449	0.490
0.450	0.500

Weight (kg)	*Mercury Concentration (ppm)*
0.450	0.570
0.451	0.563
0.452	0.385
0.452	0.665
0.453	0.505
0.453	0.657
0.453	0.785
0.454	0.190
0.454	0.250
0.454	0.280
0.454	0.750
0.455	0.193
0.456	0.140
0.458	0.615
0.458	0.882
0.459	0.315
0.459	0.967
0.460	0.370
0.460	0.420
0.461	0.200
0.462	0.313
0.463	0.175
0.465	0.150
0.468	0.150
0.468	0.205
0.468	0.273
0.468	0.530
0.469	0.492
0.470	0.050
0.470	0.135
0.470	0.835
0.473	0.383
0.474	0.683
0.476	0.425
0.477	0.175
0.478	0.195
0.478	0.660
0.479	0.090
0.481	0.183
0.482	0.345
0.482	0.360

Weight (kg)	*Mercury Concentration (ppm)*
0.482	0.365
0.482	0.475
0.483	0.130
0.483	0.170
0.483	0.570
0.483	0.733
0.484	0.180
0.484	0.530
0.485	0.220
0.485	0.260
0.486	1.228
0.487	0.367
0.489	0.108
0.490	0.200
0.490	0.255
0.492	0.720
0.493	0.170
0.493	0.743
0.496	0.420
0.496	0.555
0.496	0.935
0.497	0.585
0.500	0.417
0.501	0.475
0.503	0.270
0.504	1.380
0.507	0.135
0.507	0.520
0.507	1.050
0.510	0.253
0.510	0.260
0.511	0.303
0.513	0.210
0.514	0.480
0.515	0.250
0.516	0.200
0.516	0.565
0.521	0.255
0.524	0.605
0.525	0.485
0.526	0.165

Weight (kg)	Mercury Concentration (ppm)
0.529	0.180
0.529	0.430
0.532	0.595
0.535	0.158
0.538	0.175
0.539	0.325
0.539	0.470
0.539	0.495
0.540	0.145
0.542	0.225
0.544	0.285
0.545	0.330
0.546	0.320
0.547	0.335
0.547	0.340
0.548	0.210
0.549	0.370
0.549	0.385
0.552	0.385
0.553	0.225
0.553	0.305
0.553	0.317
0.553	0.345
0.553	0.485
0.556	0.300
0.560	0.280
0.562	0.335
0.567	0.350
0.567	0.370
0.567	0.425
0.567	0.575
0.568	0.770
0.569	0.450
0.571	0.133
0.572	0.535
0.573	0.300
0.573	0.515
0.577	0.115
0.577	0.470
0.578	0.185
0.579	0.440
0.579	0.545
0.580	0.533
0.581	0.595
0.582	0.280

Weight (kg)	Mercury Concentration (ppm)
0.582	0.290
0.582	0.415
0.583	0.125
0.589	0.110
0.589	0.465
0.589	0.475
0.590	0.625
0.596	0.147
0.596	0.295
0.596	0.465
0.601	0.550
0.602	0.645
0.604	0.630
0.605	0.305
0.605	0.560
0.607	0.435
0.608	0.145
0.608	0.765
0.609	0.220
0.609	0.225
0.609	0.287
0.609	0.555
0.610	0.240
0.610	0.320
0.611	0.247
0.611	0.270
0.617	0.495
0.620	0.575
0.622	0.550
0.624	0.450
0.630	0.510
0.630	0.530
0.632	0.323
0.632	0.400
0.632	0.440
0.635	1.200
0.636	0.370
0.640	0.527
0.642	0.445
0.644	0.430
0.644	0.540
0.647	0.307
0.648	0.250
0.648	0.623
0.649	0.520

Weight (kg)	Mercury Concentration (ppm)
0.650	0.370
0.653	0.550
0.655	1.081
0.658	0.220
0.658	0.750
0.662	0.200
0.663	0.475
0.667	0.330
0.668	0.700
0.669	0.180
0.670	0.160
0.675	0.445
0.675	0.705
0.680	0.485
0.680	0.555
0.684	0.310
0.687	0.145
0.690	0.310
0.690	1.020
0.691	0.073
0.692	0.487
0.695	0.530
0.700	0.365
0.704	0.147
0.704	0.257
0.704	0.273
0.707	0.730
0.709	0.360
0.711	0.667
0.717	0.892
0.718	0.313
0.723	0.290
0.723	0.460
0.724	0.663
0.725	0.820
0.731	0.067
0.737	0.610
0.737	0.630
0.746	0.490
0.746	0.497
0.751	0.240
0.762	0.573
0.765	0.490
0.766	0.225
0.766	0.258

Weight (kg)	Mercury Concentration (ppm)
0.778	0.550
0.778	0.557
0.780	0.505
0.783	1.603
0.784	0.200
0.786	0.515
0.787	0.100
0.787	0.430
0.790	0.760
0.792	0.110
0.792	0.145
0.793	0.500
0.794	0.450
0.805	0.423
0.808	0.360
0.808	0.453
0.811	1.240
0.815	0.085
0.815	0.820
0.816	0.435
0.818	0.670
0.819	0.728
0.822	0.190
0.824	0.165
0.824	0.495
0.826	0.263
0.829	0.107
0.831	0.390
0.831	0.858
0.834	0.590
0.835	0.125
0.836	0.285
0.836	0.720
0.842	0.505
0.842	0.537
0.850	0.535
0.851	0.605
0.851	0.703
0.851	0.860
0.855	0.087
0.861	0.420
0.868	0.145
0.869	0.502
0.870	0.117
0.878	0.975

Weight (kg)	Mercury Concentration (ppm)
0.879	0.290
0.879	0.360
0.881	0.110
0.881	0.713
0.882	0.450
0.883	0.605
0.885	0.485
0.893	0.340
0.895	0.450
0.906	0.762
0.907	0.270
0.907	0.280
0.907	0.380
0.907	0.420
0.907	0.445
0.908	0.365
0.913	0.565
0.913	0.597
0.919	0.575
0.920	0.445
0.921	0.507
0.921	0.777
0.923	1.015
0.928	0.250
0.933	0.780
0.933	1.040
0.936	0.263
0.937	1.065
0.940	0.570
0.948	0.310
0.962	0.542
0.964	0.130
0.978	0.410
0.978	0.552
0.978	0.660
0.978	0.715
0.987	0.660
0.992	0.397
0.993	0.470
1.007	0.150
1.010	1.030
1.021	0.400
1.021	0.500
1.021	0.530
1.023	0.555
1.030	0.180
1.034	0.590
1.035	0.433
1.035	0.670
1.035	0.675
1.036	0.165
1.038	0.580
1.049	0.585
1.049	0.645
1.049	0.730
1.050	0.310
1.062	0.905
1.063	0.845
1.064	0.710
1.065	0.450
1.073	0.268
1.077	0.215
1.080	0.655
1.092	0.390
1.097	0.347
1.106	0.515
1.106	0.725
1.111	0.163
1.120	0.445
1.121	0.280
1.134	0.470
1.135	0.300
1.145	1.265
1.149	0.810
1.155	1.050
1.156	0.555
1.159	0.492
1.163	0.230
1.168	0.287
1.171	0.785
1.172	0.802
1.175	0.210
1.175	0.505
1.176	0.320
1.180	1.550
1.189	0.590
1.191	0.400
1.193	0.425
1.204	0.580
1.204	1.150
1.205	0.430
1.209	0.950
1.217	0.665
1.219	0.750
1.219	0.885
1.220	0.713
1.226	0.470
1.227	0.755
1.229	0.590
1.233	0.285
1.233	0.905
1.234	0.880
1.244	0.750
1.247	0.695
1.247	0.710
1.247	0.823
1.261	0.570
1.276	0.457
1.286	0.773
1.290	0.317
1.295	0.663
1.299	0.550
1.300	1.110
1.304	0.900
1.305	0.850
1.305	0.880
1.312	0.253
1.316	0.975
1.332	0.775
1.353	0.865
1.353	1.400
1.389	0.970
1.390	1.018
1.393	0.492
1.400	0.620
1.403	0.570
1.405	0.667
1.405	0.870
1.406	1.265
1.440	0.565
1.460	0.710
1.490	0.325
1.490	0.820
1.491	0.763
1.503	0.480
1.504	0.770
1.505	0.295
1.505	1.250
1.515	0.270
1.517	0.440
1.525	0.725
1.531	0.820
1.531	1.130
1.535	0.540
1.544	0.610
1.545	0.907
1.556	1.385
1.559	0.673
1.566	0.550
1.567	1.570
1.573	0.993
1.575	0.385
1.578	0.627
1.585	0.795
1.588	0.297
1.593	0.665
1.596	0.370
1.597	0.675
1.598	1.010
1.610	0.477
1.610	0.710
1.619	0.710
1.630	1.043
1.644	0.680
1.648	0.765
1.651	0.220
1.656	0.610
1.658	0.625
1.670	1.678
1.680	0.527
1.687	0.795
1.687	0.845
1.701	0.340
1.704	0.250
1.710	0.590
1.715	1.120
1.718	0.920
1.724	0.540
1.744	0.320
1.765	1.185

Weight (kg)	Mercury Concentration (ppm)
1.768	1.295
1.772	1.053
1.781	0.800
1.788	0.350
1.801	0.840
1.808	1.520
1.809	0.720
1.829	1.485
1.833	0.667
1.834	0.417
1.843	0.660
1.844	0.800
1.856	1.630
1.901	1.140
1.909	0.645
1.910	0.725
1.914	0.360
1.914	0.542
1.920	0.950
1.928	0.465
1.942	0.605
1.950	0.637
1.954	0.550
1.955	0.635
1.956	0.525
1.956	0.827
1.958	0.837
1.970	1.000
1.984	0.777
1.986	0.915
1.993	1.070
1.996	1.430
2.013	0.460
2.025	1.635
2.037	0.505
2.058	1.160
2.070	1.080
2.071	1.220
2.076	0.927
2.076	0.965
2.078	1.185
2.082	0.480
2.084	0.730
2.115	0.430
2.127	1.120

Weight (kg)	Mercury Concentration (ppm)
2.130	0.863
2.142	1.157
2.155	0.410
2.155	0.555
2.155	1.197
2.177	0.950
2.197	1.020
2.235	0.723
2.241	0.795
2.250	1.103
2.258	0.623
2.280	0.710
2.282	0.335
2.282	1.190
2.307	0.740
2.310	0.580
2.346	0.713
2.381	0.365
2.399	1.607
2.446	0.730
2.470	1.100
2.481	1.003
2.523	0.685
2.523	1.550
2.535	0.420
2.557	0.600
2.566	0.710
2.579	1.295
2.608	0.415
2.608	0.650
2.676	1.160
2.688	0.817
2.693	0.625
2.723	1.015
2.805	1.070
2.807	1.030
2.809	1.000
2.811	1.425
2.823	1.018
2.834	0.810
2.850	1.820
2.855	1.055
2.863	0.705
2.863	1.065
2.904	1.025

Weight (kg)	Mercury Concentration (ppm)
2.938	0.713
2.958	1.100
2.983	0.815
3.055	0.935
3.063	0.700
3.075	0.650
3.092	1.783
3.175	1.710
3.187	0.890
3.214	2.310
3.226	0.905
3.317	1.065
3.350	0.750
3.359	0.925
3.469	0.935
3.483	1.000
3.512	1.280
3.544	0.440
3.880	0.910
3.973	0.860
4.082	0.420
4.239	1.178
4.351	1.013
4.798	0.870
4.876	1.900
5.811	1.310
6.004	1.220
7.627	0.990

Appendix E

Monte Carlo Simulations Using Crystal Ball

A basic familiarity of Excel and Crystal Ball is assumed.

Traditional Monte Carlo Simulations

Crystal Ball is a user–friendly add–in for Microsoft Excel used to run Monte Carlo simulations. Steps for the traditional Monte Carlo simulation procedure are not given here as the procedure is outlined in the Crystal Ball users manual (Sargent and Wainwright, 1996).

Hierarchical Monte Carlo Simulations

The first step in the hierarchical simulation is to randomly select a value or level for the dependent variables (e.g., age and gender for this research). This is easily accomplished by assigning a percent to each possible class or value using a custom distribution in Crystal Ball (Sargent and Wainwright, 1996).

Next, a value is randomly selected from the hierarchical distributions specific to the dependent values selected above (i.e., age–specific or gender–specific distributions). In this research, the S–distribution parameters were required at this time for the specific distribution of interest. Specific quantiles of the S–distribution were estimated using the approximation equations given in Chapter 3 and Appendix A.

The appropriate parameter values were assigned using either a nested IF function or a logical function TRUE in Excel. An example of each is given below for the assignment of one of four age–dependent parameter values. For the example, the parameter value is 0.5 if cell A1 equals one, 0.6 if A1 equals two, 0.7 if A1 equals three, and 0.8 if A1 equals four.

Nested IF: `=IF(A1=1, 0.5, IF(A1=2, 0.6, IF(A1=3, 0.7, 0.8)))`

TRUE: `=((A1=1)*0.5)+((A1=2)*0.6)+((A1=3)*0.7)+((A1=4)*0.8)`

The IF can only be nested seven times, but the TRUE function has no such limitation. In addition, the TRUE function evaluates more quickly and efficiently in Excel.

The values from the nested IF or the TRUE function can now be used in the parameter fields of the input variables (i.e., Crystal Ball assumption cells) as described in the users manual (Sargent and Wainwright, 1996). Once a cell reference has been entered in any parameter field, two radio buttons become available in the assumption window. Select the radio button "dynamic" so that the parameter field will be recalculated for each iteration in the simulation.

Two–Dimensional Monte Carlo Simulations

The easiest way to run a two–dimensional simulation is using the *Two–Dimensional Simulation Extender* included with Crystal Ball Pro (Werckman and Wainwright, 1998). Documentation for this Extender is provided in the previous reference.

Unfortunately, the Extender does have the following limitations: the maximum number of outer loop iterations is 100, the maximum number of inner loop iterations is 1000, and only values for the output variable can be extracted or saved.

The two–dimensional simulations were performed in this research by first selecting parameter values for each of the outer loops. The uncertainty distributions characterizing the parameter values can be assigned to cells in the worksheet. The references for these cells can now be entered in the parameter fields of the input variables. Select the radio button "static" to have these parameter values calculated only once for the entire outer loop.

Now separate simulations, similar to the traditional simulation, are performed for each outer loop. The copy and paste functions can be used to set up several outer loop simulations to run consecutively.

Hierarchical Two–Dimensional Monte Carlo Simulations

As with the two–dimensional simulation, the first step in hierarchical two–dimensional simulation is to select parameter values for each of the outer loops using the uncertainty distributions. This can be accomplished using the process described in the *Two–Dimensional Monte Carlo Simulations* section of this appendix. Remember to select the radio button "static" to have these parameter values calculated only once for the entire outer loop.

Next, a value or level is randomly selected for the dependent variables (e.g., age and gender for this research) using custom distributions in Crystal Ball (Sargent and Wainwright, 1996).

A value is now randomly selected from the input distributions specific to the dependent values selected above (i.e., age–specific or gender–specific distributions), where the parameters for each input distribution are obtained using the nested IF function or the logical function TRUE as described in the *Hierarchical Monte Carlo Simulations* section of this appendix. Remember to select the radio button "dynamic" for these assumption cells so that the parameter field is updated each iteration.

Separate simulations are performed for each outer loop. The copy and paste functions can be used to set up several outer loop simulations to be run consecutively.

List of References

Agency for Toxic Substances and Disease Registry. Toxicological Profile for Mercury (Update). Atlanta, GA: U.S. Department of Health and Human Services, Public Health Service, Agency for Toxic Substances and Disease Registry, ATSDR/TP–93/10, 1993, p. 357.

Agency for Toxic Substances and Disease Registry. Toxicological Profile for Mercury (Update). Atlanta, GA: U.S. Department of Health and Human Services, Public Health Service, Agency for Toxic Substances and Disease Registry, ATSDR/TP–98/10, 1998, p. 485.

Agency for Toxic Substances and Disease Registry. Toxicological Profile for Toxaphene. Atlanta, GA: U.S. Department of Health and Human Services, Public Health Service, Agency for Toxic Substances and Disease Registry, ATSDR/TP–90/26, 1990, p. 161.

Albert, C.M., C.H. Hennekens, C.J. O'Donnell, U.A. Ajani, V.J. Carey, W.C. Willett, J.N. Ruskin, and J.E. Manson. "Fish Consumption and Risk of Sudden Cardiac Death." Journal of the American Medical Association. 279(1):23–28, 1998.

Balthis, W.L. "Application of Hierarchical Monte Carlo Simulation to the Estimation of Human Exposure to Mercury Via Consumption of King Mackerel (*Scomberomorus cavalla).*" Ph.D. dissertation, Medical University of South Carolina, 1998.

Balthis, W.L., E.O. Voit, and G.M. Meaburn. "Setting Prediction Limits for Mercury Concentrations in Fish Having High Bioaccumulation Potential." Envirometrics. 7: 429–439, 1996.

Bogen, K.T. "Methods to Approximate Joint Uncertainty and Variability in Risk." Risk Analysis. 15(3): 411–419, 1995.

Brainard, J. and D.E. Burmaster. "Bivariate Distributions for Height and Weight of Men and Women in the United States." Risk Analysis. 12(2):267–275, 1992.

Brand, K.P. and M.J. Small. "Updating Uncertainty in an Integrated Risk Assessment: Conceptual Framework and Methods." Risk Analysis. 15(6): 719-731, 1995.

Bukowski, J., L. Korn, and D. Wartenberg. "Correlated Inputs in Quantitative Risk Assessments: The Effects of Distributional Shape." Risk Analysis. 15(2): 215–219, 1995.

Burmaster, D.E. and P.D. Anderson. "Principles of Good Practice for the Use of Monte Carlo Techniques in Human Health and Ecological Risk Assessments." Risk Analysis. 14(4): 477–481, 1994.

Burmaster, D.E., and E.A.C. Crouch. "Lognormal Distributions for Body Weight as a Function of Age for Males and Females in the United States, 1976–1980." Risk Analysis. 17(4):499–505, 1997.

Burmaster, D.E. and D.A. Hull. "Using Lognormal Distributions and Lognormal Probability Plots in Probabilistic Risk Assessments." Human and Ecological Risk Assessment. 3(2): 235–255, 1997.

Burmaster, D.E. and K. von Stackelberg. "Using Monte Carlo Simulations in Public Health Risk Assessments: Estimating and Presenting Full Distributions of Risk." Journal of Exposure Analysis and Environmental Epidemiology. 1(4): 491–512, 1991.

Burmaster, D.E. and A.M. Wilson. "An Introduction to Second–Order Random Variables in Human Health Risk Assessments." Human and Ecological Risk Assessment. 2(4): 892–919, 1996.

Calabrese, E.J. Nutrition and Environmental Health: The Influence of Nutritional Status on Pollutant Toxicity and Carcinogenicity. Volume 2 – Minerals and Macronutrients. New York: John Wiley and Sons, 1981, p. 468.

Carrington, C.D. and P.M. Bolger. "Uncertainty and Risk Assessment." Human and Ecological Risk Assessment. 4(2):253–257, 1998.

Carrington, C.D., G.M. Cramer, and P.M. Bolger. "A Risk Assessment for Methylmercury in Tuna." Water, Air and Soil Pollution. 97: 273–283, 1997.

Clarkson, T.W. "Methylmercury: Loaves Versus Fishes." CIIT Activities. 17(5): 2–6, 1997.

Cohen, J.T., M.A. Lampson, and T.S. Bowers. "The Use of Two–Stage Monte Carlo Simulation Techniques to Characterize Variability and Uncertainty in Risk Analysis." Human and Ecological Risk Assessment. 2(4): 939–971, 1996.

Cronin, W.J. IV, E.J. Oswald, M.L. Shelley, J.W. Fisher, and C.D. Flemming. "A Trichloroethylene Risk Assessment Using a Monte Carlo Analysis of Parameter Uncertainty in Conjunction with Physiologically–Based Pharmacokinetic Modeling." Risk Analysis. 15(5): 555–565, 1995.

Davidson, P.W., G.J. Myers, C. Cox, C. Axtell, C. Shamlaye, J. Sloane–Reeves, E. Cernichiari, L. Needleham, A. Choi, Y. Wang, M. Berlin, and T.W. Clarkson. "Effects of Prenatal and Postnatal Methylmercury Exposure From Fish

Consumption on Neurodevelopment: Outcomes at 66 Months of Age in the Seychelles Child Development Study." Journal of the American Medical Association. 280(8): 701–707, 1998.

Davidson, P.W., G.J. Myers, C. Cox, C.F. Shamlaye, D.O. Marsh, M.A. Tanner, M. Berlin, J. Sloane–Reeves, E. Cernichiari, O. Choisy, A. Choi, and T.W. Clarkson. "Longitudinal Neurodevelopmental Study of Seychellois Children Following *in utero* Exposure to Methylmercury from Maternal Fish Ingestion: Outcomes at 19 and 29 Months." NeuroToxicology. 16(4): 677–688, 1995.

Daviglus, M.L., J. Stamler, A.J. Orencia, A.R. Dyer, K. Liu, P. Greenland, M.K. Walsh, D. Morris, and R.B. Shekelle. "Fish Consumption and the 30–Year Risk of Fatal Myocardial Infarction." New England Journal of Medicine. 336(15): 1046–1053, 1997.

Dubois, D. and H. Prade. "Operations on Fuzzy Numbers." International Journal of Systems Science. 9:613–626, 1978.

Egeland, G.M. and J.P. Middaugh. "Balancing Fish Consumption Benefits with Mercury Exposure." Science. 278(5345): 1904–1905, 1997.

Eisler, R. Mercury Hazards to Fish, Wildlife, and Invertebrates: A Synoptic Review. U.S. Fish and Wildlife Service. Biological Report No. 85(1.10), 1987, p. 90.

Environmental Protection Agency. Exposure Factors Handbook. Washington, D.C.: U.S. Environmental Protection Agency, Office of Health and Environmental Assessment, EPA 600/8–89/043, 1990, various pagination.

Environmental Protection Agency. Guidance for Assessing Chemical Contamination Data for Use in Fish Advisories. Volume I: Fish Sampling and Analysis. Washington, D.C.: U.S. Environmental Protection Agency, Office of Science and Technology, EPA 823–R–93–00, 1993, various pagination.

Environmental Protection Agency. Guidance for Assessing Chemical Contamination Data for Use in Fish Advisories. Volume II: Risk Assessment and Fish Consumption Limits. Washington, D.C.: U.S. Environmental Protection Agency, Office of Science and Technology, EPA 823–B–94–004, 1994, various pagination.

Environmental Protection Agency. "Guidelines for Exposure Assessment." Federal Register. 57(104): 22888–22938, May 29, 1992.

Environmental Protection Agency. Guiding Principles for Monte Carlo Analysis. Washington, D.C.: U.S. Environmental Protection Agency, Risk Assessment Forum, EPA/630/R–97/001, 1997a, p. 36.

Environmental Protection Agency. Mercury Study Report to Congress. Volume I: Executive Summary. Washington, D.C.: U.S. Environmental Protection Agency, Office of Air Quality Planning & Standards and Office of Research and Development, EPA–452/R–97–003, 1997b, various pagination.

Environmental Protection Agency. Mercury Study Report to Congress. Volume IV: An Assessment of Exposure to Mercury in the United States. Washington, D.C.: U.S. Environmental Protection Agency, Office of Air Quality Planning & Standards and Office of Research and Development, EPA–452/R–97–006, 1997c, various pagination.

Environmental Protection Agency. Mercury Study Report to Congress. Volume V: Health Effects of Mercury and Mercury Compounds. Washington, D.C.: U.S. Environmental Protection Agency, Office of Air Quality Planning & Standards and Office of Research and Development, EPA–452/R–97–007, 1997d, various pagination.

Environmental Protection Agency. The Integrated Risk Information System (IRIS). Online. Washington, D.C.: U.S. Environmental Protection Agency, Office of Health and Environmental Assessment, Office of Research and Development, 1996.

Finley, B. and D. Paustenbach. "The Benefits of Probabilistic Exposure Assessment: Three Case Studies Involving Contaminated Air, Water, and Soil." Risk Analysis. 14(1): 53–73, 1994.

Finley, B., D. Proctor, P. Scott, N. Harrington, D. Paustenbach, and P. Price. "Recommended Distributions for Exposure Factors Frequently Used in Health Risk Assessment." Risk Analysis. 14(4): 533–553, 1994.

Frey, H.C. and D.S. Rhodes. "Characterization and Simulation of Uncertain Frequency Distributions: Effects of Distribution Choice, Variability, Uncertainty, and Parameter Dependence." Human and Ecological Risk Assessment. 4(2): 423–468, 1998.

Frey, H.C. and D.S. Rhodes. "Characterizing, Simulating, and Analyzing Variability and Uncertainty: An Illustration of Methods Using an Air Toxics Emissions Example." Human and Ecological Risk Assessment. 2(4): 762–797, 1996.

Grandjean, P., P. Weihe, P.J. Jorgensen, T. Clarkson, E. Cernichiari, and T. Videro. "Impact of Maternal Seafood Diet on Fetal Exposure to Mercury, Selenium and Lead." Archives of Environmental Health. 47(3): 185–195, 1992.

Grandjean, P., P. Weihe, and R.F. White. "Milestone Development in Infants Exposed to Methylmercury from Human Milk." NeuroToxicology. 16(1): 27–35, 1995.

Grandjean, P., P. Weihe, R.F. White, F. Debes, S. Araki, K. Yokoyama, K. Murata, N. Sorensen, R. Dahl, and P.J. Jorgensen. "Cognitive Deficit in 7-Year-Old Children With Prenatal Exposure to Methylmercury." Neurotoxicology and Teratology. 19(6): 417–428, 1997.

Haimes, Y.Y., T. Barry, and J.H. Lambert, eds. "When and How Can You Specify a Probability Distribution When You Don't Know Much." Risk Analysis. 14(5): 661–706, 1994.

Hall, R.A., E.G. Zook, and G.M. Meaburn. National Marine Fisheries Service Survey of Trace Elements in the Fishery Resources. Washington, D.C.: U.S. Department of Commerce, National Marine Fisheries Service, Technical Report NMFS SSRF–721, 1978, p. 313.

Hastings, C., Jr. Approximations for Digital Computers. Princeton, NJ: Princeton University Press, 1955, p. 201.

Hattis, D. and D.E. Burmaster. "Assessment of Variability and Uncertainty Distributions for Practical Risk Analyses." Risk Analysis. 14(5): 713–730, 1994.

Hoffman, F.O. and R.H. Gardner. "Evaluation of Uncertainties in Radiological Assessment Models." In Radiological Assessment: A Textbook on Environmental Dose Analysis. Till, J.E. and H.R. Meyer, eds. Prepared for Division of Systems Integration, Office of Nuclear Reactor Regulation, U.S. Nuclear Regulatory Comission. Washington D.C.: The Division, NUREG/CR–3332, ORNL–5968, NRC FIN B0766, 1983, various pagination.

Hoffman, F.O. and J.S. Hammonds. "Propagation of Uncertainty in Risk Assessments: The Need to Distinguish Between Uncertainty Due to Lack of Knowledge and Uncertainty Due to Variability." Risk Analysis. 14(5): 707–712, 1994.

Hogg, R.V. and A.T. Craig. Introduction to Mathematical Statistics: Fourth Edition. New York: Macmillan Publishing Company, Inc., 1978, p. 438.

Iman, R.L. and J.C. Helton. "An Investigation of Uncertainty and Sensitivity Analysis Techniques for Computer Models." Risk Analysis. 8(1): 71–90, 1988.

Iman, R.L. and J.C. Helton. "The Repeatability of Uncertainty and Sensitivity Analyses for Complex Probabilistic Risk Assessments." Risk Analysis. 11(4): 591–606, 1991.

International Atomic Energy Agency. Evaluating the Reliability of Predictions Made Using Environmental Transport Models. Vienna, Austria: International Atomic Energy Agency, Safety Series No. 100, 1989, p. 106.

Jacobs, H.L., H.D. Kahn, K.A. Stralka, and D.B. Phan. "Estimates of per Capita Fish Consumption in the U.S. Based on the Continuing Survey of Food Intake by Individuals (CSFII)." Risk Analysis. 18(3): 283–291, 1998.

Johnson, H.M. and I. Doré (eds). Annual Report on the United States Seafood Industry. Bellevue, WA: H.M. Johnson & Associates, 1993, p. 62.

Johnson, H.M. and I. Doré (eds). Annual Report on the United States Seafood Industry. Bellevue, WA: H.M. Johnson & Associates, 1998.

Jukes, T.H. "Mercury in Fish." Journal of the American Medical Association. 233(9): 1001–1002, 1975.

Keenan, R.E., B.L. Finley, and P.S. Price. "Exposure Assessment: Then, Now, and Quantum Leaps in the Future." Risk Analysis. 14(3): 225–230, 1994.

Lee, D.H.K., ed. Metallic Contaminants and Human Health. New York: Academic Press, 1972, p. 241.

Lipfert, F.W., P.D. Moskowitz, V. Fthenakis, and L. Saroff. "Probabilistic Assessment of Health Risks of Methylmercury from Burning Coal." NeuroToxicology. 17(1): 197–212, 1996.

Lipton, D.W. "The Resurgence of the U.S. Swordfish Market." Marine Fisheries Review. 48(3): 24–27, 1986.

MacIntosh, D.L., G.W. Suter II, and F.O. Hoffman. "Uses of Probabilistic Exposure Models in Ecological Risk Assessments of Contaminated Fish." Risk Analysis. 14(4): 405–419, 1994.

Marsh, D.O., T.W. Clarkson, C. Cox, G.J. Myers, L. Amin–Zaki, and S. Al–Tikriti. "Fetal Methylmercury Poisoning: Relationship Between Concentration in Single Strands of Maternal Hair and Child Effects." Archives of Neurology. 44(10): 1017–1022, 1987.

Marsh, D.O., T.W. Clarkson, G.J. Myers, P.W. Davidson, C. Cox, E. Cernichiari, M.A. Tanner, W. Lednar, C. Shamlaye, O. Choisy, C. Hoareau, and M. Berlin. "The Seychelles Study of Fetal Methylmercury Exposure and Child Development: Introduction." NeuroToxicology. 16(4): 583–596, 1995.

McKeown–Eyssen, G.E., J. Ruedy, and A. Neims. "Methylmercury Exposure in Northern Quebec. II: Neurologic Finds in Children." American Journal of Epidemiology. 118(4): 470–479, 1983.

McKinney, J.D., ed. Environmental Health Chemistry: The Chemistry of Environmental Agents as Potential Human Hazards. Ann Arbor, MI: Ann Arbor Science Publishers, Inc., 1981, p. 656.

McKone, T.E. "Uncertainty and Variability in Human Exposures to Soil Contaminants Through Home–Grown Food: A Monte Carlo Assessment." Risk Analysis. 14(4): 449–463, 1994.

McKone, T.E. and K.T. Bogen. "Predicting the Uncertainties in Risk Assessment." Environmental Science & Technology. 25(10): 1674–1681, 1991.

McKone, T.E. and P.B. Ryan. "Human Exposure to Chemicals Through Food Chains: An Uncertainty Analysis." Environmental Science & Technology. 25(9): 1154–1163, 1989.

Metzger, J.N., R.A. Fjeld, J.S. Hammonds, and F.O. Hoffman. "Evaluation of Software for Propagating Uncertainty Through Risk Assessment Models." Human and Ecological Risk Assessment. 4(2): 263–290, 1998.

Morgan, M.G. and M. Henrion. Uncertainty: A Guide to Dealing with Uncertainty in Quantitative Risk and Policy Analysis. New York: Cambridge University Press, 1990, p. 332.

Murphy, B.L. "Dealing with Uncertainty in Risk Assessment." Human and Ecological Risk Assessment. 4(3): 685–699, 1998.

Myers, G.J., D.O. Marsh, P.W. Davidson, C. Cox, C.F. Shamlaye, M. Tanner, A. Choi, E. Cernichiari, O. Choisy, and T.W. Clarkson. "Main Neurodevelopmental Study of Seychellois Children Following *in utero* Exposure to Methylmercury from a Maternal Fish Diet: Outcome at Six Months." NeuroToxicology. 16(4): 653–664, 1995.

National Center for Health Statistics. Analytic and Reporting Guidelines: The Third National Health and Nutrition Examination Survey, NHANES III (1988–94). Hyattsville, MD: U.S. Department of Health and Human Services, Public Health Service, Centers for Disease Control and Prevention, National Center for Health Statistics. 1996, p. 47.

National Center for Health Statistics. Plan and operation of the Third National Health and Nutrition Examination Survey, 1988–94. Washington, D.C.: U.S. Department of Health and Human Services, Public Health Service, Centers for Disease Control and Prevention, National Center for Health Statistics. Vital and Health Statistics 1(32), 1994, p. 407.

National Oceanic and Atmospheric Administration. Analysis of Consumer Perspectives on Fish and Seafood. Washington D.C.: U.S. Department of Commerce, National Oceanic and Atmospheric Administration, 1991, p. 33.

Officer, C.B. and J.H. Ryther. "Swordfish and Mercury: A Case History." Oceanus. 24(1): 34–41, 1981.

Palisade Corporation. @Risk: Advanced Risk Analysis for Spreadsheets. Windows Version July, 1997. Newfield, NY: Palisade Corporation, 1997a, p. 318.

Palisade Corporation. BestFit: Probability Distribution Fitting for Windows. Windows Version June, 1997. Newfield, NY: Palisade Corporation, 1997b, p. 133.

Price, P.S., S.H. Su, J.R. Harrington, and R.E. Keenan. "Uncertainty and Variation in Indirect Exposure Assessments: An Analysis of Exposure to Tetrachlorodibenzo–p–Dioxin from a Beef Consumption Pathway." Risk Analysis. 16(2): 263–277, 1996.

Rai, S.N., D. Krewski, and S. Bartlett. "A General Framework for the Analysis of Uncertainty and Variability in Risk Assessment." Human and Ecological Risk Assessment. 2(4): 972–989, 1996.

Richardson, G.M. and M. Allan. "A Monte Carlo Assessment of Mercury Exposure and Risks from Dental Amalgam." Human and Ecological Risk Assessment. 2(4): 709–761, 1996.

Rom, W.N., ed. Environmental and Occupational Medicine: Second Edition. Boston: Little, Brown and Company, 1992, p. 1493.

Rowe, W.D. "Understanding Uncertainty." Risk Analysis. 14(5): 743–750, 1994.

Ruffle, B., D.E. Burmaster, P.D. Anderson, and H.D. Gordon. "Lognormal Distributions for Fish Consumption by the General U.S. Population." Risk Analysis. 14(4): 395–404, 1994.

Rugen, P. and B. Callahan. "An Overview of Monte Carlo, A Fifty Year Prospective." Human and Ecological Risk Assessment. 2(4): 671–680, 1996.

Rupp, E.M. "Age Dependent Values of Dietary Intake for Assessing Human Exposures to Environmental Pollutants." Health Physics. 30: 151–163, 1980.

Rupp, E.M., F.L. Miller, and C.F. Baes III. "Some Results of Recent Surveys of Fish and Shellfish Consumption by Age and Region of U.S. Residents." Health Physics. 39: 165–175, 1980.

Ryan, P.B. "An Overview of Human Exposure Modeling." Journal of Exposure Analysis and Environmental Epidemiology. 1(4): 453–474, 1991.

Sargent, R. and E. Wainwright (eds). Crystal Ball: Forecasting & Risk Analysis for Spreadsheet Users. Version 4.0. Broomfield, CO: CGPress, 1996, p. 288.

Seiler, F.A. and J.L. Alvarez. "On the Selection of Distributions for Stochastic Variables." Risk Analysis. 16(1): 5–18, 1996.

Shamlaye, C.F., D.O. Marsh, G.J. Myers, C. Cox, P.W. Davidson, O. Choisy, E. Cernichiari, A. Choi, M.A. Tanner, and T.W. Clarkson. "The Seychelles Child Development Study on Neurodevelopmental Outcomes In Children Following *in utero* Exposure to Methylmercury from a Maternal Fish Diet: Background and Demographics." NeuroToxicology. 16(4): 597–612, 1995.

Smith, A.E., P.B. Ryan, and J.S. Evans. "The Effect of Neglecting Correlations When Propagating Uncertainty and Estimating the Population Distribution of Risk." Risk Analysis. 12(4): 467–474, 1992.

Stanford Research Institute (SRI) International. Seafood Consumption Data Analysis: Final Report. Environmental Protection Agency, Task 11, Contract 68–01–3887, 1980, p. 44.

Thompson, K.M., D.E. Burmaster, and E.A.C. Crouch. "Monte Carlo Techniques for Quantitative Uncertainty Analysis in Public Health Risk Assessments." Risk Analysis. 12(1): 53–63, 1992.

Thompson, K.M. and J.D. Graham. "Going Beyond the Single Number: Using Probabilistic Risk Assessment to Improve Risk Management." Human and Ecological Risk Assessment. 2(4): 1008–1034, 1996.

Voit, E.O. "Dynamic Trends in Distributions." Biometrical Journal. 5: 587–603, 1996.

Voit, E.O. "The S–Distribution: A Tool for Approximation and Classification of Univariate, Unimodal Probability Distributions." Biometrical Journal. 34(7): 855-878, 1992.

Voit, E.O. and P.F. Rust. "Tutorial: S–System Analysis of Continuous Univariate Probability Distributions." Journal of Statistical Computation and Simulation. 42: 187–249, 1992.

Voit, E.O. and L.H. Schwacke. "Scalability Properties of the S–Distribution." Biometrical Journal. 40(6): 665–684, 1998.

Voit, E.O. and S. Yu. "The S–Distribution: Approximation of Discrete Distributions." Biometrical Journal. 36(2): 205–219, 1994.

Voit, E.O., W.L. Balthis, and R.A. Holser. "Conditional Monte Carlo Modeling with S–Systems." Proceedings: International Congress on Modeling and Simulation. M. McAleer and A. Jakeman, eds. 3: 1223-1234, 1993.

Voit, E.O., W.L. Balthis, and R.A. Holser. "Hierarchical Monte Carlo Modeling with S–Distributions." Environment International. 21(5): 627–635, 1995.

Waldron, H.A. and A. Scott. "Metals." In: Raffle, P.A.B., P.H. Adams, P.J. Baxter, and W.R. Lee, eds. Hunter's Diseases of Occupations. London: Edward Arnold Publishers, 1994, p. 804.

Werckman, C. and E. Wainwright (eds). Getting Started with Crystal Ball Pro. Broomfield, CO: CGPress, 1998, p. 74.

World Health Organization. Environmental Health Criteria 101: Methylmercury. Geneva, Switzerland: World Health Organization, International Programme on Chemical Safety, 1990, p. 144.

Yager, R.R. "Fuzzy Prediction Based on Regression Models." Information Sciences. 26: 45–63, 1982.

Yu, S. and E.O. Voit. "A Simple, Flexible Failure Model." Biometrical Journal. 5: 595–609, 1995.